THE POTENTIAL OF DISSOCIATED METHANOL AS A FUEL FOR SPARK IGNITION ENGINES

Ian Malcolm Robinson

Thesis submitted to the Faculty of Engineering, University of Cape Town in fulfilment of the Degree of Master of Science in Mechanical Engineering

Cape Town 1983

ABSTRACT

This thesis examines the potential of dissociated methancl to increase the thermal efficiency or reduce the exhaust emissions of an internal combustion engine. It is assumed that liquid methancl will be dissociated onboard a vehicle using engine waste heat to produce a gas consisting of hydrogen and carbon monoxide in a molar ratio of 2:1.

Tests were conducted on a single cylinder engine using liquid, vaporised and dissociated methanol fuels. The dissociated methanol was derived from bottled hydrogen and carbon monoxide. Indicated thermal efficiency together with methane, methanol and formaldehyde exhaust emissions were measured. The effect of the carbon monoxide in the dissociated methanol on efficiency was investigated by operating the engine on both hydrogen and carbon monoxide separately.

The results for thermal efficiency showed that the presence of carbon monoxide resulted in a lower efficiency than for pure hydrogen. However, if the waste heat recovered in the dissociation reaction is not included in the calorific value of the fuel, then dissociated methanol offers a significant improvement in thermal efficiency compared to liquid methanol. Vaporised methanol offers efficiencies comparable to dissociated methanol for mixtures leaner than stoichiometric, again benefitting from the recovered heat.

The results for exhaust emissions showed that methanol and formaldehyde emissions were effectively eliminated and methane emissions significantly reduced with dissociated methanol fueling. Vaporised methanol fueling reduced emissions of these species to approximately $\frac{1}{3}$ of the value with liquid methanol fueling. NOx emissions may be expected to increase for both vaporised and dissociated methanol.

Preliminary design considerations indicated that there is probably insufficient high temperature energy in the exhaust gas to dissociate all the engine's fuel requirement. As a result it was concluded that while vaporised methanol could not

match the increase in efficiency or the reduction in exhaust emissions of dissociated methanol, its greater practicability for onboard implementation probably makes it a better candidate for future development.

ACKNOWLEDGEMENTS

The author wishes to express his thanks to:

Professor R.K. Dutkiewicz for the freedom permitted under his supervision.

Professor R.M. Stegen and Mr. A.D.B. Yates for their technical advice on all aspects of the work.

Mr. R. Nates for his development work with the MBTH method of aldehyde detection.

The staff of the Energy Research Institute, all of whom have contributed to this thesis.

Mrs. M. Stewart for typing the thesis.

The CSIR for their financial support.

Finally, the author wishes to pay tribute to Mr. D.M. Finlayson for the excellence in construction of experimental apparatus. His advice, experience and patience were instrumental in the successful conclusion of this investigation.

CONTENTS

LIST OF TABLES

LIST OF FIGURES

Page

1. INTRODUCTION

Literature published on research into methanol as a fuel for internal combustion engines has concentrated almost exclusively on its performance as a liquid fuel. However, it is well known that methanol can be dissociated to hydrogen and either carbon monoxide or carbon dioxide. The present investigation is concerned with the dissociation of methanol to hydrogen and carbon monoxide, represented by the following reaction:

$$CH_3OH \rightleftharpoons 2H_2 + CO$$

Two factors are of importance in such a dissociation reaction:

(i) The reaction is highly endothermic. This reaction may be effected using waste heat which would otherwise be rejected from the combustion cycle. This in itself should be responsible for an increase in the thermal efficiency.

(ii) The product gas is rich in hydrogen. The combustion properties and characteristics of the gas mixture have been reported to be similar to those of pure hydrogen, which is accepted as having a particularly high thermal efficiency at lean fuel-air ratios.

Initially, these benefits were seen in isolation. The use of an endothermic dissociation reaction specifically to recover waste heat was probably first employed, with gasoline as the fuel, in the Boston Reformed Fuel Car [1]. But it was the hydrogen rich composition of the dissociated methanol product gas which led researchers in the field of hydrogen as a potential automotive fuel to the concept of methanol dissociation as an efficient means of onboard hydrogen storage for vehicle applications [2, 3].

It appears that three criteria must be investigated before a decision can be made regarding the potential of onboard dissociation of methanol:

(i) Practicability of dissociation onboard a vehicle.
(ii) Effect on overall thermal efficiency
(iii) Effect on exhaust emission

Regarding the practicability of onboard dissociation, it has already been shown to be thermodynamically and technically possible [4]. At present, much more development is needed before an optimum system can be reached. It would be advantageous if the need for such development could be definitively established before ccmmencement of the development work. That is, if positive trends in thermal efficiency or exhaust emissions following dissociation were proven, development of a dissociation reactor for onboard use could be justified.

Fortunately it appears that meaningful indications of trends in thermal efficiency and exhaust emissions for operation on dissociated methanol can be obtained without incurring the development cost of a dissociation reactor by operation on bottled hydrogen and carbon monoxide. This report presents the results of such an investigation. The results of both previous work and the present investigation are used to determine the potential of dissociating methanol as a means to improving thermal efficiency or reducing exhaust emissions. In addition, attention is given to the benefits that may be achieved by vaporising the methanol, a procedure seen as offering most of the benefits of dissociated methanol, but on a reduced magnitude. Finally, consideration is given to the design of a system capable of dissociating methanol onboard a vehicle.

2. PREVIOUS WORK ON ENGINE EFFICIENCY

2.1 Introduction

One difficulty in assessing the potential improvements in thermal efficiency with dissociated methanol fueling is the unique composition of the fuel. Reports on the performance of the hydrogen and carbon monoxide mixture are extremely rare. However, the combustion performance of the mixture has been reported to be similar to that of hydrogen [4]. This was substantiated by showing the similarity between hydrogen and dissociated methanol for certain combustion parameters. Table 1 is a comparison of selected combustion parameters for methanol, hydrogen and dissociated methanol [4, 5]. Unfortunately there are no published results for operation on carbon monoxide, so the actual effect of carbon monoxide on the combustion performance of the hydrogen in the product gas is not known at this stage.

Table 1: Comparison of Combustion Parameters at Ambient Conditions

Parameter	Methanol	Hydrogen	Dissociated Methanol
Laminar flame speed (m/s) (stoichiometric mixture)	0,55	3,0	2,15
Minimum ignition energy (mJ) (stoichiometric mixture)	0,22	0,02	0,02
Equivalence ratio for lean combustion limit	0,52	0,10	0,13
Quench distance (mm)	1,6	0,64	N/A

Thus it appears that engine performance on dissociated methanol can be predicted from performance on pure hydrogen. This approach has been adopted in the discussion that follows.

2.2 Improvements in Combustion with Hydrogen Fueling

Oxidation of hydrogen is governed primarily by relatively fast, nearly thermally neutral bimolecular branching chain reactions. By contrast, hydrocarbon oxidation involves thermal chain mechanisms due to the slower endothermic reactions associated with the fuel breakdown. As a result of this non-thermal chain branching process in hydrogen, it has wide flammability limits, relatively high flame speed and low ignition energy[5].

The potential improvements in thermal efficiency offered by hydrogen over methanol have been ascribed to numerous factors. The effect of all these factors will now be considered.

(i) The thermodynamic cycle of hydrogen fueled engines is closer to the theoretical Otto cycle than that of methanol fueled engines. The reason for this is the higher flame speed which makes combustion closer to top dead centre possible. Turbulence in the cylinder should increase the laminar flame speed of hydrogen and methanol by the same ratio, resulting in an in-cylinder flame speed five times higher for hydrogen.

(ii) The wide flammability limits of hydrogen permit satisfactory operation at much leaner mixtures than with methanol. Hydrogen engines in automotive applications are commonly run at an equivalence ratio (the actual fuel-air ratio divided by the stoichiometric fuel-air ratio) of 0,6 [4]while for methanol engines this value is 0,95 [6]. This improves the thermal efficiency directly since the ratio of specific heats is increased and the degree of dissociation following combustion reduced as a result of the lower peak temperature [7].

(iii) There is no inadequate vaporisation with hydrogen as occurs with liquid methanol. Liquid methanol that condenses on the cylinder walls will be in a thermal and hydrodynamic boundary layer and may well escape reaction, to be swept out of the cylinder with the exhaust gas as unburnt fuel.

(iv) Complete combustion occurs even very near the cylinder walls with hydrogen as a result of the very small quench distance.

(v) Hydrogen diffuses rapidly to produce a homogeneous mixture in the combustion chamber. In contrast, the non homogeneous charge occuring with liquid methanol will contain pockets of mixture too rich for complete combustion.

(vi) The wide flammability limits also make it possible to vary the equivalence ratio over a wide range under vehicle operating conditions: $0,4 < \phi < 1,1$. This characteristic of hydrogen makes it possible to use quality governing to regulate the power output - throttling losses may be nearly eliminated by throttling only the hydrogen and admitting the air unthrottled to the engine. At 50% load the power wasted through throttling may be equivalent to as much as 80% of the brake power [8] . Many of the spectacular claims made for improvement in brake thermal efficiency in multicylinder automotive applications have exploited this fact [9, 10].

(vii) The absence of carbon in the fuel results in a flame with very low luminosity. This reduces heat loss to the cylinder walls by radiation. Unfortunately, in this respect dissociated methanol will have no advantage over liquid methanol.

(viii) It has been proposed that the reason for the higher thermal efficiency of methanol compared to gasoline is due to the dissociation of methanol to hydrogen and carbon monoxide in the combustion chamber during

compression. The combustion of the hydrogen and carbon monoxide was then believed to be responsible for the improvement in efficiency [11]. This was shown to be incorrect since the calculations for the dissociation reaction were based on equilibrium conditions and neglected the presence of air. Insufficient time is available for equilibrium to be reached and actual measurements showed that hydrogen and carbon monoxide were absent both during compression and immediately ahead of the flame front [12].

2.3 Difficulties Associated with Hydrogen Fueling

A problem that is experienced with gaseous fuels is the displacement of air by fuel in the fuel-air charge. In other words, there is a loss in the volumetric energy density of the charge. Theoretical comparison of volumetric energy density for stoichiometric mixtures of hydrogen and methanol (with the methanol remaining essentially as a liquid in the inlet manifold) indicates a 20% loss for hydrogen. There is no indication in the literature that this will in any way reduce the indicated thermal efficiency. Certainly, brake thermal efficiency will be reduced since friction losses will constitute a larger percentage of the power developed.

This problem of reduced power output with hydrogen is made more acute if it is desired to operate in the lean region at rated output. This can be dealt with by improving cylinder charging, for instance by injecting hydrogen after the inlet valve has closed or by turbocharging [13].

Undesirable combustion is a characteristic which has frequently been reported with hydrogen. The cause and effect are inextricable in a large number of conflicting reports. The only coherent outcome appears to be the need to operate hydrogen fueled engines at compression ratios no higher than 8 with mixture strengths below stoichiometric if engine operation is to appear similar to that on gasoline.

Thus far hydrogen and dissociated methanol have been regarded as having similar combustion performance. There is, however, one significant difference: for hydrogen and liquid methanol the number of moles of the stoichiometric mixture decreases by approximately 15% due to combustion before post flame dissociation occurs. For dissociated methanol the figure is 33%. Considered in isolation, this would reduce efficiency by 21% in comparison with hydrogen or liquid methanol.

2.4 Results from Previous Investigations

The object of this section was to establish the relative thermal efficiency as a function of equivalence ratio for liquid, vaporised and dissociated methanol (or pure hydrogen) from previous investigations.

This approach presented several problems:

(i) The type of engine varied from single cylinder test engines to multicylinder automotive engines in different reports.

(ii) The compression ratios varied from 5 to 12.

(iii) Only one report covered the performance of both liquid and dissociated methanol (bottled hydrogen and carbon monoxide) [14].

(iv) Two further reports cover the performance of dissociated methanol [4, 15]. However, the data in one of these reports is incompatible with the present data [15].

Fortunately there is sufficient published information to enable two of these problems to be resolved. The effect of engine type was not amenable to the treatment used below, but was limited to only a few reports.

The problem of lack of results for dissociated methanol has already been resolved by the assumption that performance on hydrogen and dissociated methanol are comparable. The problem

of different compression ratios was resolved by establishing the effect of compression ratio on efficiency. Sufficient work has been published on the effect of compression ratio on efficiency to enable a representative trend to be established. Least squares exponential regression was applied to the results in [16, 17, 18], all from single cylinder test engines, to obtain an expression relating the compression ratio and efficiency:

$$\frac{\eta}{\eta'} = \frac{\ln CR}{4,26} + 0,511$$

where CR = compression used in the investigation

η = indicated efficiency at a compression ratio of CR

η' = indicated efficiency corrected to a compression ratio of 8

Unfortunately it is extremely rare for comparative tests to be performed on hydrogen and methanol. However, results from each tested separately are readily available in published literature and by second order polynomial least squares regression, representative curves relating efficiency to equivalence ratio may be obtained separately for methanol and hydrogen.

Results from single cylinder engine tests were selected for this task since they offered both a direct comparison with the results from the present investigation and are generally obtained under more stringent experimental conditions than results for multi-cylinder engines.

2.4.1 Results for Liquid Methanol

The results from four investigations were used to establish the relationship between equivalence ratio and efficiency for methanol, figure 1. It can be seen that while the trend in efficiency with equivalence ratio is the same for all reports, there is a significant difference in the values obtained for efficiency. The difference between the highest and lowest values is approximately 14% of the measured efficiency. The cause for this discrepancy may lie either in the definition of efficiency or in the experimental method.

In the definition of efficiency there is no agreement on whether the net or gross calorific value of the fuel should be used.

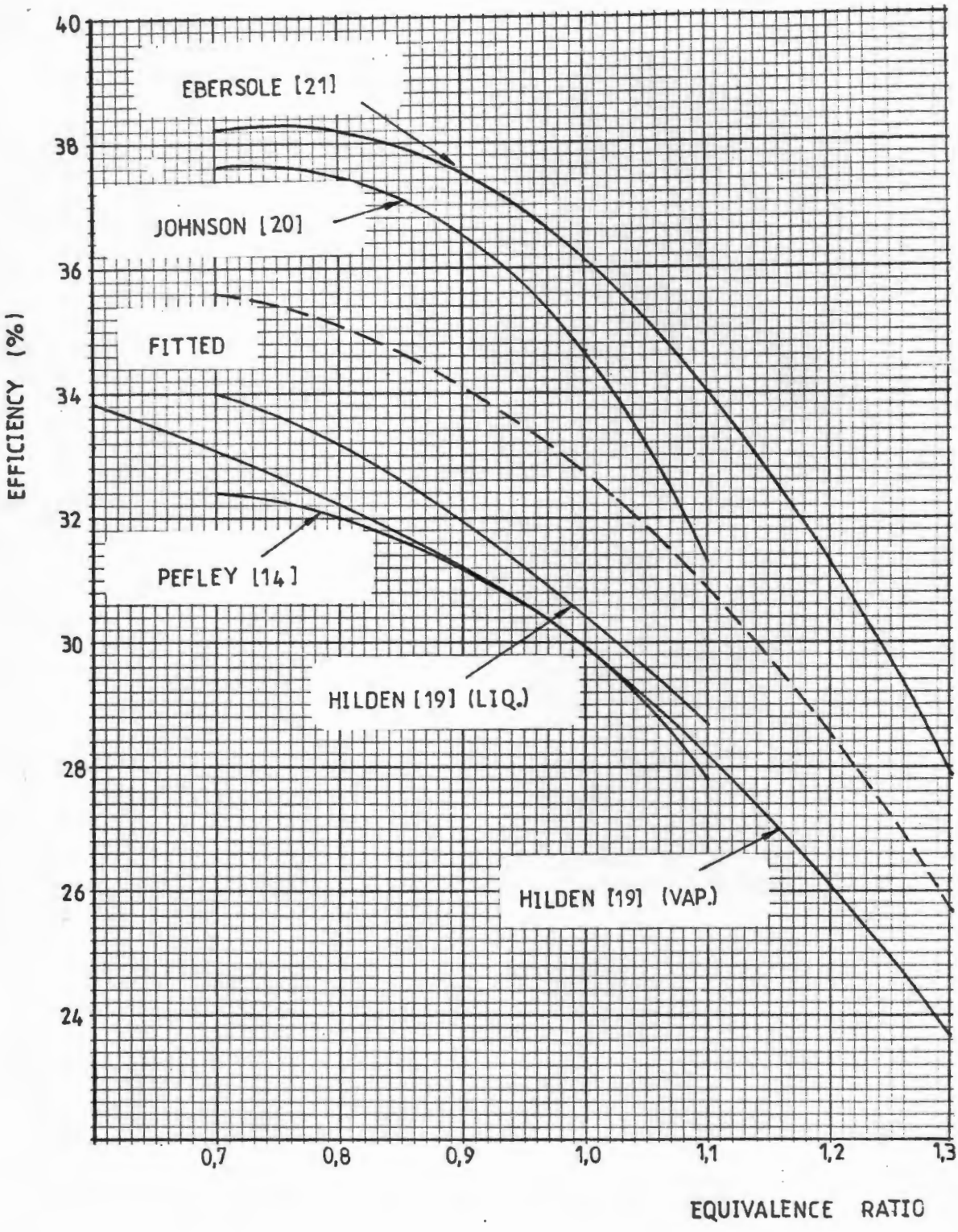

Figure 1. Efficiency for Methanol Fueling from the Literature

While generally the net value is used, it is also permissible to use the 6% higher gross value. Few reports indicate which value was used.

Considering now the experimental method, all the investigations used Co-operative Fuels Research (CFR) engines with wide open throttle and the spark timing set to the minimum advance for best torque (MBT). Compression ratio was corrected to 8 by the method developed previously. Mixture preparation in the intake system appeared to cause some difficulty in all the investigations. The high latent and sensible heats for methanol together with low volumetric energy density means that for comparable power output, the methanol-air mixture requires nine times the heat of a gasoline-air mixture to achieve complete vaporisation. To compensate for this, various degrees of air preheat were used upstream of the carburettor in all investigations. However, Hilden and Parks [19] produced results for the two extremes, no air preheat and complete vaporisation. The change this caused in efficiency is insignificant compared to the difference between different investigations.

One remaining aspect concerns the fact that indicated efficiencies are being considered. This implies that some means of measuring the indicated power of the engine was employed. Mention was seldom made in the reports of how this was done, although it is generally either obtained directly from a pressure-volume indicator card or by adding the friction power to the brake power. Indicated efficiency measured by these two methods should not, however, differ by more than about 2% [17].

Further than this, discrepancies must be due to an accumulation of relatively small uncertainties inherent in the different experimental procedures.

2.4.2 Results for Hydrogen

Again results from four investigations were used to establish the relationship between equivalence ratio and efficiency for hydrogen, figure 2. As for methanol there is a significant difference in the values obtained for efficiency and in addition

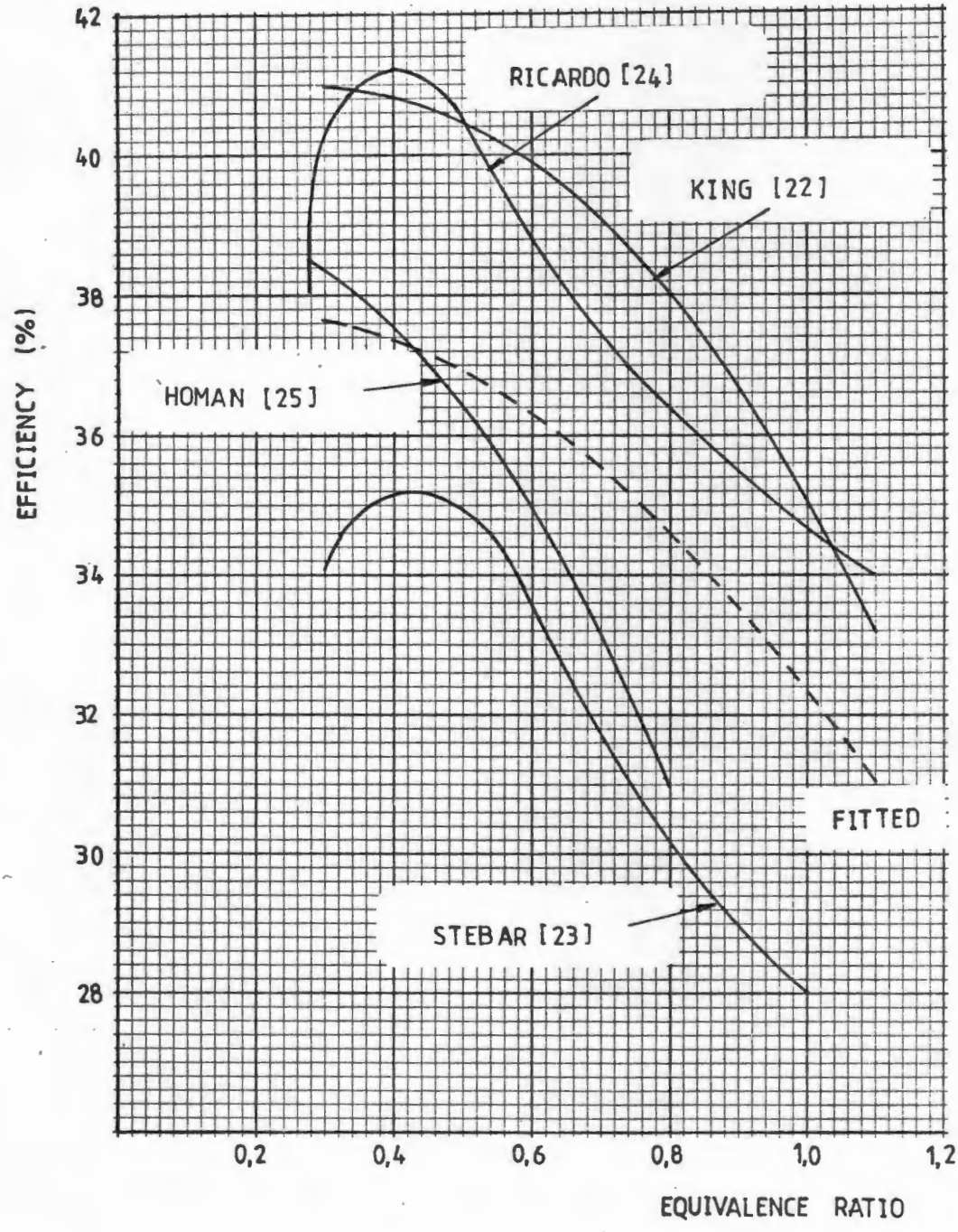

Figure 2. Efficiency for Hydrogen Fueling from the Literature

the trend in efficiency for equivalence ratios less than 0,5 also differs.

Concerning experimental conditions, the engine speeds, spark timing and throttle setting were as for the methanol tests. Three of the engines were CFR engines, while Ricardo [24] used a Ricardo engine. Since indicated efficiency is a measure of the power delivered to the piston, different friction losses will not affect the results. One difference between engines which may be significant is the shape of the combustion chamber. In the CFR engine this is disc shaped, with a flat cylinder head and flat piston while the Ricardo had a convex piston with a flat head. This difference should favour the CFR engine with regard to efficiency, although the results indicate the opposite.

In considering the discrepancies in efficiency, it is important to note that the high flame speed and low ignition energy of hydrogen may give rise to undesirable combustion phenomena, a subject which will be dealt with later. For the present it is sufficient to note that numerous relatively minor modifications were made to overcome problems such as backfiring down the intake system and knocking. Thus three of the investigations were made using hydrogen-air mixtures blended before the intake valve while Homan [25] employed direct cylinder injection of hydrogen after the closing of the inlet valve.

All the investigators had their own unique methods of ensuring the absence of hot spots within the combustion chamber; for instance, King [22] used sodium cooled exhaust valves. These measures were instituted to achieve normal combustion and no attention was paid to their effect on efficiency.

These engine modifications are also suspected of being the reason why two of the curves drop for equivalence ratios less than 0,4 while the others continue to rise. Specifically, these modifications are believed to influence the equivalence ratio at which misfire occurs.

The equivalence ratio for coherent upward propagating flames is 0,24 under conditions of standard temperature and pressure.

Once the mixture in the cylinder at ignition becomes leaner than the flammability limit, misfires may be expected with increasing frequency as the equivalence ratio is further reduced.

Now the efficiency may be expected to rise, although at a diminishing rate, as the equivalence ratio is reduced until misfire occurs. At this point unburnt fuel is expelled through the exhaust and there is a sudden drop in efficiency. With methanol, misfire is commonly first detected at equivalence ratios between 0,7 and 0,8. This means that an engine running on methanol will have an indicated mean effective pressure of the order of 8 bar, while on hydrogen this value will be between 1 and 2 bar. This is of significance in terms of how unstable the engine is at misfire.

Because of the interest in regulating the power output of hydrogen engines by quality governing alone, the engines have been operated at extremely lean mixtures, the only limiting factors being "unstable operation" and "misfire" these two terms being used interchangeably. However, from the author's experience a misfire frequency as low as 1 in 100 when operating on methanol is more easily detected by the operator than a misfire frequency as high as 1 in 5 when operating on hydrogen. When a hydrogen engine begins misfiring there is in fact no apparent loss in stability of operation.

Thus it is believed that both Stebar and Parks [23] and Ricardo [24] were operating in the true misfire region for equivalence ratios less than 0,4 which would account for the sudden drop in efficiency.

The curve fitted to all the hydrogen results by a second order polynomial does not show this reduction in efficiency at very lean mixtures.

2.4.3 Results for Vaporised Methanol

The problem of supplying sufficient heat for adequate vaporisation of the liquid methanol-air charge has already been mentioned. In this regard, a gaseous fuel has the advantage of achieving a nearly homogeneous charge in the cylinder at ignition and does

not suffer from the problem of liquid fuel escaping reaction in the quench zone surrounding the cylinder walls. It appears that vaporising the methanol before admission to the cylinder might thus offer a gain both due to improved combustion and recovery of waste heat to achieve vaporisation. Accordingly, results from previous investigations were sought.

One investigation was carried out by Hilden and Parks [19] and the results are recorded together with those for liquid methanol in figure 1. No indication is given in the report whether the calorific value of the methanol used in the calculation of the efficiency is for the liquid or the vapour. The heat of vaporisation corresponds to approximately 6% of the lower calorific value for liquid methanol. Thus, if the calorific value used in the calculation was for the vapour, then recovery of waste heat to vaporise the fuel would be equivalent to an increase of approximately 2 percentage points in efficiency i.e. the efficiency would now be approximately 1 percentage point above the efficiency curve for liquid methanol.

A second investigation was carried out by Mischke [17] who used a six cylinder direct injection diesel engine converted to spark ignition. The investigation concentrated on quality control of output in the upper load range and efficiency there was reported to be comparable to the diesel engine. Results of brake specific fuel consumption with equivalence ratio were provided only for methanol vapour. Since this engine has an unknown relationship to the single cylinder test engines referred to previously. The results were regarded as incompatible.

2.4.4 Results for Dissociated Methanol

Three investigations of dissociated methanol were found in the literature. Pefley [14] and Inagaki [4] produced results for single cylinder engines running on bottled hydrogen and carbon monoxide at similar compression ratios. Pefley used a CFR engine running at 900 rpm while Inagaki used an engine of unknown type with 20% less swept volume and running at 1 600 rpm. These two sets of results are shown in figure 3. These results are clearly not compatible.

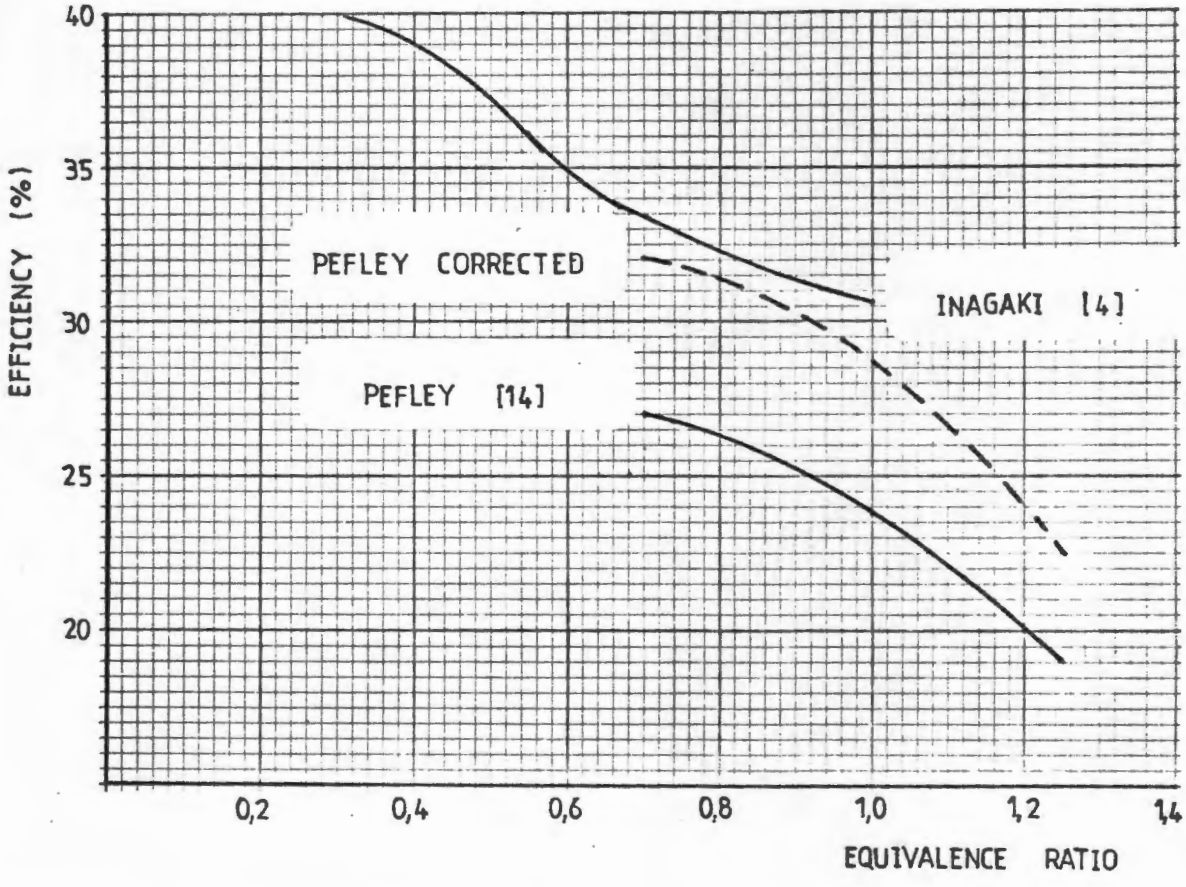

Figure 3. Efficiency for Dissociated Methanol Fueling from the Literature

At this point it is necessary to consider the fact that the energy required to dissociate liquid methanol is equivalent to 20% of the net calorific value or dissociated methanol has 120% of the energy of liquid methanol on an equal mass basis. So once again uncertainty arises as to what calorific value the investigators have used in the efficiency calculation.

Considering Inagaki's results, there are two reasons to support the belief that the calorific value for liquid methanol was used in the efficiency calculation:

(i) The efficiency already exceeds that of certain of the results quoted previously for pure hydrogen.

(ii) The case for onboard dissociation of methanol was being presented and efficiency would thus have been presented in the most favourable manner possible.

Now, if Pefley's results are assumed to be based on the calorific value of the hydrogen and carbon monoxide mixture then correcting them to a base of liquid methanol brings them into agreement with those of Inagaki, figure 3.

Another aspect in which Pefley's results raise doubt is the way in which the efficiency curve flattens out at an equivalence ratio of 0,7, suggesting the lean misfire limit was being approached. In view of the wide flammability limits for hydrogen this is a most surprising result.

The third investigation, by Finegold [15], deals with a four cylinder engine running on the product gas from the dissociation reaction. Results were provided for brake thermal efficiency as a function of torque in comparison with gasoline at a speed of 1 000 rpm. Maximum gain (48%) occurred at about maximum torque, which was estimated to occur at an equivalence ratio of 1,1. In order to relate this gain to methanol, the four investigations used previously to derive the methanol results were used to derive a representative efficiency for gasoline. From this curve, a 48% gain in efficiency over gasoline at an equivalence ratio of 1,1 translates to an absolute indicated efficiency of 42,9%. After correction from a compression ratio

of 14 to compression ratio of 8, the efficiency is 37,9%. This is some 26% above the efficiency obtained by Inagaki and appears unrealistic.

Finally, the results for efficiency of the different fuels are presented in figure 4, the results for dissociated methanol being those quoted by Inagaki but with the curve smoothed to that of a second order polynomial.

2.5 Summary

The effect of vaporised and dissociated methanol on thermal efficiency was obscured by the uncertainty in the calorific values of the fuels used in the calculation of efficiency. However, it was clear that hydrogen fueling was marginally less efficient than liquid methanol fueling at the same equivalence ratio. This was surprising in view of the improvements in combustion performance which accompany hydrogen fueling. Clearly, this was a point that warranted further investigation.

It appears that the addition of carbon monoxide to hydrogen will further reduce engine efficiency. Ultimately, only the recovery of waste heat may increase the efficiency for dissociated methanol above that for liquid methanol.

The potential of vaporising methanol as a means of waste heat recovery was another aspect that warranted further investigation.

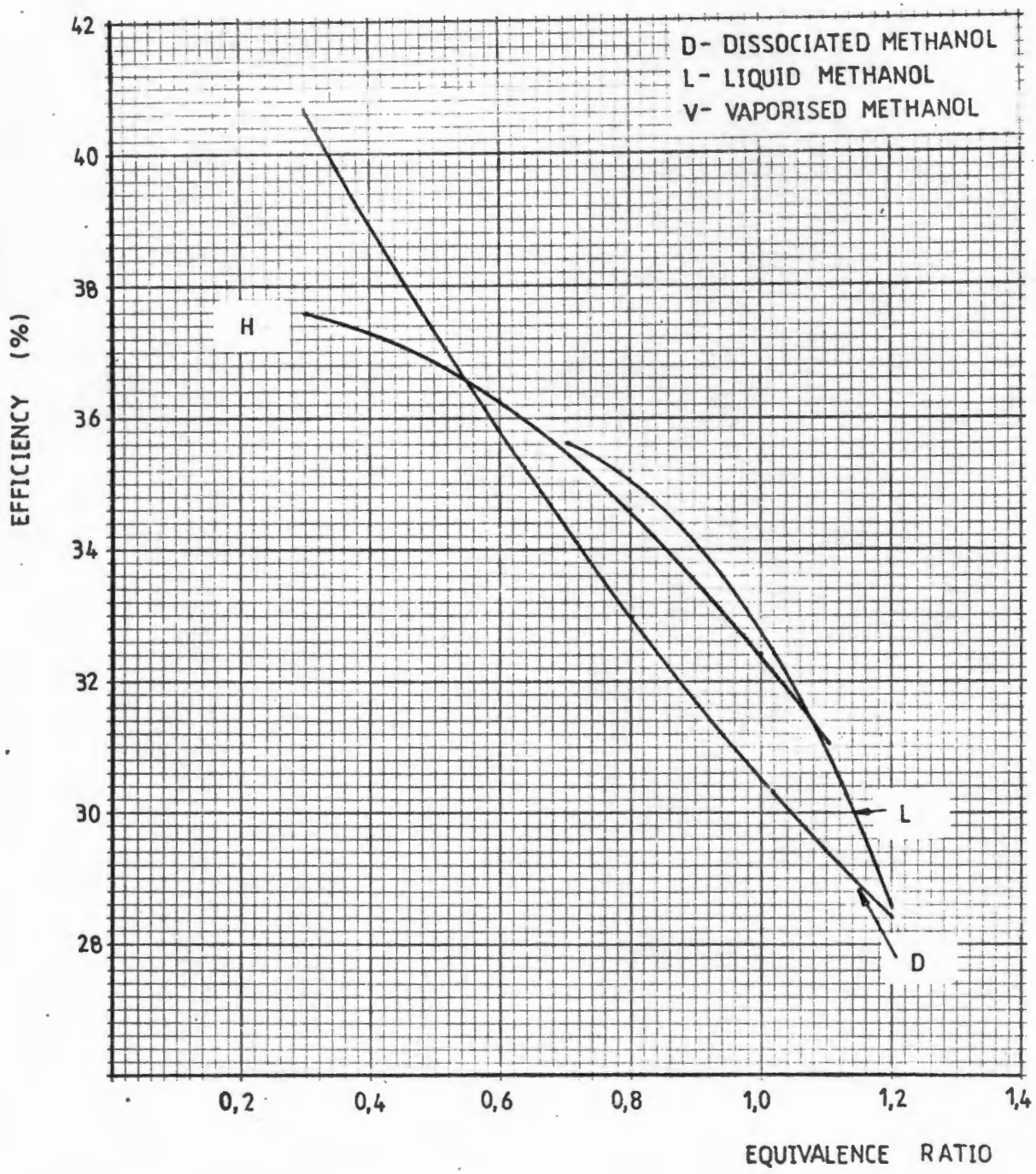

Figure 4. Effect of Fuel Type on Efficiency from the Literature

3. PREVIOUS WORK ON EXHAUST EMISSIONS

3.1 Introduction

There are a large number of species which may be identified in the exhaust of a methanol fueled engine, many of them only in trace concentrations. Two simple criteria may be used to establish which species warrant further investigation:

(i) Species which are closely related to the completeness of fuel oxidation. These were identified as carbon monoxide and methanol.

(ii) Species which are toxicologically or environmentally important. These were identified as oxides of nitrogen (NOx) and aldehydes.

Results from previous investigations will be used to establish the trends in these emissions with equivalence ratio. There are two reasons why results from different investigations cannot be meaningfully combined, as was done with efficiency:

(i) Differences in test equipment. For repeatable emissions measurement, it is extremely important that experimental conditions be as nearly identical as possible. Factors such as combustion chamber shape are known to have a significant effect on emissions. This influences both the magnitude and trend of the methanol and aldehyde curves.

(ii) Different methods of analysis. While analysis of carbon monoxide and NOx is characterised by a uniform approach, this is not true for methanol and aldehydes. Each investigation has its own equipment and procedures for measuring methanol and aldehydes and unfortunately results clearly reflect this.

As a result it was decided simply to present the separate results from at least four investigations of liquid methanol which had the greatest similarity in test equipment and procedures. In addition, reduction in emissions reported by Hilden and Parks [19] for vaporised methanol and Pefley [14] for dissociated

methanol will also be presented. The results from the excellent work by Hilden and Parks are unfortunately reported in mass specific units. The volumetric efficiency needed to convert these to concentrations was derived from the work of Ebersole and Manning [21] on a similar engine. The discussion that follows considers the source and concentration of each species separately.

3.2 Carbon Monoxide Emissions

3.2.1 Source of CO Emissions

Carbon monoxide is an intermediate product in the combustion process. In mixtures richer than stoichiometric there is insufficient oxygen available for the complete oxidation of the carbon in the fuel and carbon monoxide is found in the exhaust in the concentration of a few volume percent. In mixtures leaner than stoichiometric there is excess oxygen available but two factors are responsible for the presence of carbon monoxide in the exhaust gas:

(i) Carbon dioxide dissociates to carbon monoxide and monatomic oxygen at the peak cycle temperature. The recombination in the expansion stroke is believed to be incomplete [27].

(ii) As a result of the nonhomogeneous fuel-air charge there will be pockets of mixture that are locally rich and will be incompletely oxidised.

Carbon monoxide is generally present in concentrations less than 1/10 volume percent in this region. Since carbon monoxide has a higher calorific value than hydrogen on an equal volume basis, its presence in the exhaust gas is clearly undesirable from an efficiency point of view.

3.2.2 Results for CO Emissions

The results from the literature figure 5, show the rapid rise in carbon monoxide emissions as the mixture becomes richer than stoichiometric. The reason for the higher values reported by Harrington [37] appears to be the spark timing. While all the

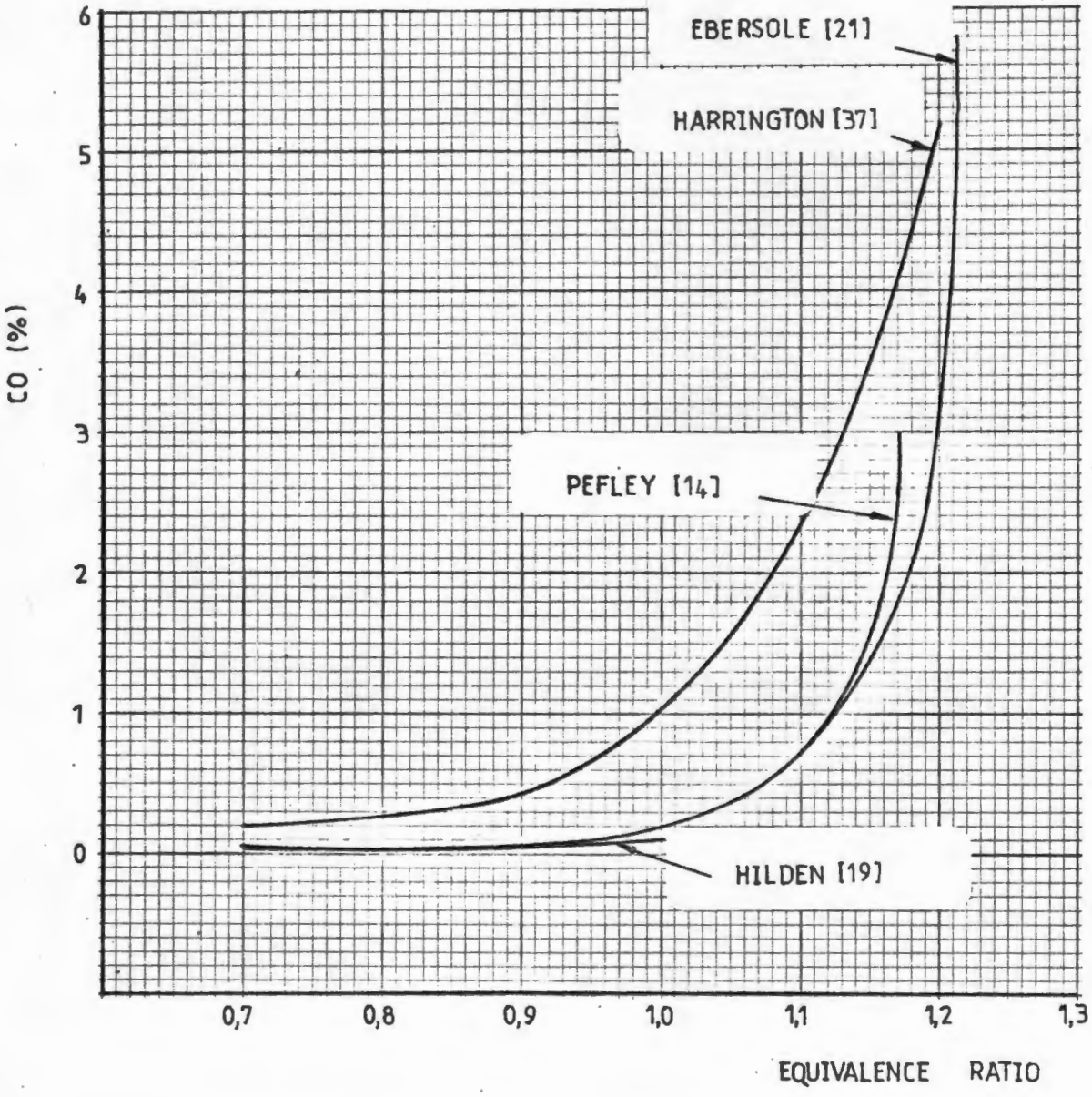

Figure 5. CO Emissions from the Literature

other investigations used MBT spark timing, Harrington maintained the timing at 15° BTDC (before top dead centre) throughout and claimed that spark timing did not affect carbon monoxide emissions. However, at lean mixtures this spark timing will result in most of the combustion occuring after top dead centre, thus missing the benefit of squish created as the piston approaches top dead centre.

Figure 9 shows that a significant reduction in carbon monoxide emissions may be expected to accompany vaporisation of the methanol. This is probably as a result of the more homogeneous fuel-air charge in the cylinder. Figure 10 shows that carbon monoxide emissions may be expected to increase with dissociated methanol fueling and mixtures close to stoichiometric. The only explanation appears to be a higher peak combustion temperature which would promote the dissociation of carbon dioxide to carbon monoxide.

3.3 Oxides of Nitrogen Emissions

3.3.1 Source of NOx Emissions

Nitric oxide (NO) is formed within the combustion chamber at the peak combustion temperature and persists during expansion and exhaust in nonequilibrium amounts. Upon exposure to additional oxygen in the atmosphere, nitrogen dioxide (NO_2) is formed [28]. This has a dark brown colour and is one of the chief elements in photochemical smog.

The dependence of NO formation on peak combustion temperature may be explained through the Zeldovich chain reaction mechanism [28]. The reactions may be represented as follows:

$$O_2 \rightleftharpoons 2O$$
$$O + N_2 \rightleftharpoons NO + N$$
$$N + O_2 \rightleftharpoons NO + O$$

This mechanism postulates that at elevated temperatures in the cylinder the molecular oxygen dissociates to atomic oxygen which reacts with molecular nitrogen to form nitric oxide and atomic nitrogen. This atomic nitrogen in turn reacts with molecular

oxygen, forming nitric oxide and atomic oxygen.

3.3.2 Results for NO_x Emissions

The results for NO_x emissions clearly show the correlation between NO formation and peak combustion temperature. Figure 6 shows that peak NO_x concentration occurs near stoichiometric mixtures where peak combustion temperature is higher than for lean or rich mixtures.

The results obtained by Ebersole and Manning [21] probably reflect differences in method of analysis rather than actual differences in NO_x emissions. While all the other investigations used chemiluminescent detection methods involving continucus reaction with ozone and detection of emitted photons, Ebersole and Manning used a colorimetric reagent.

Both vaporised and dissociated methanol show a considerable increase in NO_x emissions, particularly near stoichiometric mixtures. This is the penalty for increasing the energy in the intake charge which results in increased cylinder temperatures.

3.4 Unburnt Fuel Emissions

Unburnt fuel (UBF) emissions from gasoline fueled engines are usually described as hydrocarbons. That description would be incorrect for methanol fueling since a large fraction of the unburnt fuel is expected to be oxygenated. By convention, UBF emissions then include any portion of the fuel which escapes reaction, together with hydrocarbon compounds either generated in the combustion process or resulting from oil ingestion. Note that aldehydes are of special interest and are reported separately from UBF emissions.

3.4.1 Source of UBF Emissions

UBF emissions may arise from two sources [29]:

(i) wall quenching

(ii) incomplete combustion

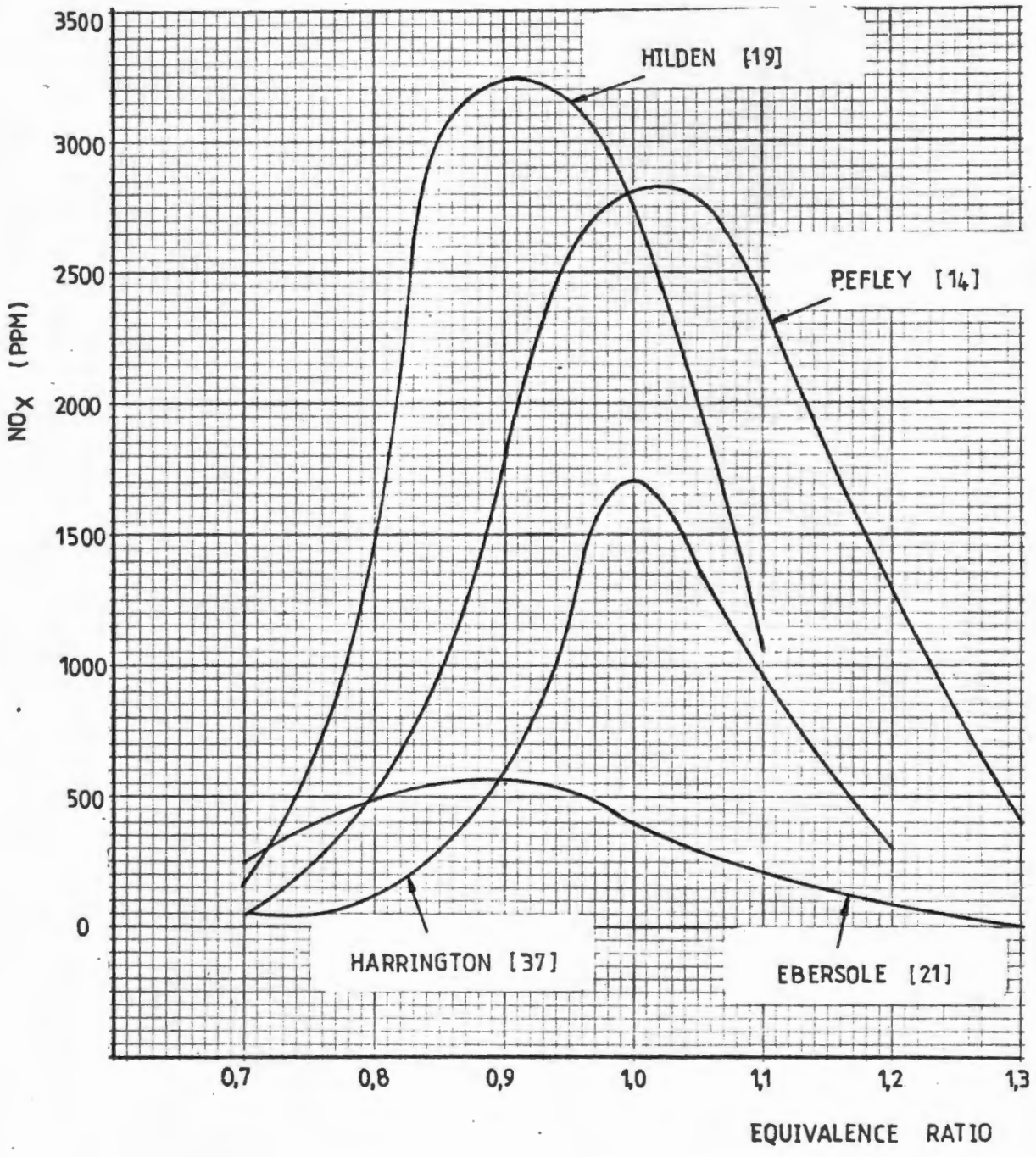

Figure 6. NO_x Emissions from the Literature

As the lean misfire limit is approached, incomplete combustion is the most important source, but under normal operating conditions it is wall quenching that is the predominant source.

Wall quenching is a combustion phenomenon which arises when a flame tries to propagate in the vicinity of a wall. The effect of the wall is a slowing down or stopping of the reaction. Wall quenching results both from chain breaking reactions and from the cooling of the layer of charge adjacent to the wall by the cool wall. During the exhaust stroke, turbulence in the cylinder scours the unburnt fuel from the wall quench zone and sweeps it out with the rest of the exhaust gas. Wall quenching is clearly evident in the UBF emissions from rich mixtures.

Incomplete combustion is known to increase significantly in lean mixtures approaching the lean misfire limit. It has been suggested that during certain cycles a flame kernel is formed but fails to develop into a full flame front, i.e. bulk quenching has occured [30]. In fact, if bulk quenching did not occur, there would be a much steeper rise in UBF emissions at the lean misfire limit, since this is generally defined as the equivalence ratio at which a certain percentage of cycles completely fail to burn.

3.4.2 Detection of UBF Emissions

The discrepancies in the results from published literature provide a good opportunity to discuss the techniques employed to measure unburnt fuel.

Measurement of UBF emissions is usually carried out by flame ionisation detector (FID). While each hydrocarbon atom has a unique response to the FID, the response of most paraffins, olefins and aromatics is within 10% of the response to propane, the standard calibration gas. However, the response to oxygenated hydrocarbons is significantly lower, from 50% to 90% of that for propane in the case of methanol [31]. The response varies both from instrument to instrument and with operating conditions, such as the hydrogen:air ratio of the mixture supplied to the flame.

Since the paraffinic and oxygenated hydrocarbons are ionized simultaneously, it is necessary to calibrate a particular instrument for the expected ratio of paraffinic to oxygenated hydrocarbons in the exhaust gas. This is where each investigation follows its own procedure:

(i) calibrate for paraffinic hydrocarbons [37]

(ii) calibrate for oxygenated hydrocarbons [21]

(iii) calibrate for mixture [19]

Procedures (ii) and (iii) are both acceptable since paraffinic hydrocarbons compose only a small percentage of total UBF emissions [19]. Pefley [14] and Ito and Yano [32] performed the analysis on gas chromatographs equipped with flame ionisation detectors but here the species are separated before introduction to the FID, so it is simply a matter of calibrating the FID for each individual species.

3.4.3 Results for UBF Emissions

The results from previous investigations, figure 7, show evidence of wall quench and incomplete combustion. The results of Hilden and Parks [19] and Ebersole and Manning [21] probably represent the extremes in mixture preparation, rather than analysis procedure. While Hilden and Parks used the standard mixture preparation system of the CFR engine, Ebersole and Manning used high pressure methanol injection to achieve atomisation just ahead of a methanol-air mixing chamber.

Figure 9 indicates that there will be a substantial reduction in UBF emissions accompanying vaporisation of the methanol. This follows from a more homogeneous fuel-air mixture with no liquid fuel in the wall quench zone. Figure 10 shows similar reductions in UBF emissions for dissociated methanol. It should be noted that although the comparison is with liquid methanol in both cases, the UBF emissions for these two investigations differ significantly, as shown in figure 7.

While the interest in UBF emissions in the present investigation was related to combustion efficiency, these emissions are also

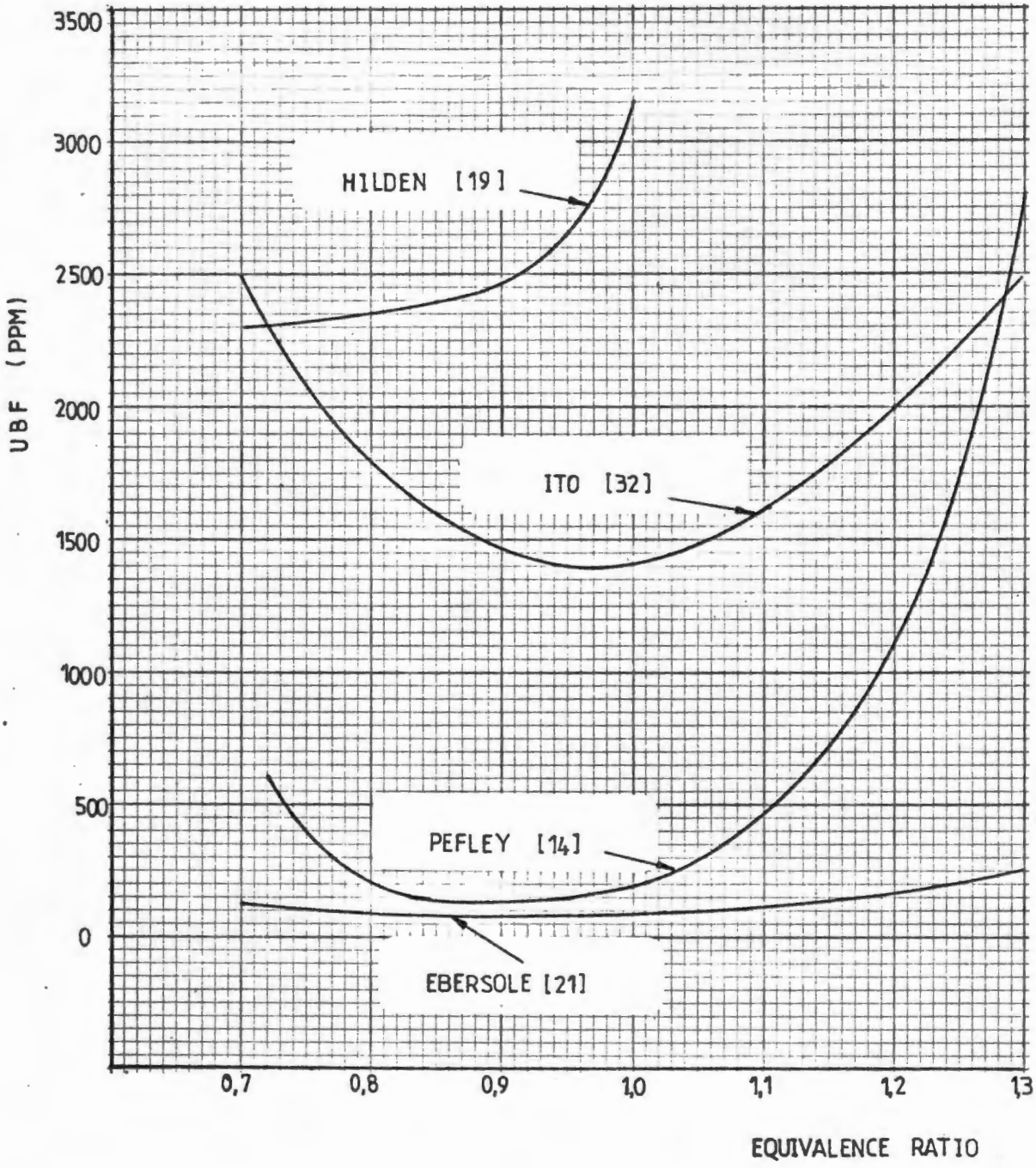

Figure 7. UBE Emissions from the Literature

regulated for the purpose of reducing photochemical smog production. This means that consideration will have to be given to the photochemical reactivity of different hydrocarbons and oxygenated hydrocarbons in the exhaust before establishing a meaningful regulatory standard or comparing UBF emissions from liquid and dissociated methanol, for instance.

3.5 Aldehyde Emissions

Aldehydes are of concern because they are an eye and throat irritant, contribute to photochemical smog production and have been identified as a potential carcinogen [31]. They are particularly significant in the context of methanol since a methanol fueled engine is generally accepted to show increased aldehyde emissions when compared to a gasoline fueled engine. An important point is that formaldehyde is an intermediate product in the formation of photochemical smog. Even in 1982 the true significance of the higher aldehyde emissions from alcohol engines was still uncertain [31].

3.5.1 Source of Aldehyde Emissions

The mechanism for the formation of formaldehyde ultimately measured in the exhaust gas is not well documented. The work of Ito and Yano [32] makes an important contribution in this field. Their findings indicate that formaldehyde formation begins in the cylinder with the oxidation of methanol that escaped reaction in the wall quench zone. Once out of the cylinder, further oxidation of methanol to formaldehyde occurs when the temperature is in the region of 400 - 500^{o}C. Above 500^{o}C oxidation of formaldehyde occurs while below 400^{o}C the formaldehyde concentration remains constant. Difficulty was experienced in correlating exhaust temperature and formaldehyde emissions for rich mixtures. In fact, the above findings did not hold for rich mixtures.

3.5.2 Detection of Aldehydes

The major difficulties in measuring aldehydes appearing in an engine exhaust are primarily due to the low concentration of aldehydes in the exhaust gas and their high reactivity. With

the most commonly used methods of detection it is necessary to convert and concentrate these highly reactive substances into more stable compounds. The three most widely used methods are discussed below.

(i) MBTH Method [33]. This method involves passing the exhaust gas through a reagent solution of 3-methyl-2-benzothiazolone (METH). The MBTH reagent solution absorbs the aldehydes present in the exhaust gas, concentrates them, and transforms them into a more stable form. The concentration of aldehydes in solution is then determined colorimetrically by measuring the optical density of the solution with a spectrophotometer. Optical density is related to concentration of aldehydes by comparison with the optical density of calibration standards. This method is generally claimed to measure total aldehydes by assuming that all aldehydes behave as formaldehyde. Analysis of absorbtion spectra of formaldehyde and acetaldehyde obtained by the MBTH method indicates they peak at a different wavelength [34]. This indicates that all aldehydes do not behave as formaldehyde, but there is sufficient overlap in the spectra to indicate that acetaldehyde will be detected, but with a reduced sensitivity.

(ii) DNPH Method [33]. Exhaust gas is passed through a solution of 2,4-dinitrophenylhydrazine (DNPH) in a manner similar to that of the MBTH method. The exhaust gas reacts with the DNPH solution to produce hydrazones. These hydrazones are mostly in solid form and are stable after separation from the DNPH solution, the hydrazones can be analysed gravimetrically, colorimetrically or chromatographically.

(iii) Chromotropic Acid Method [34]. This method basically follows the MBTH method except that the reagent in this case is chromotropic acid dissolved in sulphuric acid. This method measures exclusively formaldehyde.

In the five investigations from which results were drawn, three investigations used the MBTH method while two further methods

were also employed. Pefley [14] employed an on-line gas chromatograph to measure aldehydes directly without any concentration or stabilisation. The puported chromatogram showed the separation of formaldehyde and detection of acetaldehyde.

The difficulty with such a method is the rapid polymerisation of formaldehyde to paraformaldehyde $(CH_2O)n$ in the presence of water vapour at temperatures as high as 150°C [35]. Paraformaldehyde would not be detected as formaldehyde on a gas chromatograph. Furthermore, it is interesting to observe that although this work was published in 1971, this method has never been used in any other published investigation despite the advantages of significantly easier analysis. In fact, an investigation conducted by Ecklund and Pefley in 1981 used the MBTH method [36].

Ito and Yano [32] employed ultraviolet derivative spectrophotometry to measure exclusively formaldehyde. This method had the advantage of supplying immediate results. Its failure to achieve more widespread usage seems to be due to the need to install on-line such a specialised piece of equipment.

Since Ito and Yano measured only formaldehyde, the question arises as to the compatibility of this method with the MBTH method, which should show some response to the presence of acetaldehyde. Fortunately, further investigations have shown that the amount of acetaldehyde present in the exhaust from pure methanol fueled engines is too small to be detected by the MBTH method [34].

3.5.3 Results for Formaldehyde Emissions

The results from previous investigations are shown in figure 8. Three of the most widely spaced results (Hilden, Pischinger and Ebersole) were obtained by using the MBTH method, which seems to indicate that these discrepancies are not due to different analysis techniques, such as MBTH or gas chromatograph. Rather, it appears that these results reflect different conditions in the exhaust pipe upstream of the sampling point and in the sampling tube itself. Only Ito and Yano reported these

conditions and it appears that attempts to explain the discrepancies found in other investigations will be mere speculation. One positive outcome of these investigations is that in general an increase in UBF emissions for lean mixtures correlate with an increase in formaldehyde emissions. For rich mixtures, the increase in UBF emissions is not accompanied by an increase in formaldehyde emissions.

The results of Hilden and Parks [19] , figure 9, show the reduction in formaldehyde emissions accompanying vaporisation of the methanol. There is a clear correlation between reduction in UBF and aldehyde emissions which supports the theory that formaldehyde is an oxidation product of unburnt methanol.

A most interesting test of this theory is the effect of dissociated methanol fueling on formaldehyde emissions in view of the negligible unburnt methanol measured in the exhaust. However, only Pefley presents results for formaldehyde emissions with dissociated methanol and the results are inconclusive. Tests were performed at three different compression ratios for liquid and dissociated methanol. The result is a meaningless scatter of data. Formaldehyde emissions are shown as being 20 ppm and 140 ppm under identical conditions. These results are inadequate to warrant serious consideration.

3.6 Summary

In comparison with liquid methanol, vaporisation of methanol was found to result in:

(i) A reduction in carbon monoxide, unburnt fuel and formaldehyde emissions.

(ii) An increase in NO_x emissions.

Dissociation of methanol was found to result in:

(i) A reduction in unburnt fuel emissions.

(ii) An increase in carbon monoxide and NO_x emissions.

(iii) An unknown change in formaldehyde emissions.

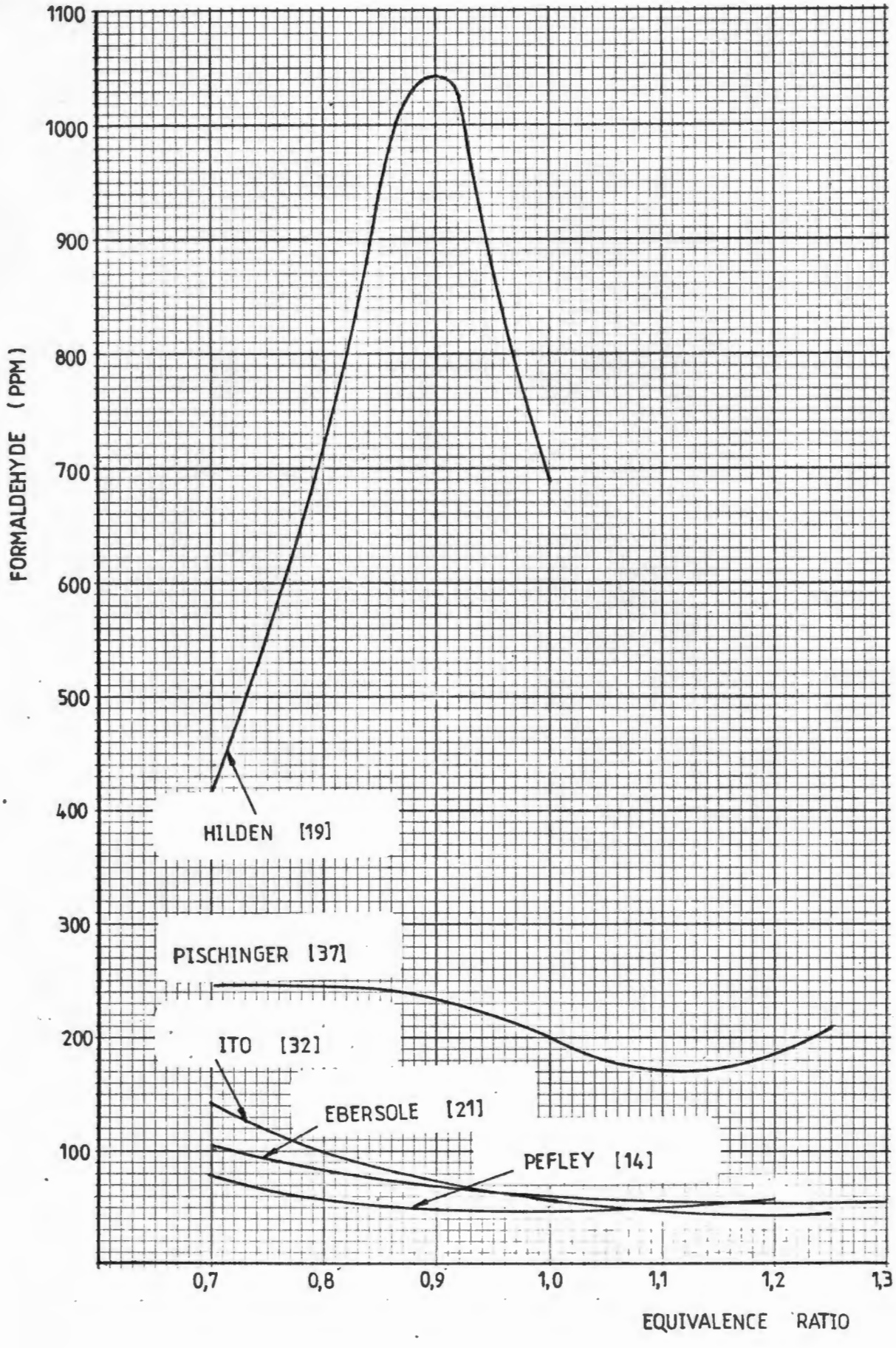

Figure 8. Formaldehyde Emissions from the Literature

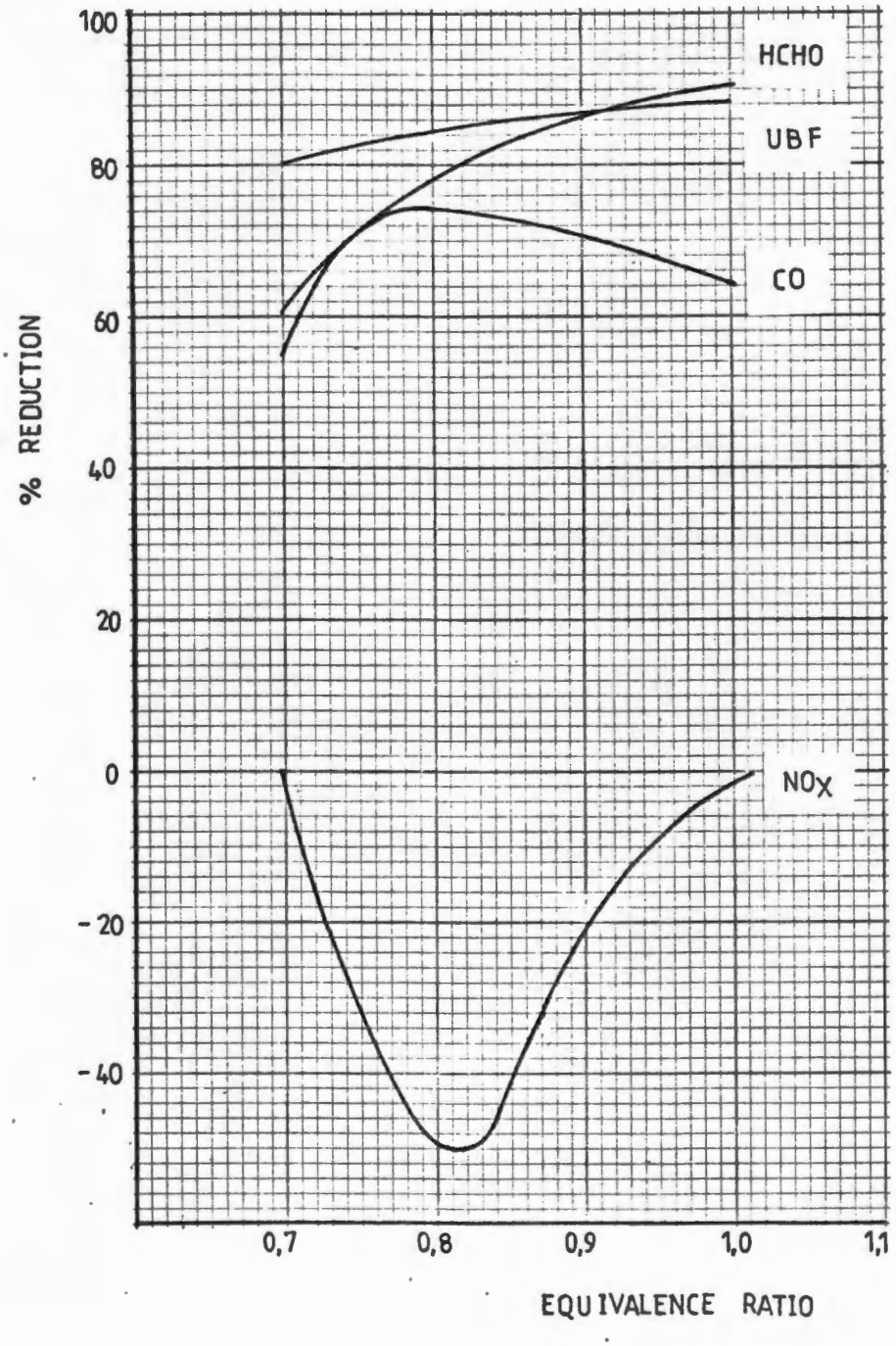

Figure 9. Reduction in Exhaust Emissions for Vaporised Methanol Fueling

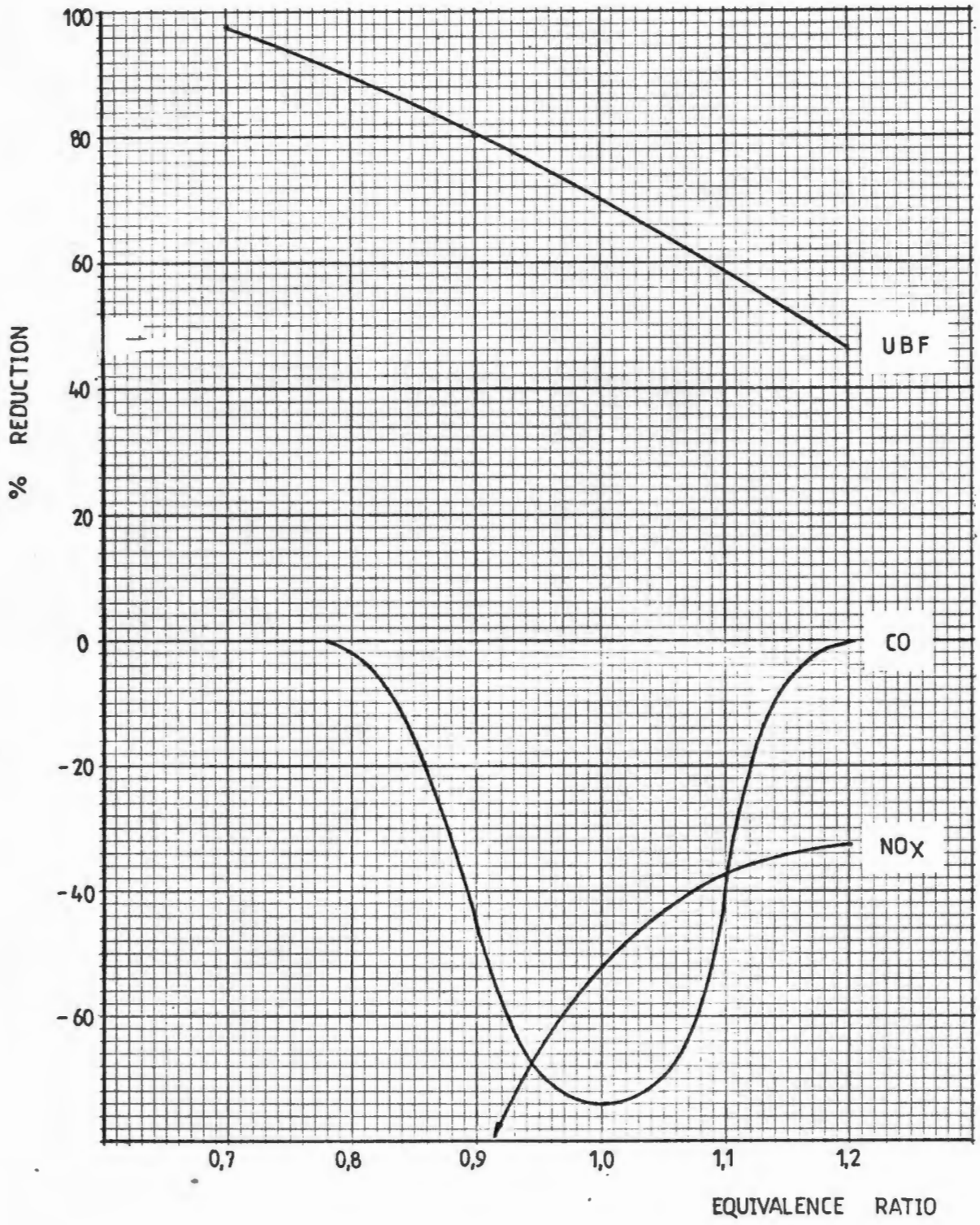

Figure 10. Reduction in Exhaust Emissions for Dissociated Methanol Fueling

A reduction in unburnt methanol emissions was found to correlate with a reduction in formaldehyde emissions and highlighted the potential of improved mixture preparation to reduce these emissions.

4. COMBUSTION IN SPARK IGNITION ENGINES

The fundamental objective of this investigation was to establish the combustion performance of a number of test fuels in a spark ignition engine. It follows that an understanding of the basic processes within the cylinder during combustion is not only desirable but is essential if the full potential of two very different fuels is to be realised. The discussion that follows will first deal with normal combustion, then abnormal combustion and finally consider the implications for a hydrogen fueled engine. Particular emphasis is laid on hydrogen throughout.

4.1 Normal Combustion

Normal combustion may be described as the desirable condition in a spark ignition engine in which combustion is initiated by a spark and remains controlled throughout the remainder of the cycle. The following description of combustion in an engine is based on the work of Benson [38].

4.1.1 Flame Development

Towards the end of the compression stroke the cylinder contains a more or less homogeneous mixture of fuel vapour and air. A spark is fired from the spark plug and as it passes from one electrode to the other it leaves a trace of flame. Combustion spreads to the envelope of the mixture containing the flame at a rate depending primarily on the temperature of the flame front and secondarily on the temperature and density of the surrounding envelope. As the flame front expands, it travels across the chamber until finally the whole of the mixture is enflamed. Depending on the degree of turbulence in the cylinder, the flame front wrinkles and perhaps breaks into eddies which speed up the process.

Two stages in the combustion process may be distinguished. The first stage corresponds to the time for the formation of the self propagating nucleus of the flame (induction period), and the second stage to the propagation of the flame throughout the combustion chamber (combustion period).

The first stage is mainly a chemical process and depends on the nature of the fuel, on the temperature and pressure of the fuel-air mixture, the concentration of residuals from the previous cycle present in the cylinder and the chemical reaction rate. It is also influenced by local turbulence.

This first portion of the charge to burn causes very little pressure rise and consequently is sometimes erroneously referred to as an ignition delay. On a pressure-crank angle indicator diagram, the first stage lies between the point at which the spark fires and the point at which the pressure curve first rises above the motoring pressure curve.

The second stage of combustion corresponds to the propagation of the flame from the initial nucleus to the consumption of all the fuel. This is both a chemical and physical process and depends on the chemical composition, the prevailing temperatures and pressures and the degree of turbulence in the cylinder. On the indicator diagram, this stage starts at the end of the first stage and ends at the point where the pressure curve begins dropping, just past the point of inflexion. Combustion duration may now be defined as the sum of stages one and two. Considering combustion as a function of only fuel-air ratio, minimum combustion duration occurs in mixtures approximately 10% rich and increases at an increasing rate for mixtures on either side of this.

The point of inflexion in the pressure curve may be used to establish the spark timing yielding optimum efficiency for a given set of operating conditions. Starting with the ignition timing sufficiently retarded so that the point of inflexion occurs well after top dead centre, advancing the ignition timing will initially increase the efficiency due to an increase in the effective expansion stroke. As the timing is advanced further, a significant pressure rise will occur before top dead centre with a resultant increase in compression work and decrease in efficiency. In general, it has been found that maximum pressure should occur between 5^{o} - 20^{o} ATDC (after top dead centre) for optimum performance and efficiency.

4.1.2 Cyclic Variation in Pressure Development

One of the fundamental characteristics of spark ignition engines is the cyclic variation in pressure development accompanying combustion. On a pressure-crank angle diagram this is most apparent in the region of peak pressure where both the magnitude of the pressure and the crank angle at which peak pressure occurs show cyclic variation. It is generally accepted that this is caused by variation in turbulence and mixture strength in the vicinity of the spark plug [39].

4.1.3 Lean Misfire Limit

When the quantity of fuel in the intake mixture is decreased, from a point of stable operation, a point is reached when the fuel-air mixture fails to burn adequately, if at all, every cycle. This condition is called misfire and is accompanied by a loss of power, sudden drop in exhaust temperature and a large increase in unburnt fuel in the exhaust gas. The frequency with which misfires occur increases as the quantity of fuel is decreased.

The lean misfire limit (LML) is the equivalence ratio at which misfire first occurs. As the LML is approached there is evidence of incomplete flame propagation (bulk quench) and/or complete failure to ignite the mixture [40]. The LML is strongly influenced by cycle to cycle variations in mixture turbulence and homogeneity.

No agreement has been reached on a definition for the LML. In previous investigations it has been defined with respect to the following parameters:

(i) Absence of a luminous flame in the combustion chamber [41].

(ii) Cylinder pressure equal to the motoring pressure [21,30].

(iii) Inflexion in the efficiency versus equivalence ratio curve [30].

(iv) Increase in the rate of UBF emissions [40].

The first and second definitions do not treat bulk quenching as a misfire.

4.2 Abnormal Combustion

A discussion of abnormal combustion is particularly relevant in the context of the present investigation with a hydrogen rich fuel. Hydrogen is particularly prone to abnormal combustion in internal combustion engines and there are many reports in the literature dealing with this phenomenon. Unfortunately there is no uniform approach to reporting abnormal combustion with hydrogen, each investigation defining descriptive terms as they see fit. The following discussion uses terms which are believed to be in most general usage, dealing first with knock (or auto-ignition) and then preignition and backfiring.

4.2.1 Knock

The following description of knock is based on the work of Benson [38]. In normal combustion, after the flame is ignited by the spark the flame front travels in a fairly uniform manner across the combustion chamber compressing the unburnt gas before it. This end gas receives heat due to both compression by the expanding gases and by radiation from the advancing flame front. Under abnormal combustion conditions the end gas spontaneously ignites ahead of the flame front. Shortly after the spontaneous ignition of the end gas a characteristic high pitch knocking sound is heard. This phenomenon is referred to as knock.

The knocking sound may be attributed to two possible sources:

(i) The impingement of a shock wave at the chamber wall, the shock wave being initiated by the spontaneous ignition source in the end gas.

(ii) The acoustic vibration of the combustion chamber contents at their resonant frequency.

In both cases there is a breakdown of the cylinder boundary layer accompanied by an increase in the heat transfer rate at the wall with the potential formation of hot spots.

The conventional assessment of knock resistance through determination of the octane number by, for instance, the ASTM Motor Method [42] is not satisfactory for hydrogen because the

required spark timing is too advanced for the particularly high flame speed. The advanced timing serves to increase the end gas pressure and temperature and hence promotes the tendency to knock, resulting in an underestimated octane number.

Hydrogen is generally reported to be susceptible to "knocking" and that "knocking" places a limit on the compression ratio-mixture strength combination [23, 24, 43, 44]. However, there are isolated reports of knock free operation at all mixture strengths [22, 45]. In one such case [45] there was definite indication of high frequency oscillations in the indicator diagram. There is no agreement in the literature about what causes this knocking. In fact, it appears that researchers are predisposed to condemn any unusual engine noise with hydrogen fueling as "knocking".

The work of King [22, 46] offers some clarification of the problem. Two terms were used to describe two different kinds of knock. Combustion knock describes an effect due to an abnormally high rate of flame propagation. Detonation knock describes an effect due to the autoignition and explosion of the end gas. These knocking sounds were described as being similar in a CFR engine. A distinction between the two types of knock was that elimination of knock by retarding the ignition gave rise to a decrease in power in the case of detonation knock but an increase in power in the case of combustion knock. It appeared that the spark timing was initially set arbitrarily and was not MBT.

The experimental results King obtained by means of indicator diagrams showed that combustion knock could occur in the absence of preignition or detonation because of the high rate of burning. Severe high amplitude cylinder pressure oscillations which are characteristic of detonation knock were successfully avoided even for equivalence ratios greater than one at a compression ratio of 10. However, rough running due to high rates of cylinder pressure rise, which is characteristic of combustion knock, was not avoided.

This roughness usually involves vibration of the crankshaft-flywheel system in bending. This may be overcome by increasing

the natural frequency of the vibrations involved such as by stiffening the crankshaft in bending [47]. Since today's engines have been optimised for gasoline combustion over a long period it is likely that engines in a future hydrogen energy economy will incorporate these changes as a matter of course.

4.2.2 Preignition and Backfire

The other two types of abnormal combustion encountered with hydrogen are preignition and backfire. These may be treated together since the mechanism appears to be the same although the phenomenon is classified according to whether the inlet valve was open or closed at the start of combustion. In backfiring, the incoming fuel-air mixture contacts a source of thermal energy of sufficient magnitude and intensity to initiate combustion during the period when the inlet valve is open. In preignition, combustion is initiated after the inlet valve has closed but before the spark occurs.

Two characteristics of hydrogen are responsible for these phenomena:

(i) Low ignition energy, an order of magnitude less than that for methanol, makes it susceptible to ignition by smaller heat sources.

(ii) High flame speed, almost an order of magnitude greater than that for methanol, contributes to the rapid growth of small flame nuclei and decreases the time available for quenching.

A suitable thermal energy source may be a high temperature zone on the interior of the combustion chamber such as a spark plug, exhaust valve or a sharp projection such as a casting imperfection or a deposit such as carbon from the pyrolysis of lubricating oil that has leaked past the piston rings [48]. Although the residual gases which remain in the combustion chamber at the end of the exhaust stroke and mix with the fresh charge were assumed to be capable of initiating combustion, it has been shown that the induction period required before ignition can occur is too short [48].

Knocking in the end gas has been proposed as a mechanism for the formation of hot spots and subsequent backfiring [49]. The process commences with the emergence of a number of knocking cycles which lead to the formation of hot spots within the combustion chamber. This is followed by a sequence of progressively earlier cycle to cycle preignitions. The preignitions in turn lead to backfiring which terminates in misfires, accompanied by combustion chamber cooling as the spent charge is inducted. The cycle may then be repeated. This mechanism is unsatisfactory as regards the explanation of backfires experienced immediately after starting.

4.3 The Hydrogen Engine

Spark ignition engines that have been optimised for operation on gasoline have been reported to be susceptible to all of the above phenomena of abnormal combustion when attempts are made to operate them without modification on hydrogen. Backfiring is the most offensive of these phenomena and three distinct approaches to solving the problem may be distinguished [48]:

(i) Elimination of potential hot spots by:

- (a) use of cold running spark plugs
- (b) use of sodium cooled exhaust valves
- (c) maintaining a clean combustion chamber free of deposits
- (d) addition of multiple piston rings to reduce oil injestion into the combustion chamber

(ii) Addition of a diluent to reduce heat production per unit volume i.e. quenching of errant flame nuclei, by:

- (a) water injection
- (b) external exhaust gas recirculation
- (c) internal exhaust gas recirculation in which valve timing is altered to increase the amount of residual gas in the cylinder.

(iii) Delayed injection of hydrogen following the admission of air.

The third approach is really a subdivision of the first approach, but its importance justifies its position.

CFR engines have been successfully operated on a premixed hydrogen-air charge supplied by devices equivalent to a gas carburettor by employing various combinations of the methods to reduce hot spots [22, 23, 24, 44, 46]. In particular, King was able to operate at best power mixtures with a compression ratio of 12 by employing all the methods for eliminating hot spots [44, 46].

More recent investigations have employed the delayed injection of hydrogen following the closure of the inlet valve [25, 45]. This enables the air to cool the combustion chamber before a flammable mixture is formed. This method has the further advantage of increasing power output to above that achieved with liquid methanol fueling.

Hydrogen injection may occur either before compression or after compression but before the spark. This latter scheme has been very successfully employed to control the rate of pressure rise by controlling the rate of hydrogen injection, obviously without the problem of preignition [22]. However, with such late injection orientation of the hydrogen jet is important if misfire is to be avoided.

5. DEVELOPMENT OF EXPERIMENTAL APPARATUS

A block diagram of the experimental apparatus is shown in figure 11.

5.1 Test Engine

All tests were conducted on a Ricardo E6 single cylinder engine. Details of the engine and operating conditions are given in table 2. A cross sectional view of the engine is shown in figure 12.

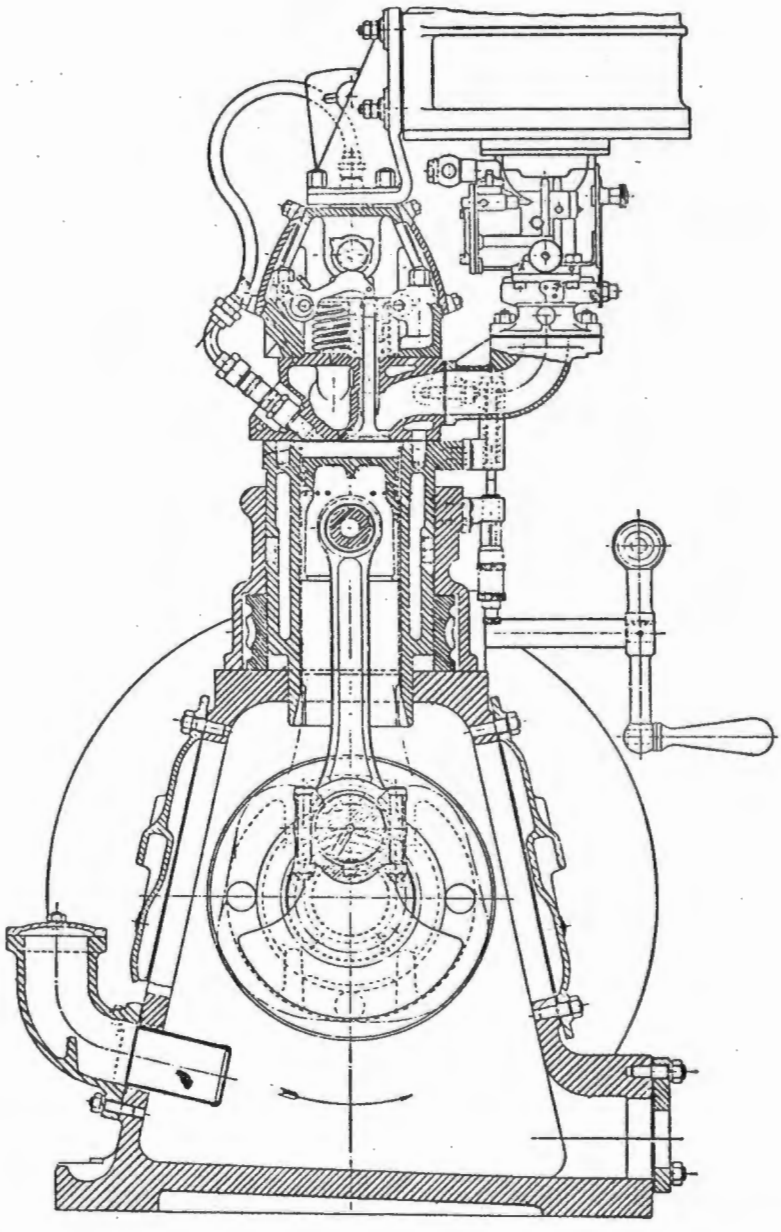

Figure 12 Cross Sectional View of Ricardo E6 Engine

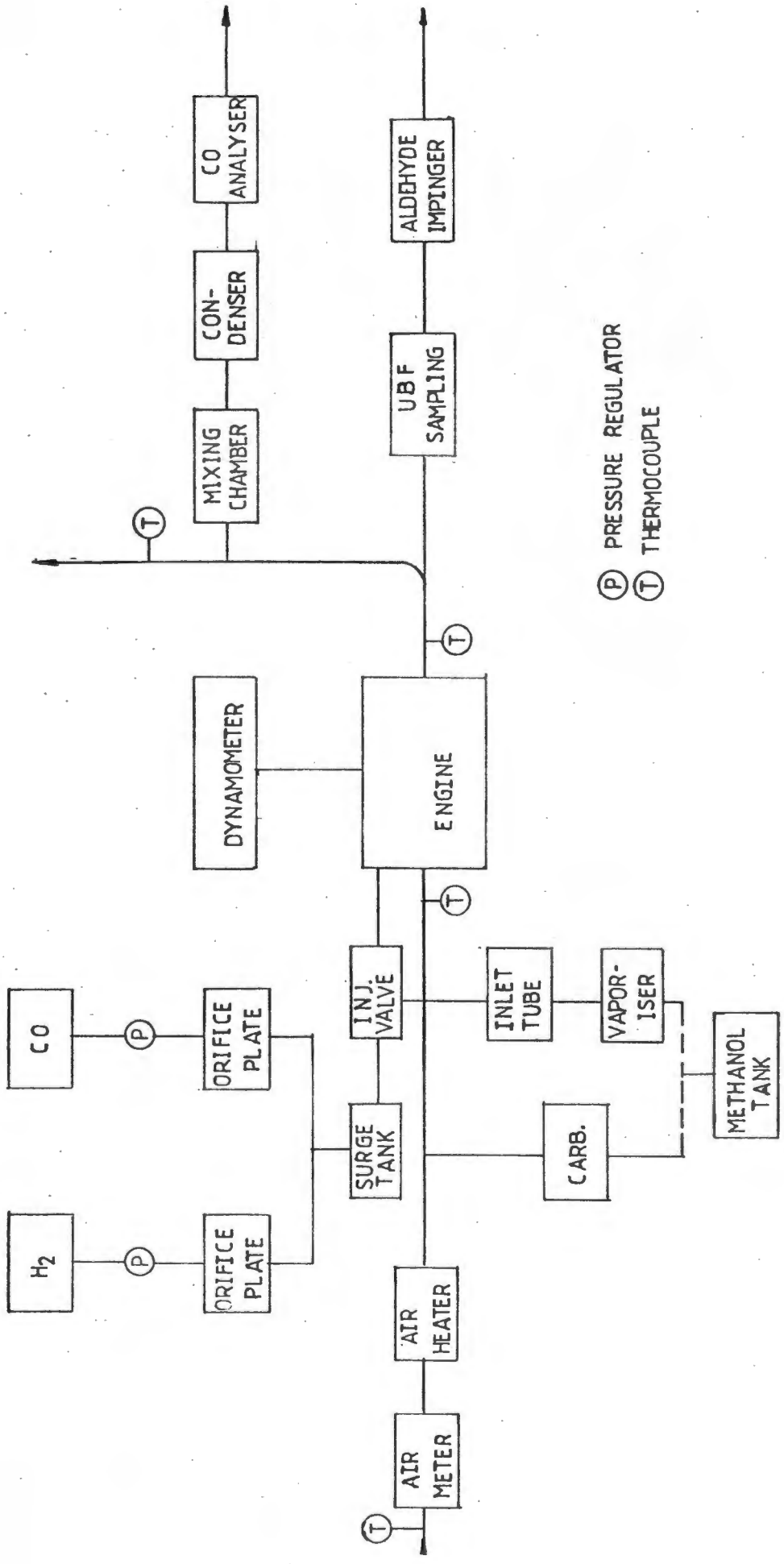

Figure 11. Block Diagram of Experimental Apparatus

The spark plug is situated at the side of the combustion chamber, between the valves. A similar hole is provided on the opposite side of the combustion chamber for a pressure transducer.

The air flow rate to the engine is measured by means of a laminar flow meter in the air intake system. Just downstream of this device (and upstream of the carburettor) is an electrical heater for preheating the air.

The lubrication system is equipped with an electrical heater in the crankcase for the purpose of warming the oil before starting and maintaining the temperature while the engine is running, if necessary. An oil-water heat exchanger enables the temperature of the oil to be controlled.

Table 2 Details of the Test Engine

Engine type	Ricardo E6
Bore	76 mm
Stroke	111 mm
Swept volume	507 cm^3
Combustion chamber shape	disc
Valve timing : inlet opens	9^{o}BTDC
inlet closes	36^{o}ABDC
exhaust opens	46^{o}BBDC
exhaust closes	8^{o}ATDC
Compression ratios	8, 12, 14
Spark plug : type	Champion N57R
gap	0,5 mm
Ignition system	Capacitive discharge
Ignition timing	MBT
Speed	900 $\pm$ 10 rpm
Throttle setting	wide open
Oil temperature	$60^{o}C \pm 2^{o}$
Coolant temperature	$71^{o}C \pm 2^{o}$

A closed circuit cooling system is used. Circulation is by an electrical pump. A coolant-water heat exchanger is provided

for temperature regulation. In the present investigation distilled water was used as the coolant and a rotameter plumbed into the coolant circuit to measure the flow rate.

The engine is coupled to a swinging field electric dynamometer. The torque developed by the dynamometer is measured by means of a brake arm attached to a balance. Switch gear enables the dynamometer to be operated as a motor to start the engine or to measure friction losses. The engine speed is measured by an electric tachometer driven by a generator coupled to the end of the dynamometer shaft.

5.2 Ignition System

A magneto was supplied as the standard ignition system. The performance of this unit was not considered adequate for reliable ignition of very lean hydrogen charges due to the particularly high ionisation potential of hydrogen. In fact, capacitive discharge ignition systems are reported as standard even in methanol tests.

The capacitive discharge ignition system which was used in the present investigation was triggered by a standard contact breaker set, the position of which was used to set the spark timing.

Figure 13a is a trace of the electric potential difference across the spark plug electrodes during firing for the magneto ignition system (time base = 500×10^{-6} sec/div.). Figure 13b is the trace with capacitive discharge ignition at the same engine conditions (time base = 100×10^{-6} sec/div.). Ground potential is two divisions from the bottom in both cases.

These figures show that there is initially a very rapid rate of increase in potential until the gap between the spark plug electrodes is ionised. The charge in the coil is then discharged across the electrodes at a small voltage difference. This is followed by resonance in the electric circuit below ionisation potential, shown by the sinusoidal curves. Two differences in the performance of the ignition systems are apparent:

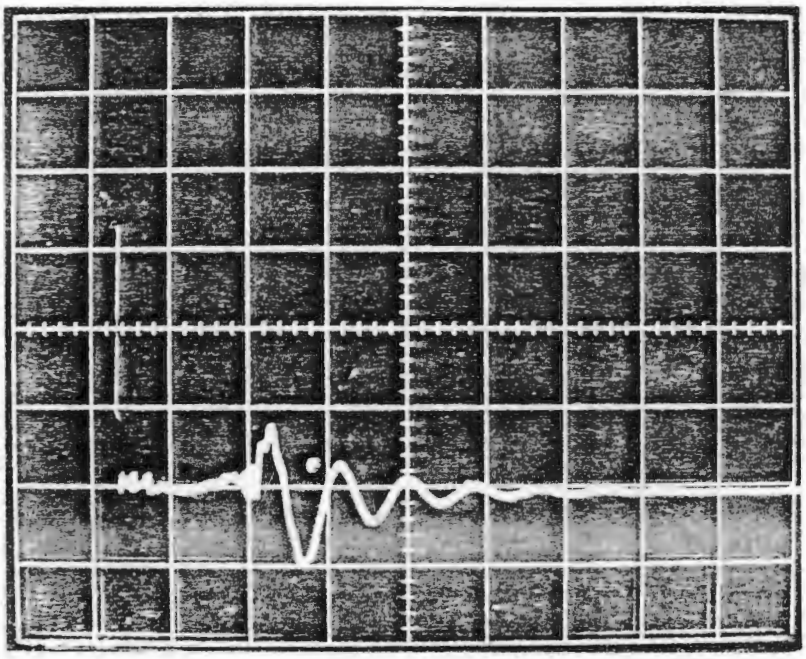

Figure 13a Potential Difference across the Spark Plug Electrodes for the Magneto Ignition System

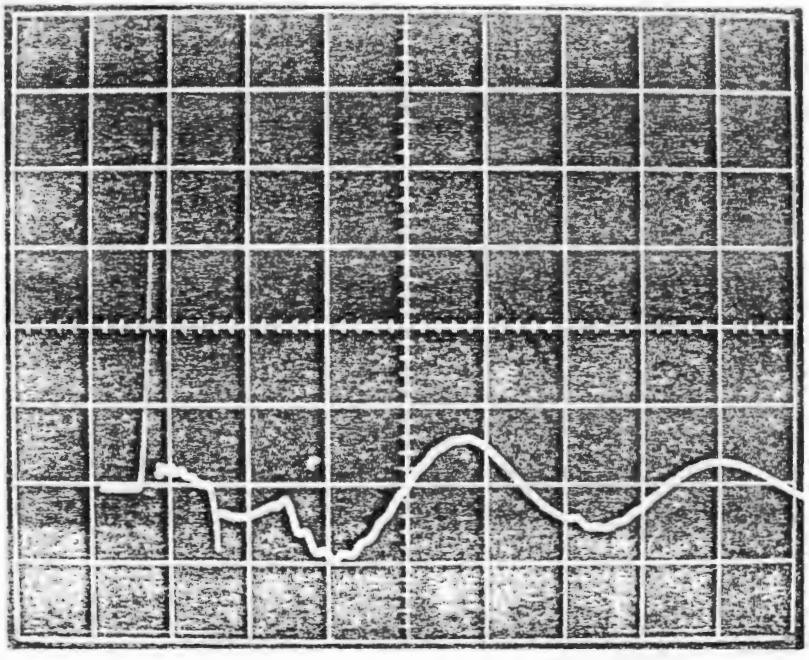

Figure 13b. Potential Difference across the Spark Plug Electrodes for the Capacitive Discharge Ignition System

(i) The capacitive discharge system provides a spark of approximately 70 x 10^{-6} sec duration as opposed to approximately 800 x 10^{-6} sec for the magneto.

(ii) The capacitive discharge system provides a 40% higher peak potential, i.e. just prior to firing. This should almost double the energy in the spark.

The shorter spark duration may give rise to increased cyclic pressure variations in terms of the model of cylinder turbulence proposed by Taylor [39]. In order to quantify this phenomenon, a term called the peak pressure scatter was defined as the ratio of the difference between the maximum and minimum cylinder pressure during combustion to the maximum pressure over approximately 1 350 cycles (3 minutes). Figure 14 shows a typical indicator diagram after 3 minutes of operation. The peak pressure scatter is the ratio of A to B expressed as a percentage.

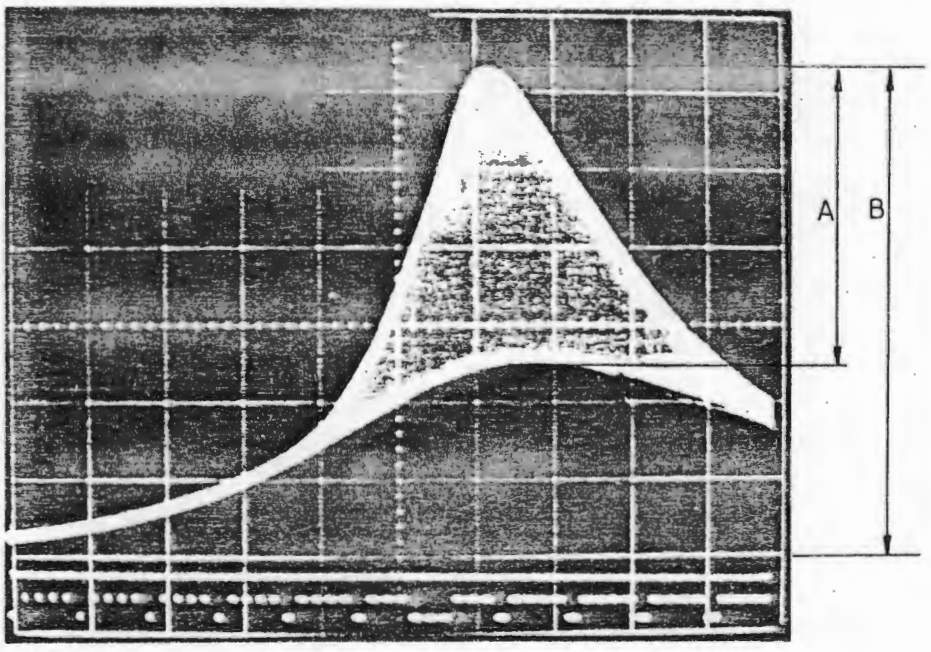

Figure 14 Typical Indicator Diagram used to determine Peak Pressure Scatter

Since the magnitude of the peak pressure does not change much over a wide range of equivalence ratios, a high value for the peak pressure scatter indicates the presence of late or incomplete combustion. When this parameter was used to assess the performance of the two ignition systems over a range of equivalence

ratios, there was no definite change in the peak pressure scatter attributable to the ignition system.

5.3 Fuel System

Different mixture preparation and induction was used for the liquid, vaporised and dissociated methanol. They will be discussed in that order.

5.3.1 Liquid Methanol

From the tank, liquid methanol passed through a measuring burette with a volume of 100 cm^3. The fuel line from the tank could be shut by means of a valve, enabling the time for the consumption of 100 cm^3 of methanol to be measured with a stopwatch. From there it passed to a conventional Solex carburettor. Methanol flow rate was adjusted by a taper needle in the fuel jet. From the carburettor, the mixture flowed along a 240 mm inlet system before entering the cylinder.

5.3.2 Vaporised Methanol

For operation on vaporised methanol, the carburettor was replaced by a transparent pyrex window. Liquid methanol from the burette passed to a centrifugal pump from which it was delivered to the vaporiser at a pressure of approximately 1,3 bar. The vaporiser is shown schematically in figure 15.

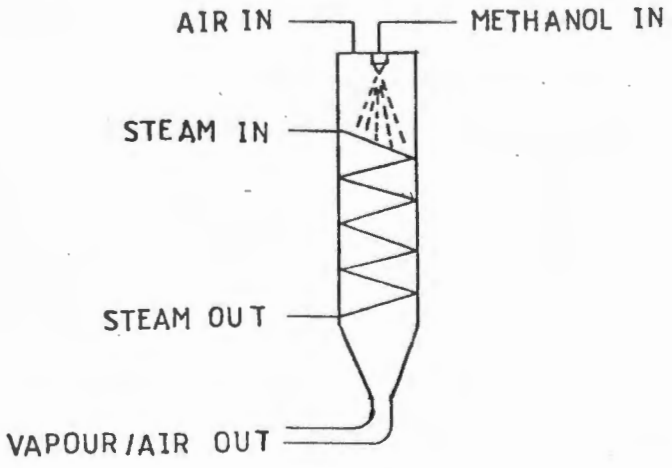

Figure 15 Methanol Vaporiser

The vaporiser was suspended alongside the air intake system with the outlet at the same height as the top of the pyrex window. Steam at a pressure of 1 bar was supplied to a heat exchanger made from 6 mm copper tubing and mounted inside the vaporiser. Methanol was sprayed into the vaporiser through a nozzle which achieved atomisation by imparting a high rotational velocity.

A pump was used to extract air from the intake, after it had passed through the flow meter, and blow it through the vaporiser. About $\frac{1}{3}$ of the air requirement of the engine was diverted in this manner. This air was used to ensure a steady supply of vapour to the engine. Without the air, the delivery pressure of the vapour was derived solely from the increase in volume accompanying vaporisation. At low flow rates this resulted in a fluctuating rate of vapour delivery.

The vapour rich air from the vaporiser was mixed with the remaining air just upstream of the pyrex window. It was thus possible to observe the condition of the vapour entering the engine. No condensation of the vapour was observed even for mixtures 30% rich. The temperature of the final mixture just upstream of the inlet valve was found to be approximately 48^{o}C which was sufficient to ensure that no condensation occurred.

5.3.3 Dissociated Methanol

For operation on dissociated methanol separate bottles of hydrogen and carbon monoxide at an initial pressure of 170 bar were used. Each gas was delivered separately from a two stage pressure regulator to an orifice plate flow meter. The delivery pressure was used to control the fuel-air ratio and in practice varied from 0,5 to 3 bar.

The flow meter was constructed in accordance with British Standards BS 1042 [50]. The orifice plate had an orifice diameter of 6,3 mm and was mounted in a PVC tube with an internal diameter of 28 mm. Even though the orifice was of the smallest permissible diameter, the flow rates for lean mixtures were so low that the resultant Reynolds numbers were off the chart of Reynolds number correction factors in the Standards. Corner tappings were selected because Reynolds

number correction factors were available for Reynolds numbers down to 10 000, whereas for D and D/2 tappings the value was 20 000.

The pressure across the orifice plate was measured with an inclined U-tube manometer filled with ethanol. The high static pressures necessary to achieve the required flow rates through the injection valve precluded the use of the conventional type of inclined manometer with a reservoir instead of a second tube. The manometer was calibrated using a precision inclined manometer at atmospheric pressure. The pressure upstream of the orifice plate was measured by means of a bourdon pressure gauge. The pressure gauge was calibrated by means of a dead-weight tester.

From the flow meter both gases flowed into a 22 l surge tank. This surge tank was used to absorb the pulsations arising from the intermittent injection of gas into the cylinder. Since the pulsations occurred 7,5 times every second with a duration of 15 msec there was no easy way to determine whether these pulsations were in fact reaching the orifice plate. If there were pulsations in the flow sufficient to cause a cyclic variation in velocity through the orifice plate, the manometer would simply respond to the root mean square velocity through the orifice. One simple test involved the replication of pressure conditions in the surge tank but with the injection valve operated manually and a rotameter fitted in the inlet line. Even opening the injection valve for an estimated period of 1/10 second produced no detectable change in flow rate measured by the rotameter. It should be noted that the maximum volume corresponding to a single pulsation was only 1/300 of the volume of the surge tank.

From the surge tank the gas passed to a rotary injection valve. The injection valve was driven off the camshaft at synchronous speed using the facility provided for a diesel pump. The valve consisted of a steel disc, rotating coaxially with the camshaft, with a highly polished face in contact with a stationary teflon disc. Contact was maintained both by means of a compression spring and gas pressure on the steel disc. A slot subtending an angle of 20° was cut in both discs and defined the injection

duration of 80 crank angle degrees. A coupling between the camshaft and the shaft carrying the steel disc enabled the crank angle at which injection started to be adjusted. Careful attention was given to the construction of the gland sealing the disc drive shaft with the result that negligible leakage was detected even with hydrogen at a pressure of 3 bar.

From the valve the gas flowed through copper tubing which entered the air inlet system upstream of the engine's inlet valve and terminated in such a manner that the gas would be injected into the cylinder once the inlet valve opened. In practice, the injection valve was set to open at approximately 30^{o} ATDC on the intake stroke. This permitted only air into the combustion chamber initially, as a measure to cool any hot spots.

An attempt had previously been made to operate the engine on a premixed hydrogen-air mixture by mixing the hydrogen with the air in the same manner as the vaporised methanol. Despite a clean combustion chamber and an extremely cold running spark plug, attempts to run the engine always terminated in a violent backfire within relatively few firing cycles. The cause of these backfires was never conclusively established but an interesting test was performed by adjusting the timing of hydrogen injection so that a premixed charge flowed into the cylinder immediately the inlet valve opened. This led to backfiring similar to that experienced previously and pointed to the fact that there must be a prominent hot spot in the combustion chamber.

A number of safety measures were adopted for operation on hydrogen and dissociated methanol:

(i) A flame arrestor was fitted in the gas line downstream from the injection valve. This prevented flame propagation down the gas line when air was mixed with the gas such as happened after the surge tank had been opened to the atmosphere for any reason.

(ii) A flap was fitted to the inlet system downstream from the air flow meter in such a manner that any increase in pressure in the inlet system, such as resulting from a backfire, would blow the flap open and rapidly

relieve the pressure, avoiding damage to the laminar flow meter.

(iii) A frangible disc was fitted to the exhaust line to relieve the pressure in the event of unburnt fuel from a misfire being ignited, for instance by a late burning cycle in which flame was still present when the exhaust valve opened.

5.4 Cylinder Pressure Measurement

Cylinder pressure measurement was accomplished by means of a piezoelectric pressure transducer mounted between the valves. The diaphragm of the transducer was flush with the cylinder head in the combustion chamber. The advantage of this was that the pressure signal obtained was free of the distortion encountered when the transducer is connected to the combustion chamber by a small bore passage. Although the pressure transducer was supplied with a calibration certificate, the calibration was verified on a deadweight tester before use.

The signal from the transducer was conditioned in a charge amplifier before being displayed on an oscilloscope. Also displayed on the oscilloscope was the output from a rotational function generator which enabled a composite pressure-crank angle diagram to be obtained on the oscilloscope.

An inductive pickup was used on the high tension ignition lead to supply an ignition signal to the oscilloscope. This was displayed as a vertical spike on the pressure curve at the crank angle at which the ignition fired. This enabled the spark advance to be read directly from the oscilloscope.

Figure 16 shows a typical pressure-crank angle diagram for operation on hydrogen. The two rows of dots indicate the crank angle at 2^{o} intervals. The cluster of three dots in the lower row is symmetrical about top dead centre. Thus it can be seen that the spark timing was set to 5^{o} ATDC. The scale on all pressure-crank angle photographs was 10 bar/div.

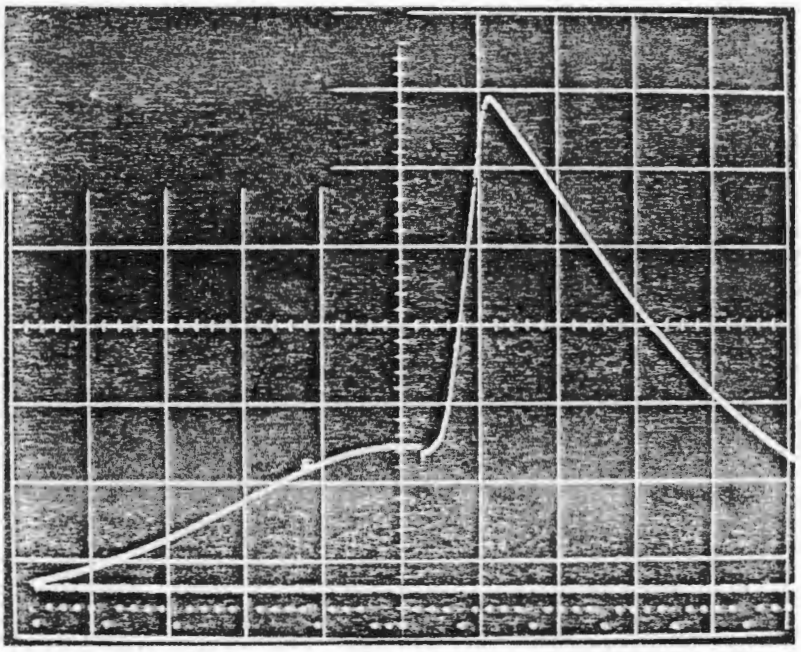

Figure 16. Typical Indicator Diagram for Operation on Hydrogen. Diagram is for a Single Cycle

5.5 Temperature Measurement

The temperatures required were those of the atmosphere, fuel-air mixture, exhaust gas and coolant entering and leaving the cylinder head.

5.5.1 Atmospheric Temperature

The atmospheric temperature was measured by an iron-constantan (iron/copper-nickel) thermocouple mounted adjacent to the air cleaner.

5.5.2 Fuel-Air Mixture Temperature

The fuel-air mixture temperature was measured by an iron-constantan thermocouple mounted approximately 60 mm upstream from the inlet valve. The thermocouple was supported on a 140 mm long PVC rod which ran along the axis of the intake system to a convenient mounting point. The thermocouple wire was carried along the PVC rod and was treated with a lacquer to

ensure that methanol did not short circuit the two wires along their length.

The mixture temperature for operation on liquid methanol was of particular interest since it would supply information from which it could be calculated how much of the methanol had been vaporised. This however posed a problem because it was clear that liquid methanol was running down the walls of the intake system and could be expected to drip onto an exposed thermocouple. The solution amounted to a crude shield: the thermocouple junction was mounted along the axis of a short piece of copper tubing which was aligned with the direction of flow. This meant that only droplets of liquid carried along in the air could reach the thermocouple.

5.5.3 Coolant Temperature

Two thermocouples were required to measure the change in temperature of the coolant flowing through the cylinder head from which heat rejected to the coolant could be calculated. The thermocouples were again iron-constantan and were inserted into the coolant stream adjacent to the cylinder head using copper tubing pockets. All exposed copper tubing was then insulated from the surroundings.

5.5.4 Exhaust Gas Temperature

The thermal energy available in the exhaust gas was of particular interest for the onboard dissociation reaction. Little published work deals with the subject. The thermal energy may be measured in a calorimeter in which the exhaust gas exchanges its heat with another fluid. Here the difficulty lies in getting the exhaust gas to the calorimeter at a temperature of 500 - 600^{o}C without loss of heat. The alternative is to measure the exhaust gas temperature and from a knowledge of its composition to calculate the enthalpy. This method was selected since the exhaust temperatures were seen as being useful in themselves.

Exhaust gas temperature measurement introduced two new problems:

(i) High absolute temperatures.

(ii) Very rapid temperature transients.

High absolute temperatures result in large heat losses from the thermocouple to the cooler surroundings. Of particular importance here is the thermal conduction along the thermocouple wires which results in heat being conducted away from the junction more rapidly than convection from the gas supplies it. The result is a measured temperature below that of the gas stream. In order to overcome this problem the thermocouple wires should be permitted to soak in the gas stream before being exposed to cooler surroundings and should be kept to the minimum diameter conversant with the life required.

The problem of transient response arises from the fact that it has been found that approximately 50% of the mass of the exhaust charge leaves the cylinder during the initial 20% of the exhaust process, a period corresponding to the blowdown phase [51]. It has also been found that the temperature during this phase shows an extremely rapid rise followed by an exponential drop [52]. These two facts together mean that much of the thermal energy in the exhaust will leave during this phase and the temperature throughout the exhaust process will have to be known if the energy in the exhaust gas is to be calculated with reasonable accuracy.

Three thermocouples were used to investigate transient response:

(i) 0,64 mm diameter chromel-alumel couple

(ii) 0,25 mm diameter iron-constantan couple

(iii) 0,13 mm diameter chromel-alumel couple

The mixture of metals was of no significance and simply reflects availability.

The thermocouples were inserted in the exhaust line immediately downstream of the exhaust valve and the outputs photographed on the oscilloscope. Figure 17a shows the result for the two chromel-alumel couples together and Figure 17b for the iron-constantan couple only. In the photographs, the lowest line

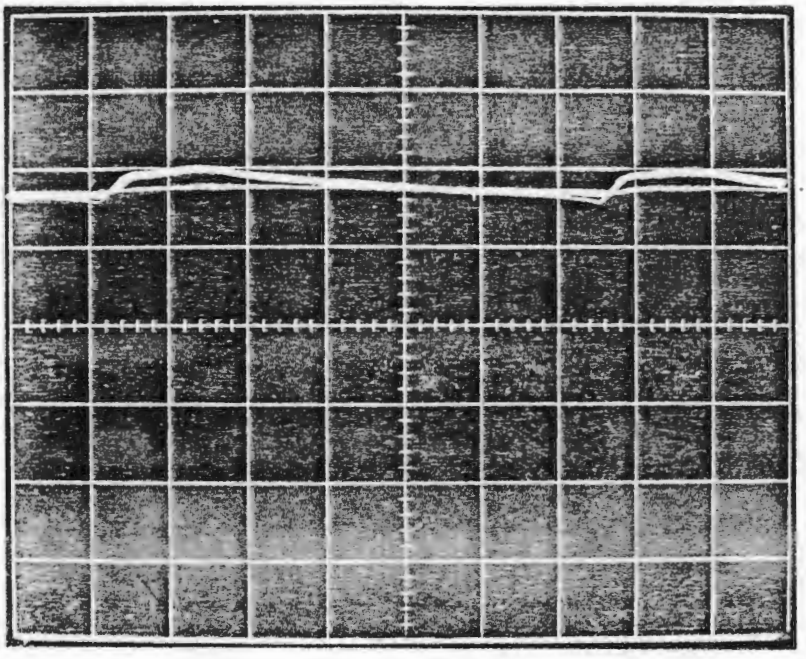

Figure 17a. Response of 0,64 mm and 0,13 mm Exhaust Thermocouples Located just Downstream of the Exhaust Valve

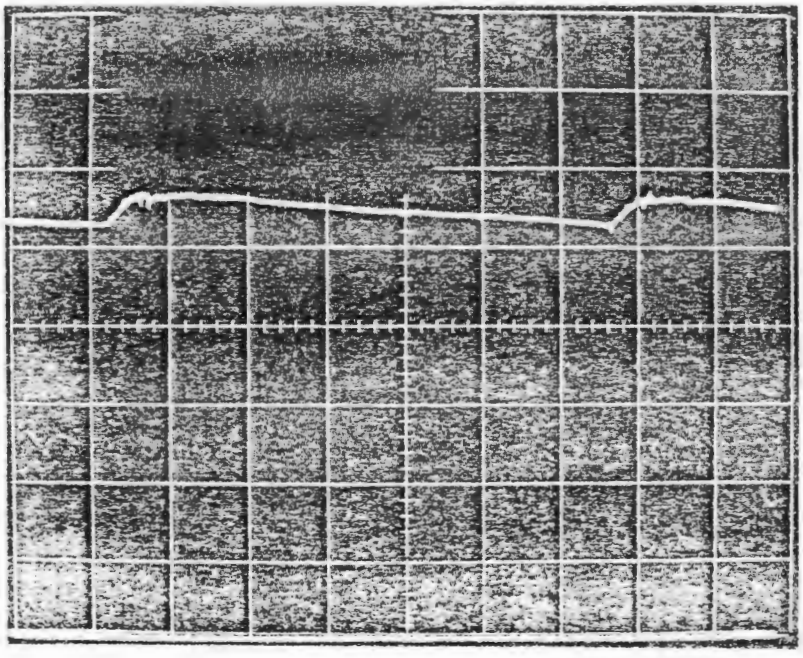

Figure 17b. Response of 0,25 mm Exhaust Thermoccuple Located just Downstream of the Exhaust Valve.

on the grid corresponds to ground potential. Both photographs were taken at the same engine speed but different fuel-air ratios. It can be seen that the large diameter chromel-alumel couple remains at a temperature close to the lowest measured by the smaller diameter one, i.e. it completely failed to detect the temperature rise at blowdown.

Both of the smaller diameter couples show a temperature difference of approximately 30°C between the highest and lowest values. Proof that these values were still too low was given by an energy balance in which indicated power and coolant heat were accurately determined. The energy balance showed that 10 - 15% of the energy available in the fuel was being lost to unaccounted sources, such as radiation. This value would normally be expected to be closer to 5%. In fact, results in the literature subsequently showed that even wire diameters of 0,05 mm were inadequate to measure half of the temperature rise above the steady state valve achieved by thicker wire [52]. Wire of 0,05 mm and smaller diameter could only be used in the exhaust gas for a few seconds before being burnt away. This would have required too much attention to be practicable.

A solution to this problem was found by using the exhaust pipe itself to create a bulk temperature that was steady with respect to time. The exhaust pipe on the engine was initially a small diameter pipe, but further along increased to three times this diameter. By carefully insulating the exhaust pipe from the point at which it emerged from the cylinder head to a distance 1,6 m downstream, it was hoped that the hot gases would exchange heat with the exhaust pipe and mix with the cooler gases to provide a uniform temperature. The pipe was insulated with insulation plaster approximately 60 mm thick and never became hotter than warm to the touch.

The 0,13 mm diameter thermocouple was inserted in the exhaust pipe about 800 mm downstream from the exhaust valve and provided an output that was invariant with respect to time. The temperature was now 100 - 120°C higher than the temperature measured simultaneously by the 0,64 mm couple at the exhaust valve. The unaccounted losses in the energy balance had now been reduced to below 5% and it was concluded that this approach was successful.

For the test programme a 0,25 mm iron-constantan thermocouple was inserted at the downstream location while the 0,64 mm chromel-alumel couple was retained at the exhaust valve. The junctions of the thermocouples were thermally insulated from the threaded plugs in which they were mounted, which were turn insulated from the cool surroundings.

5.5.5 Thermocouple Output Conversion

All thermocouple temperatures were measured by a datalogger which was capable of converting the thermocouple potentials to temperature. The thermocouples were connected directly to a single isothermal connector block which automatically compensated for the second junction formed at ambient temperature. A reference junction in an ice bath was thus not necessary. Calibration of the instrument was verified by adding a reference junction to a single thermocouple which was then used to measure ambient and exhaust temperature. Millivolt readings from the circuit with the reference junction were converted to temperature and offered reasonable agreement with the value obtained directly both for the chromel-alumel and iron-constantan thermoccuples.

5.6 Emissions Analysis

Apparatus was available for the measurement of CO, UBF and formaldehyde. No apparatus was available for the measurement of NO_x emissions.

5.6.1 CO Measurement

The sample of gas to be analysed for CO was withdrawn from the centre of the exhaust gas stream at a distance of approximately 800 mm downstream from the exhaust valve. The sample was drawn through stainless steel tubing to a condenser which cooled the sample to room temperature, the condensate being collected in a water trap. The sample then passed through silica gel drying agent and a filter to remove any particulate matter before being admitted to the nondispersive infra red analyser.

Calibration was carried out according to the manufacturer's instructions using a calibration standard of 5,2 % CO.

Calibration gas was supplied to the instrument using the same route followed by the sample after the sample line had been disconnected at the exhaust pipe. Interference from vapours of water and methanol was assessed by supplying the instrument with a sample of air saturated with water and methanol separately. In both cases there was no measurable interference.

5.6.2 UBF Measurement

UBF emissions for methanol fueling were expected to consist mainly of methanol with a small quantity of paraffinic hydrocarbons. For dissociated methanol fueling UBF should strictly include H_2 and CO together with the expected hydrocarbons. However, from the complex chemistry of combustion for hydrogen and carbon containing fuels it appears that unburnt fuel will be present in the exhaust gas as a hydrocarbon [53]. A thermal conductivity detector was not available for the gas chromatograph so that H_2 in the exhaust gas was not measured.

A nondispersive infrared analyser for hydrocarbons was available. However, since the instrument wasn't internally heated, methanol and water had to be condensed out of the sample before analysis. Even with the condenser in an ice bath, the vapour pressure exerted by the methanol removed any chance of measuring the methane concentration. The instrument was capable of measuring the hydrocarbon emissions with dissociated methanol, but this method of hydrocarbon analysis remains extremely susceptible to interference from other species in the exhaust and is seldom used today [54].

UBF is most commonly measured in a heated flame ionisation detector (FID). However, as mentioned previously, this instrument has a different response to methanol and paraffinic hydrocarbons and it is necessary to know the relative percentage of each present in the exhaust gas before accurate calibration can be attempted.

For the present investigation a gas chromatograph equipped with an FID was available, although remote from the engine. A system was developed to facilitate the storage and transportation of an exhaust gas sample. Sample bottles with a volume of 150 cm^3 were formed from pyrex tubing. A septum was fitted to an

injection port at one end and a high vacuum ground glass stopcock to the other. The sample bottles were silanized to minimise adsorption of polar molecules (such as methanol) onto the glass.

A sample was obtained by partially evacuating the sample bottle through the stopcock with a vacuum pump. The bottle was then connected to a stainless steel sample line the other end of which terminated in the exhaust gas stream approximately 160 mm from the exhaust valve. The gas temperature in the sample line was maintained at 130 - 150^{o}C by electrical heating tape. The exhaust gas sample was drawn into the bottle through the stopcock.

A syringe was then used to obtain a sample via the septum for injection into the gas chromatograph. A 2 m long, 6 mm silanized glass column was used in the gas chromatograph. The principal species the column packing was required to separate were methane, methanol and formaldehyde. A Porapak Q packing was selected on the basis of the excellent results reported by Pefley [14] for Porapak T, but with the advantage of more favourable separation for the thermal conductivity detector being used at that time. The FID response was then calibrated separately for methane and methanol.

5.6.3 Formaldehyde Measurement

Formaldehyde was expected to be the predominant aldehyde present in the exhaust gas. Because formaldehyde is more reactive than the other exhaust species of interest, it is necessary to have some knowledge of the reactions it may undergo at the temperatures encountered. The following discussion is based on reference [35].

Both liquid and gaseous formaldehyde polymerise readily at ordinary temperatures and can be kept in pure monomeric state only for a limited time. Dry formaldehyde gas shows no polymerisation at 80 - 100^{o}C. However, even a trace of water provokes rapid polymerisation. Formaldehyde gas 90 - 100% pure must be kept at 100 - 150^{o}C or above to avoid polymerisation. In aqueous solution, dissolved formaldehyde is present as an equilibrium mixture of the monohydrate and a series of low molecular weight polymeric hydrates. Commercial formaldehyde

is generally sold as formalin. Formalin contains 37% formaldehyde by weight and 8 - 15% methanol which prevents polymerisation.

The first attempts to detect formaldehyde in the exhaust gas were made on the gas chromatograph while a sample was being analysed for UBF. Methane and methanol were detected in that order, but only a relatively slight baseline drift developed from the retention time for formaldehyde, figure 18a. The baseline had already been corrected for column bleeding during temperature programming.

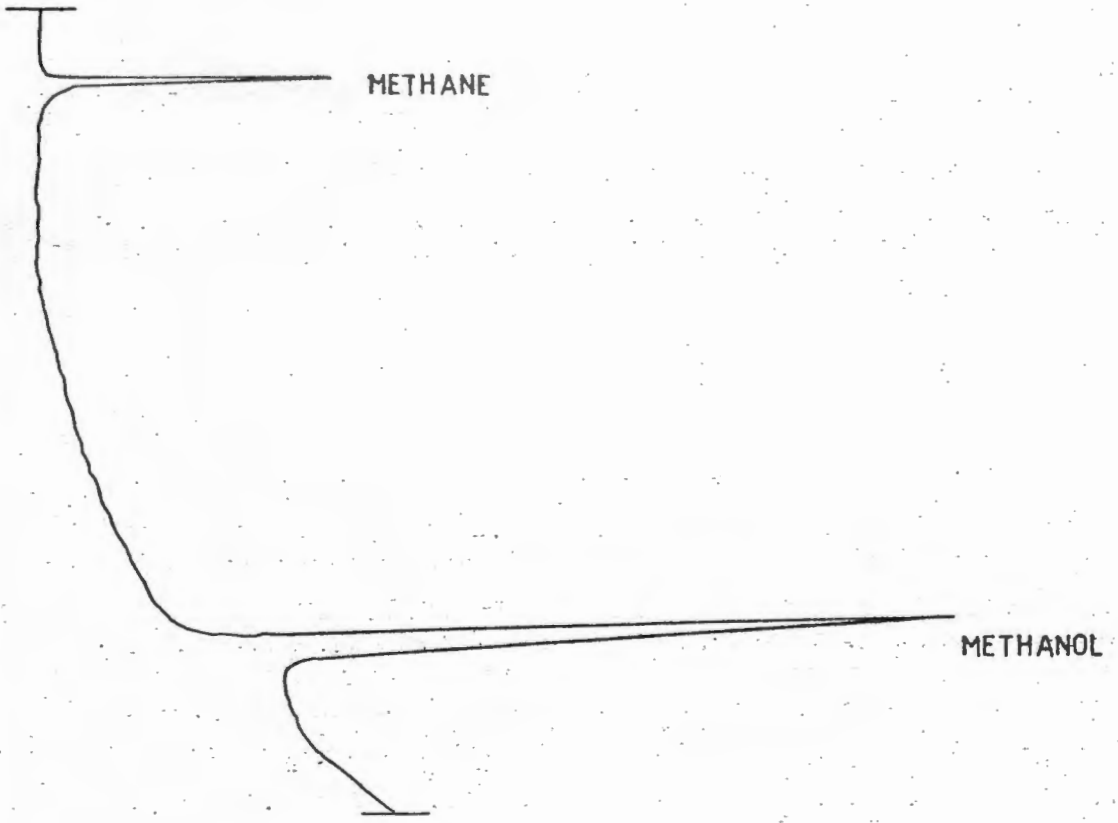

Figure 18a. Exhaust Gas Chromatogram

By contrast, in a sample of formalin distinct peaks for formaldehyde and methanol were obtained, figure 18b. The amount of formaldehyde in this sample was calculated to be equivalent to a gas sample when the exhaust gas had a formaldehyde concentration of 200 ppm. Already some tailing of the formaldehyde peak is evident, probably due to adsorbtion. Formaldehyde is an extremely polar compound and may be expected to be adsorbed onto a conventional column packing. However, Porapak is a porous polystyrene polymer, fabricated into beads which should not adsorb polar compounds [14]. In addition

to this, the column itself had been silanized.

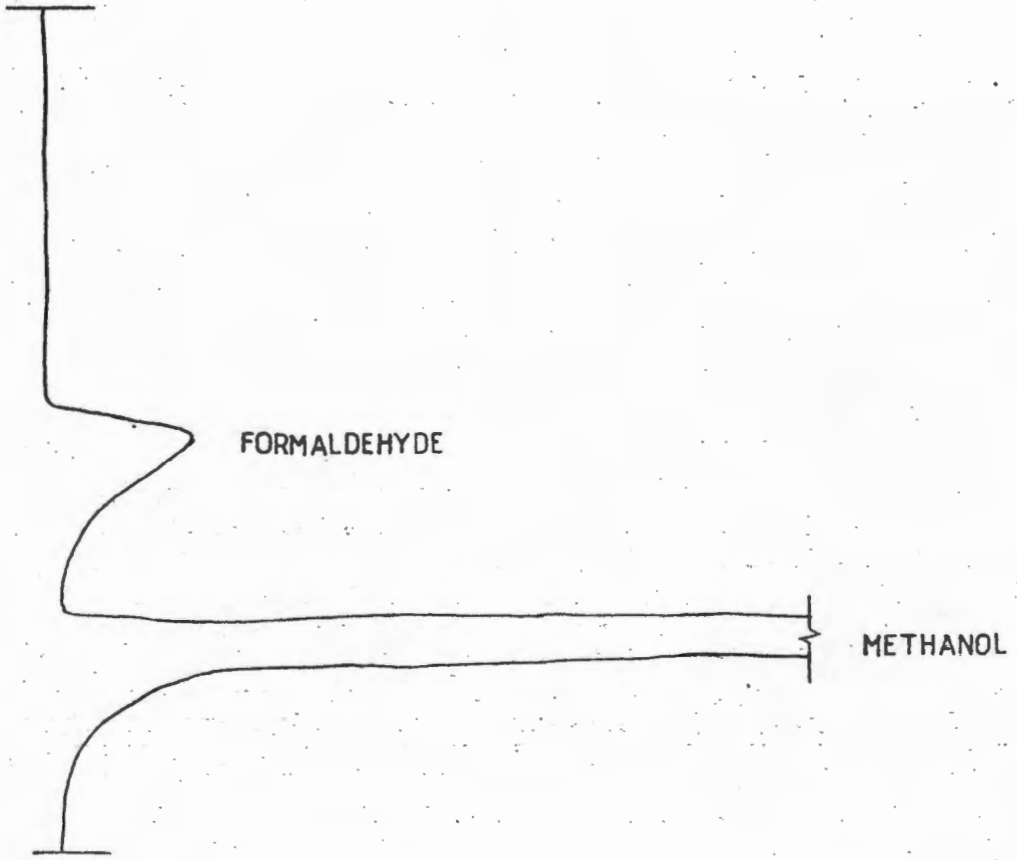

Figure 18b. Formalin Chromatogram

The next step was to install an impinger by means of which the exhaust gas could be bubbled through a liquid. The impinger was installed at the same point where UBF samples were collected from the heated sample line. The insulation of the exhaust pipe had raised the gas temperature to above 500°C for a distance of 1,6 m downstream from the exhaust valve. As has already been mentioned, reactions involving methanol and formaldehyde will be active at this temperature. Thus formaldehyde and UBF emissions measured some distance downstream will not be representative of these emissions with an air cooled exhaust pipe. For this reason the sample was withdrawn just 160 mm downstream from the exhaust valve and the insulation was not expected to influence the temperature significantly over such a short distance.

The impinger consisted of a No. 1 frit in a 38 mm flask. The exhaust gas was drawn through the impinger by a rotary vacuum pump. The flow rate was measured by two rotameters - one for low flow rates and the other for high flow rates. The rotameters were calibrated with exhaust gas by adding a wet test meter to

the sample line.

This apparatus was first used to bubble the exhaust gas through distilled water, since distilled water has been found to have a high collection efficiency for formaldehyde [34]. The aim was to increase the concentration of formaldehyde and investigate its effect on the chromatogram. The result was a considerable baseline drift, commencing at approximately the retention time for formaldehyde and continuing past the methanol peak.

Now, any formaldehyde that was in the exhaust gas would exist predominantly in the polymerised form in both of the above methods. Thus it was suspected that the polymers of formaldehyde did not alute as a distinct peak or even as a series of peaks. In order to test this hypothesis, a sample of paraformaldehyde was thermally depolymerised, the formaldehyde gas so evolved being bubbled through distilled water. When a sample of this solution was analysed on the gas chromatograph, the now characteristic baseline drift was observed.

It was assumed that the formaldehyde entering the impinger was still the monomer, since the sample line was heated to 130 - 150^{o}C. Thus a solution of 15% methanol in distilled water was prepared and exhaust gas bubbled through this. When a sample of this solution was analysed on the gas chromatograph, still no formaldehyde could be detected. As a result of these tests it appears reasonable that polymerisation was occuring prior to the impinger, probably due to the presence of water vapour in the exhaust gas.

These tests showed that there is no simple method available to measure formaldehyde on a gas chromatograph. The next step was to assess the various wet chemistry techniques available.

The chromotropic acid method was rejected because it measured exclusively formaldehyde. While this is adequate for liquid methanol fueling, the position is less clear for dissociated methanol. The results of a comparative study have shown that there is no clear distinction between the performance of the DNPH and MBTH methods when used to measure total aldehydes in methanol fueling [34]. The DNPH method has the advantage of

being able to quantify the various aldehydes present with suitable processing of the hydrazones. However, the MBTH method was the most commonly used in the investigations reviewed. In addition, the MBTH method had already been used by the Energy Research Institute of the University of Cape Town and suitable hardware developed.

The original MBTH method was developed by Sawicki in 1961 [55]. Various modifications have been proposed to increase sensitivity and reduce interference. The most significant of these appears to be the addition of sulphamic acid to reduce interference from SO_2, proposed by Nebel [56]. This method was used in the present investigation. The absorbance was measured at 635 nm with a spectrophotometer.

The greatest sensitivity of the absorbance measurement is achieved at mid-scale on the spectrophotometer. This meant that the volume of the exhaust gas to be drawn through the impinger was effectively fixed for a given type of fuel and the flow rate and sampling duration had to be adjusted to match this value. High flow rates were undesirable because of reduced collection efficiency while long sample times were vulnerable to drift in engine conditions.

Once the approximate sample volume had been established various combinations of sample flow rate and time were examined for their effect on repeatability. From these tests it appeared that repeatability was dependent on the method used in handling the impinger between collections rather than on flow rates. It appeared that formaldehyde rich condensate was forming in the impinger downtube between tests. This was responsible for erratic results when the condensate was washed into the MBTH solution. Washing the impinger in distilled water between tests overcame this problem.

In practice the flow rate was adjusted to offer convenience of operation. Of necessity this was approximately $4\frac{1}{2}$ times higher for dissociated methanol than for liquid or vaporised methanol, because of the extremely low concentration of formaldehyde and the need for short sampling times to conserve fuel.

The repeatability of the MBTH method itself to measure formaldehyde was assessed by processing 5 samples obtained from the same parent solution. The results agreed to within the resolution of the spectrophotometer.

Calibration was performed by adding known amounts of formaldehyde tc the MBTH solution and then processing as for the exhaust sample. Details are contained in Appendix E. The formaldehyde was used in the form of formalin, the formaldehyde content of which was assayed by a commercial laboratory in a sodium bisulphite titration.

Methanol was present in both the calibration and exhaust gas samples, the concentration being many times higher in the exhaust gas than in the formalin. As a result, the effect of methanol at a concentration of 10 000 ppm in the exhaust gas was investigated during calibration tests. No measurable interference was observed.

The next chapter will discuss the actual experimental procedure followed.

6. EXPERIMENTAL PROCEDURE

This Chapter deals with the specific procedure followed in the laboratory.

6.1 Engine Operation

6.1.1 Engine Constants

The investigation of the potential of dissociated methanol was carried out under the following conditions, considered to be representative of performance in a reciprocating internal combustion engine.

(i) Engine speed of 900 rpm. The majority of single cylinder engine tests are conducted at 900 - 1200 rpm. In addition, the cost of the bottled gases dictated that fuel consumption should be a minimum at a given fuel-air ratio.

(ii) Compression ratio of 8. This was again representative of many single cylinder engine tests.

(iii) Wide open throttle. It has been shown that at least the relationship between equivalence ratio and efficiency is little affected by load [17].

(iv) MBT spark timing. Spark timing other than MBT is generally only used to investigate its effect on certain emission species.

The present work was not concerned with the effect of these parameters on efficiency and exhaust emissions. However, the effect on engine performance of compression ratios of 8, 12 and 14 was investigated for liquid methanol. A compression ratio of 14 was selected as the highest useful compression ratio since it was found to be the point above which increasing compression ratio had little effect on indicated efficiency.

6.1.2 Mixture Preparation

The electrical resistance heater in the intake system was used to investigate the effect of air preheat on engine performance when fueled on liquid methanol. In the literature, air preheat is generally employed to improve mixture preparation with methanol even when exhaust emissions are not of interest.

The amount of heat supplied to the air was kept constant for all fuel-air ratios. This resulted in the free stream temperature for lean mixtures being about 8°C higher than for rich mixtures. The alternative, adjusting the amount of pre-heat to maintain constant mixture temperature, required inordinately long stabilisation times because of the slow response of mixture temperature to preheat.

Air preheat of 300 W and 1000 W was tested. The former provided free stream temperatures comparable to those of vaporised methanol, with a mean mixture temperature of 48°C, although from the cold intake walls it was concluded that a fair amount of methanol remained unvaporised. The latter (1000 W) provided the maximum preheat available with a mean mixture temperature of 118°C. Under equilibrium conditions, this preheat was sufficient to ensure complete vaporisation.

6.1.3 Spark Timing

It has already been mentioned that the crank angle at which the point of inflexion in the pressure-crank angle diagram occurs may be used to optimise spark timing and should then be between 5° and 20° ATDC.

A series of tests were conducted to investigate the relationship between the crank angle at which peak pressure occured and the indicated power at a constant fuel-air ratio. Figure 19 shows the results for liquid methanol at a compression ratio of 12. Note that the efficiency and torque will be directly proportional to the power. The cyclic variation in pressure development meant that the crank angle corresponding to peak pressure had to be averaged by eye. By using the storage facility of the oscilloscope, the variation in this angle was estimated to be $\pm$ 2°, except near the lean limit, where the variation became significantly greater.

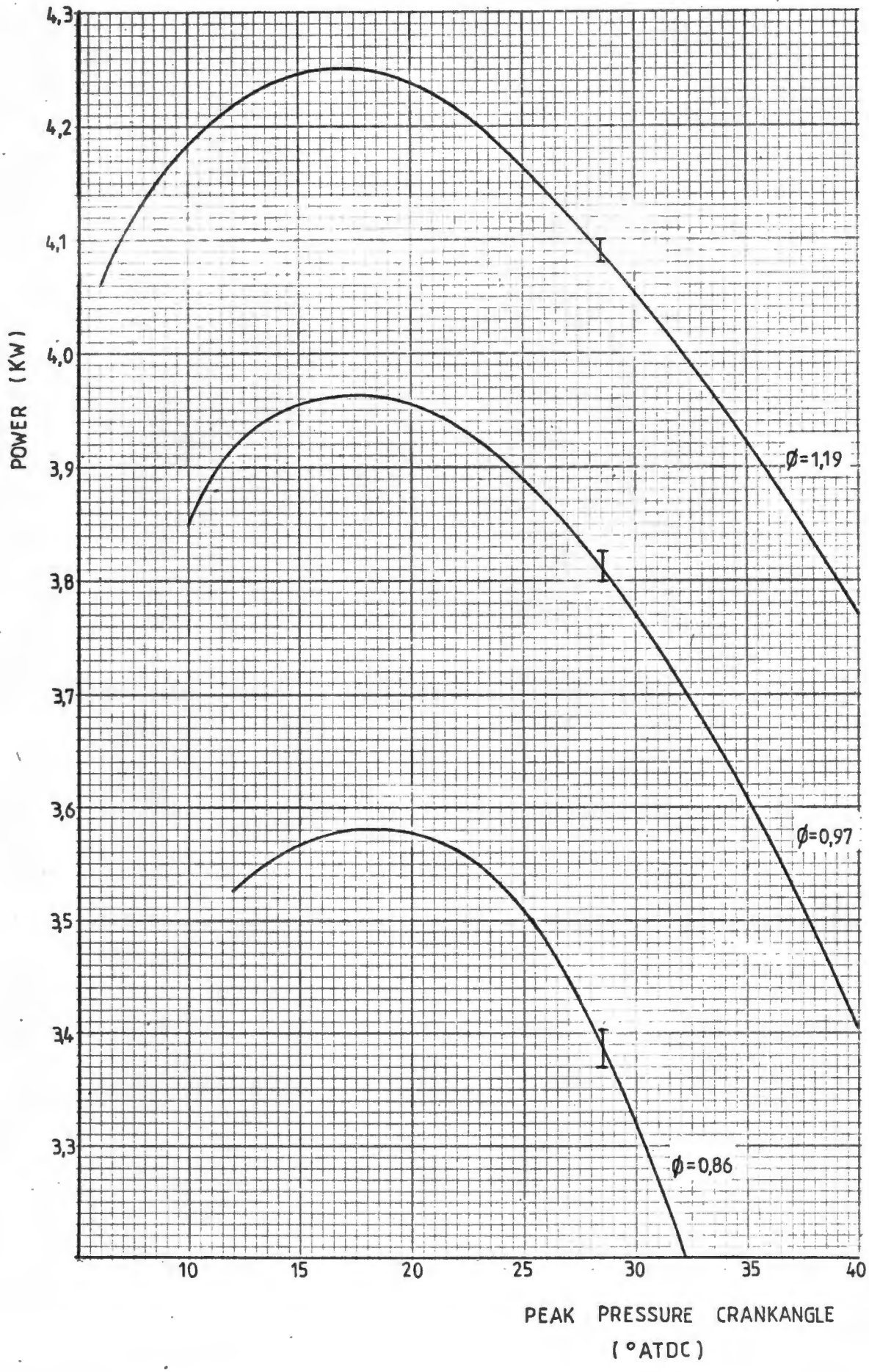

Figure 19. Effect of Peak Pressure Crankangle on Power for Three Equivalence Ratios

Figure 19 shows that the concept of there being a plateau in the efficiency versus spark timing curve to be valid. Hence "minimum advance for best torque" or MBT spark timing may be realised. However, variation in the peak pressure crank angle over the range of fuel-air ratios is about the same magnitude as the difference between minimum advance for best torque and simply the advance for absolute maximum torque. Hence it appears that the concept of a minimum advance is not really applicable here, but will be used to indicate that spark timing was adjusted to give peak pressure at a crank angle of 18^{o} ATDC.

This test was repeated for vaporised methanol and hydrogen and in each case a peak pressure crank angle of 18^{o} ATDC was found to be close to maximum torque.

6.1.4 LML Detection

For the purpose of the present investigation the lean misfire limit was defined as the equivalence ratio at which approximately 0,5 - 1,5% of the cycles were motored.

Detection of the LML was accomplished with the aid of the pressure-crank angle diagram. The first stage was to detect that a misfire had occured. The second stage was to determine the frequency of misfire.

Figure 20a is a typical indicator diagram obtained on reducing the fuel flow at constant speed. The lowest curve was a motored cycle since it is symmetrical about top dead centre (the crank angle marker is blurred by speed fluctuations) and the peak pressure thus occurs before that of even a bulk quenched cycle. By increasing the time base of the oscilloscope figure 20b is obtained, in which the vertical lines correspond to the peak pressures of each cycle. In this way 78 consecutive cycles can be examined at one time. The motoring cycles were known to have a height of two divisions after comparison with the trace obtained when the spark plug was short circuited.

The fuel flow rate could then be finely adjusted until successive diagrams like figure 20b just showed one misfire. In reality,

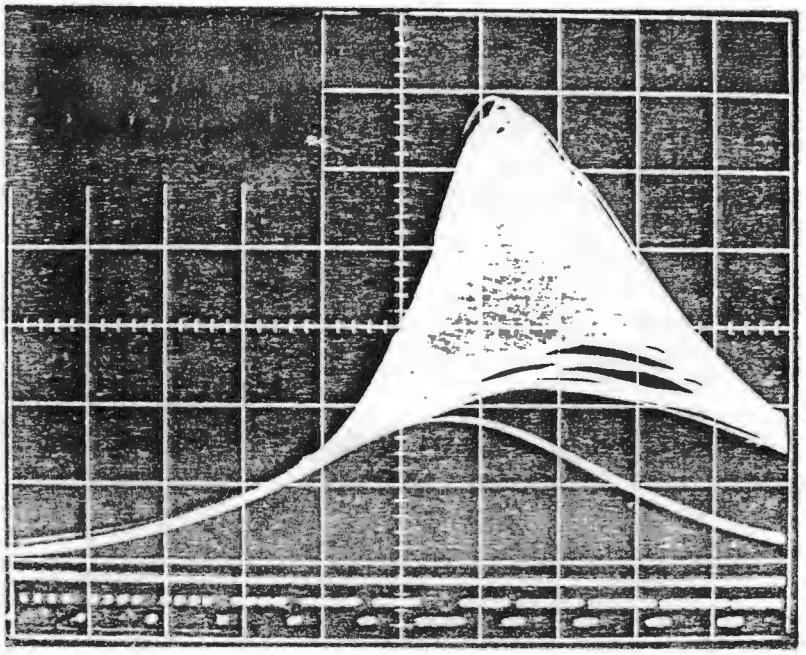

Figure 20a. Typical Indicator Diagram Used to Determine the Presence of a Misfire

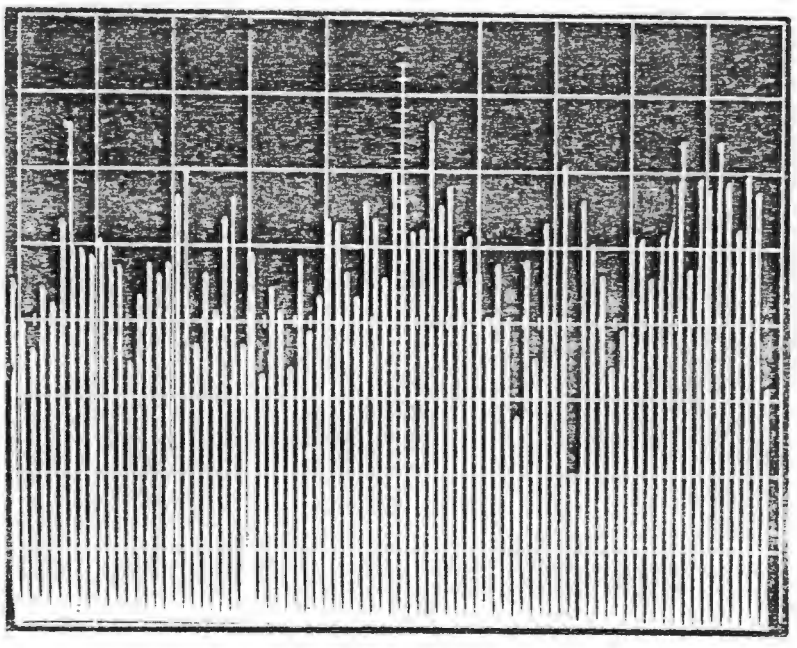

Figure 20b. Typical Indicator Diagram Used to Determine the Frequency of Misfire

this would have been closer to one misfire every 156 cycles. At this mixture strength engine operation remained steady over a period of several minutes, although there was a detectable but momentary loss of speed accompanying each misfire. The results also showed that the efficiency versus equivalence ratio curve was fairly flat at this point and did not show the rapid drop associated with frequent misfires.

6.1.5 Test Procedure

Prior to beginning the test programme, the engine was overhauled in accordance with the manufacturer's instructions. The combustion chamber was cleaned of all deposits and the clearance volume measured to enable accurate determination of the compression ratio from the micrometer reading.

The electric oil heater was used to bring the oil close to operating temperature before starting. The engine was then started by motoring, the motor being switched to load once combustion was sustained. The engine was warmed up until both coolant and oil temperatures had stabilised at approximately 70^{o}C and 60^{o}C respectively. This warm up phase lasted at least one hour and was accomplished with liquid methanol when dissociated methanol was being tested in order to conserve gas.

The fuel-air ratio could be set approximately by observing a rotameter in the methanol delivery line. With dissociated methanol the hydrogen and carbon monoxide pressure regulators had to be adjusted until the manometers indicated the required 2:1 flow rate. Tests were conducted over the full range of fuel-air ratios from LML to 30% rich.

Next the spark timing was adjusted to give peak cylinder pressure at 18^{o} ATDC and the field current adjusted to give an engine speed of 900 rpm.

Exhaust gas temperature measured by the downstream thermocouple required an excessive amount of time to stabilise. However, a linear relationship was found between this temperature and the temperature measured by the thermocouple adjacent to the exhaust

valve and in subsequent tests measurements were made using the upstream thermocouple and converting them to the correct value. The linear relationship was effectively the same for all fuels used.

Coolant temperature difference then became the parameter which required the longest stabilisation time. The difference in coolant temperature between cylinder head inlet and outlet was monitored and once this had stabilised the test could begin. All measurements at a given condition were repeated until agreement was satisfactory and values were then averaged.

At the end of the test session the fuel supply was cut off, the dynamometer switched to motor and the friction losses measured. Over the whole test period, friction losses only varied by about 4%.

6.2 Emissions Measurement

6.2.1 CO Emissions

CO Emissions were measured continuously and an almost immediate response to changes in engine conditions was observed. The only attention the CO analyser required was periodic calibration. The primary calibration was performed using the standard calibration gas and clean air. Secondary calibration could then be performed electronically. Experience showed that primary calibration was necessary only weekly, while secondary calibration was performed before each test session and checked at the end of each session.

6.2.2 UBF Emissions

The sample bottles used for UBF collection were washed with acetone and then purged with clean air before use. A vacuum pump was used in conjunction with a mercury manometer to reduce the bottle pressure to about 70 kPa. The bottle was then connected to the heated sampling line and the exhaust gas drawn in. The samples were stored in bottles for 2 - 3 hours before analysis on the gas chromatograph. Analyses could be performed a minimum of 10 minutes after collection and it was found that

no change could be detected in the sample composition after this period. Thus the 2 - 3 hour delay before analysis was considered acceptable.

A precision syringe was used to inject 0,3 ml of the contents of the sample bottle into the gas chromatograph. The column temperature was optimised for the separation of methane and methanol: following injection of the sample the temperature was held at 50°C for 1 minute, followed by a temperature rise of 20°C/min. until 120°C was reached and held for 4 minutes. The gas flow rates to the chromatograph were as follows:

(i) nitrogen carrier gas - 50 ml/min

(ii) hydrogen for FID - 30 ml/min

(iii) air for FID - 300 ml /min

A typical chromatogram is shown in figure 21. The chromatogram was analysed by means of an on-line computer. The area of the peaks was automatically calculated by the rule of trapezoids (Newton-Cotes two point formula). Note that the peaks are plotted to different scales in the chromatogram.

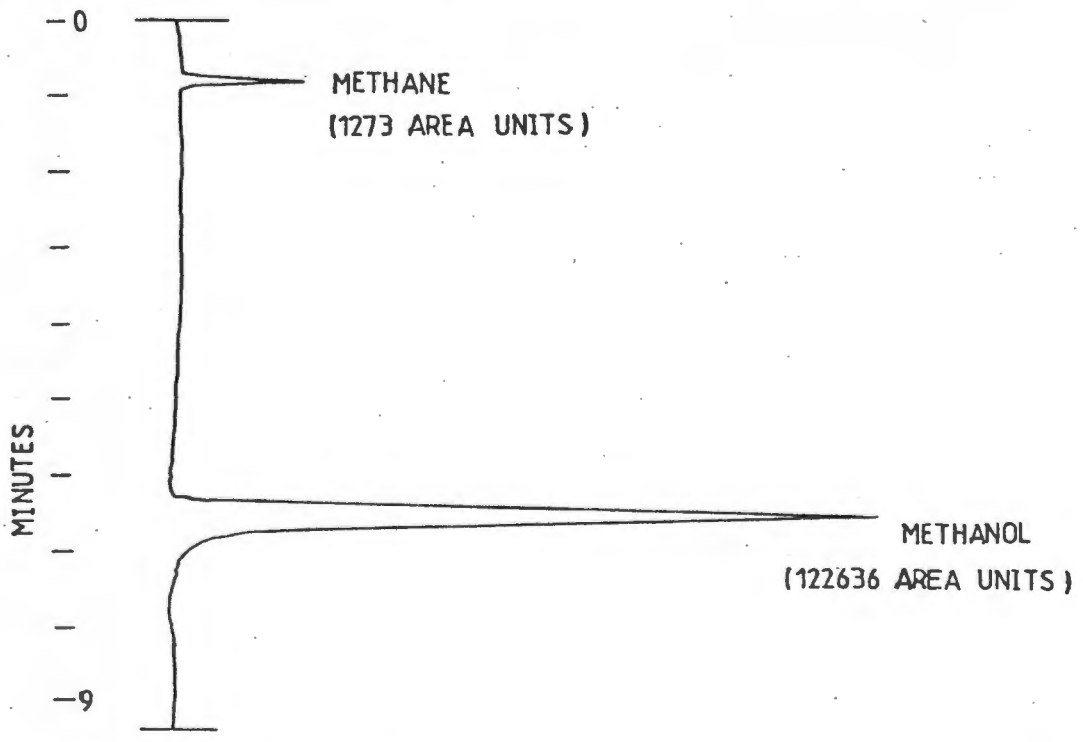

Figure 21. Typical Chromatogram for Methane and Methanol

The computer had the facility to store the results of a blank run (no sample injected) as a baseline and then to subtract this baseline from the sample chromatogram before plotting. Following conditioning of the column, a blank run yielded a nearly flat baseline. On injection of a sample, baseline drift was experienced from approximately the time formaldehyde was expected to elute. This was not really a problem since baseline interpolation for the peaks was correctly performed by the computer. Following the first sample run, another blank run was performed, again showing baseline drift probably due to the presence of adsorbed formaldehyde polymers. Since the amount of baseline drift did not increase much with successive samples, the result of this blank run could be stored as a new baseline. Subsequent chromatograms using this baseline had much reduced drift.

Using the calibration data in Appendix E, the area units under the peak could be converted directly into concentrations.

6.2.3 Formaldehyde Emissions

The MBTH method used follows that proposed by Nebel [56]. The MBTH reagent and ferric chloride solution were both used on the same day that they were prepared. 20 ml of MBTH reagent was used in the impinger.

Initially, two impingers in series were used. However, the formaldehyde collected in the second impinger was less than 1% of that collected in the first impinger with liquid and vaporised methanol fueling. Since higher flow rates were used for dissociated methanol this test was repeated then. In this case the formaldehyde in the second impinger was below the detection threshold. Thus it was considered reasonable to use a single impinger for all the tests and no correction was made to the results obtained. The sample volumes, together with the sampling times, were as follows:

(i) liquid methanol : 6 l /4 min

(ii) vaporised methanol: 6 l /4 min

(iii) dissociated methanol: 14 l /2 min

Exhaust gas was drawn through distilled water in the impinger between tests. A three-way valve enabled the vacuum pump to be kept running continuously and the time during which exhaust gas passed through the MBTH solution to be measured accurately.

A 1 ml aliquot from the impinger was processed in a volumetric flask. The absorbance was measured with a spectrophotometer within 2 - 3 min. of adding the acetone. The absorbance was converted directly to concentration using the calibration in Appendix E.

7. RESULTS OF EXPERIMENTAL WORK

7.1 Content of Results

Certain performance parameters of the engine were seen as contributing to knowledge of the combustion characteristics of the fuels. Measurement of the following parameters was made with that object in view:

(i) indicated efficiency

(ii) indicated power

(iii) heat in exhaust gas

(iv) heat in engine coolant

(v) exhaust gas temperature

(vi) combustion duration

(vii) peak pressure scatter

(viii) carbon monoxide in exhaust gas (strictly, this belongs under emissions)

The effect of compression ratio, air preheat and fuel type on these parameters was investigated. Compression ratios of 8, 12 and 14 were investigated with no preheat and liquid methanol. Air preheat of 0,300 and 1000 W was investigated at a compression ratio of 8 with liquid methanol. Liquid, vaporised and dissociated methanol, together with hydrogen and carbon monoxide fuels were investigated at a compression ratio of 8.

Three exhaust emission species were identified as being of importance either with respect to combustion efficiency or pollution:

(i) methane

(ii) methanol

(iii) formaldehyde

The effect of liquid, vaporised and dissociated methanol fueling on these species was investigated.

7.2 Processing of Results

An outline of the method used to calculate the various terms in the energy balance is provided in Appendices A and B. The complete set of results for the performance parameters from 191 individual tests is tabulated in Appendix C.

The results for the various emissions species are tabulated in Appendix F.

7.3 Data Reduction

The results of the experimental work related the dependent variable to the independent variable through, on average, 20 data points. Plotting the data points alone was not sufficient to indicate a clear, unambiguous relationship and it became clear that it was necessary to obtain a regression of the measured variable against the independent variable. Curve fitting by eye was rejected because of its subjective nature.

Ultimately, second order polynomial least squares regression was used for the majority of the curves, excluding CO emissions and peak pressure scatter. One standard error of the estimate was represented by an I at a convenient point on the curve. The details of the data reduction are contained in Appendix G.

7.4 Precision of Results

The precision of results is a measure of agreement between repeated determinations of the apparent result, the actual result being constant. The standard error of the estimate was used to indicate the overall precision of the results and whether differences in the measured variables between fuels were significant or trivial. There was evidence that the efficiency curve did not repeat exactly on different days, so the individual effects of rapid changes or incorrect measurements of friction losses and atmospheric pressure and temperature were investigated for stoichiometric operation on methanol.

A difference of two divisions in the balance reading for motoring load (equivalent to 2 oz.) resulted in efficiency changing by 0,6% of its original value. A difference of 10 mm in the barometer reading resulted in efficiency changing by 0,3% if still plotted for stoichiometric conditions. Similarly a change of $2^{o}C$ in the ambient temperature resulted in a 0,3% change in efficiency. If all three of these changes occured undetected and the effects were additive, then the indicated efficiency would be $33,2 \pm 0,4\%$. This is a most unlikely condition and indicates that these parameters alone were not responsible for the variation in efficiency.

For operation on bottled gas, the flow measurement by orifice plate was less accurate (not as near the actual value) than timing the volume flow of methanol. The maximum tolerance on the flow rate measured by the orifice plate within which the true value was expected to be was estimated at 2,6% using the methods of BS 1042 [50]. For methanol, this value was less than 1%.

7.5 Presentation of Results

The most important decision in the presentation of the results was the selection of the independent variable for comparison of the results from different fuels. The choice lay between indicated power and equivalence ratio. For example, should efficiencies be compared on the basis of equal power or equivalence ratio? Equivalence ratio was selected as the independent variable because loss of power accompanying operation on gaseous fuels or at lean mixtures can easily be compensated for by increasing swept volume or turbocharging.

The equivalence ratio is defined as the actual fuel-air ratio divided by the stoichiometric fuel-air ratio.

The efficiency and exhaust and coolant energy are presented as a percentage of the net energy in the fuel.

Exhaust emission species were presented on a concentration basis, since the loss in power with operation on dissociated methanol was accompanied by a corresponding decrease in the

number of moles of exhaust gas.

The effect of compression ratio on selected performance parameters of the engine is given in figures 22 - 27. The effect of air preheat on selected performance parameters is given in figures 28 - 34. The effect of fuel type on performance parameters is given in figures 35 - 43. Figure 42 shows the efficiencies that could be expected if waste heat was used to vaporise or dissociate the fuel, that is, the calorific value of the fuel was considered to be that of liquid methanol in all cases.

Figures 44 - 46 show the effect of fuel type on emissions. It should be noted that for dissociated methanol fueling, methanol emissions were below the detection threshold of 10 ppm and formaldehyde was at all times less than 1 ppm.

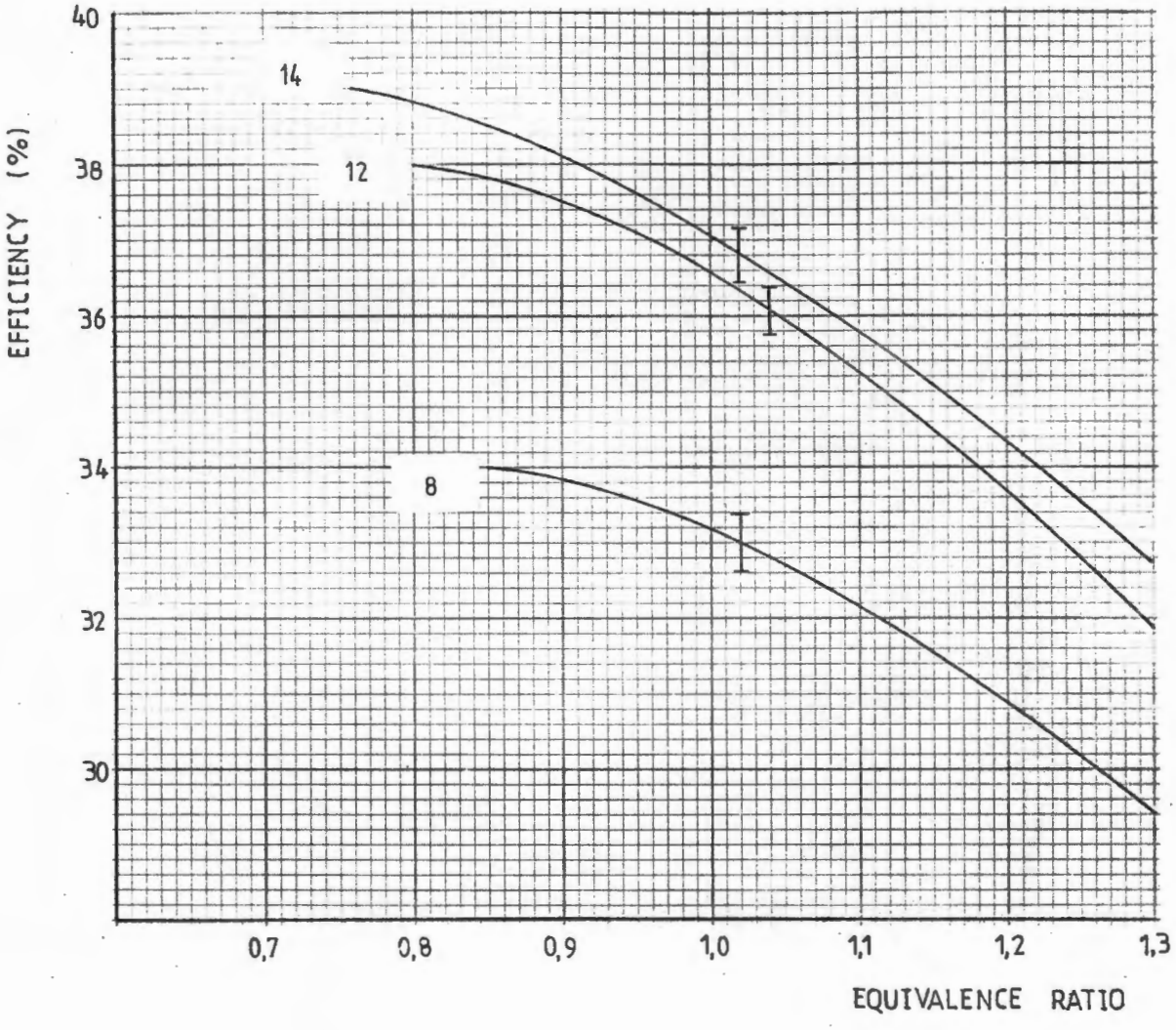

Figure 22. Effect of Compression Ratio on Efficiency

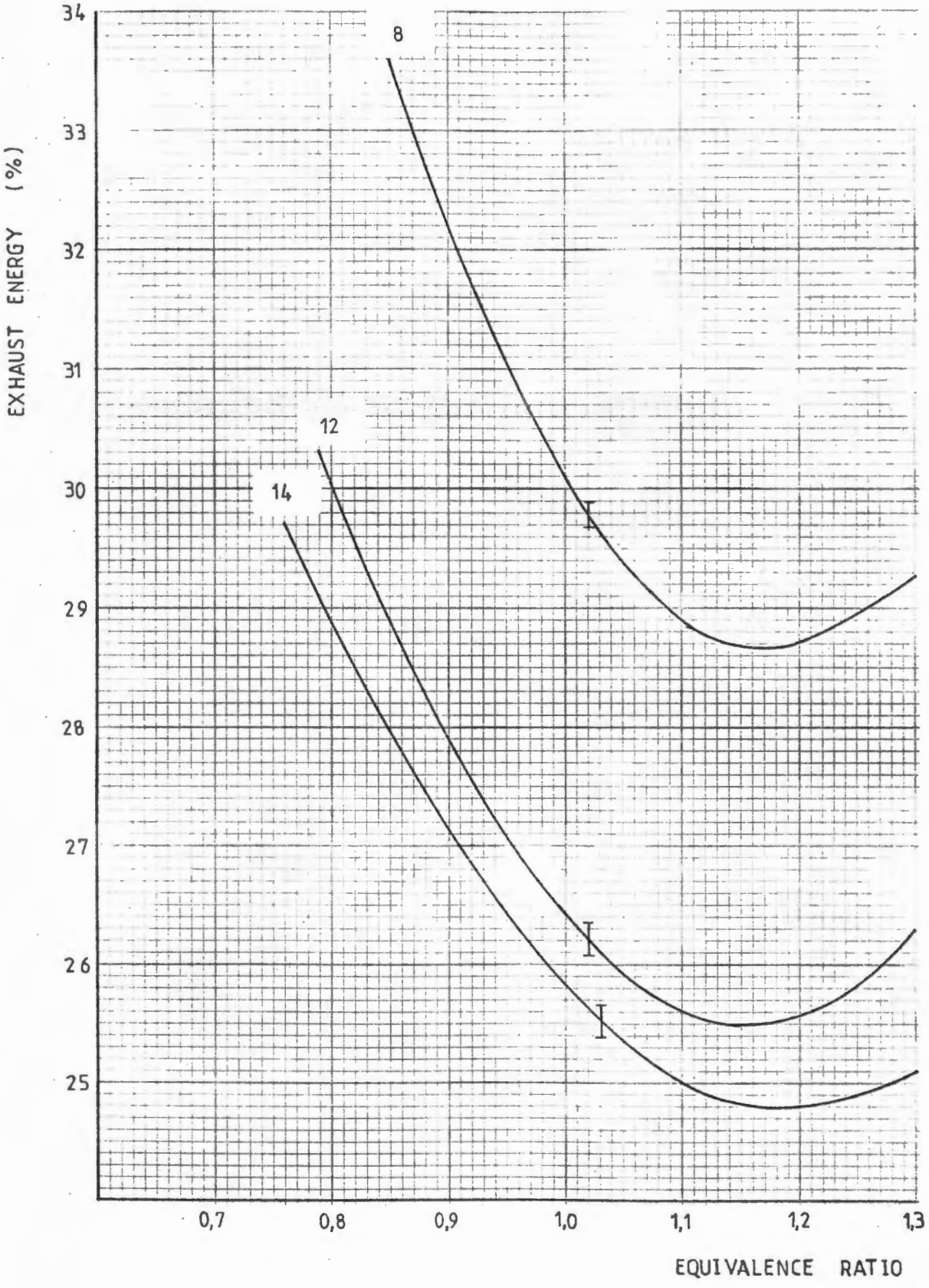

Figure 23. Effect of Compression Ratio on Exhaust Energy

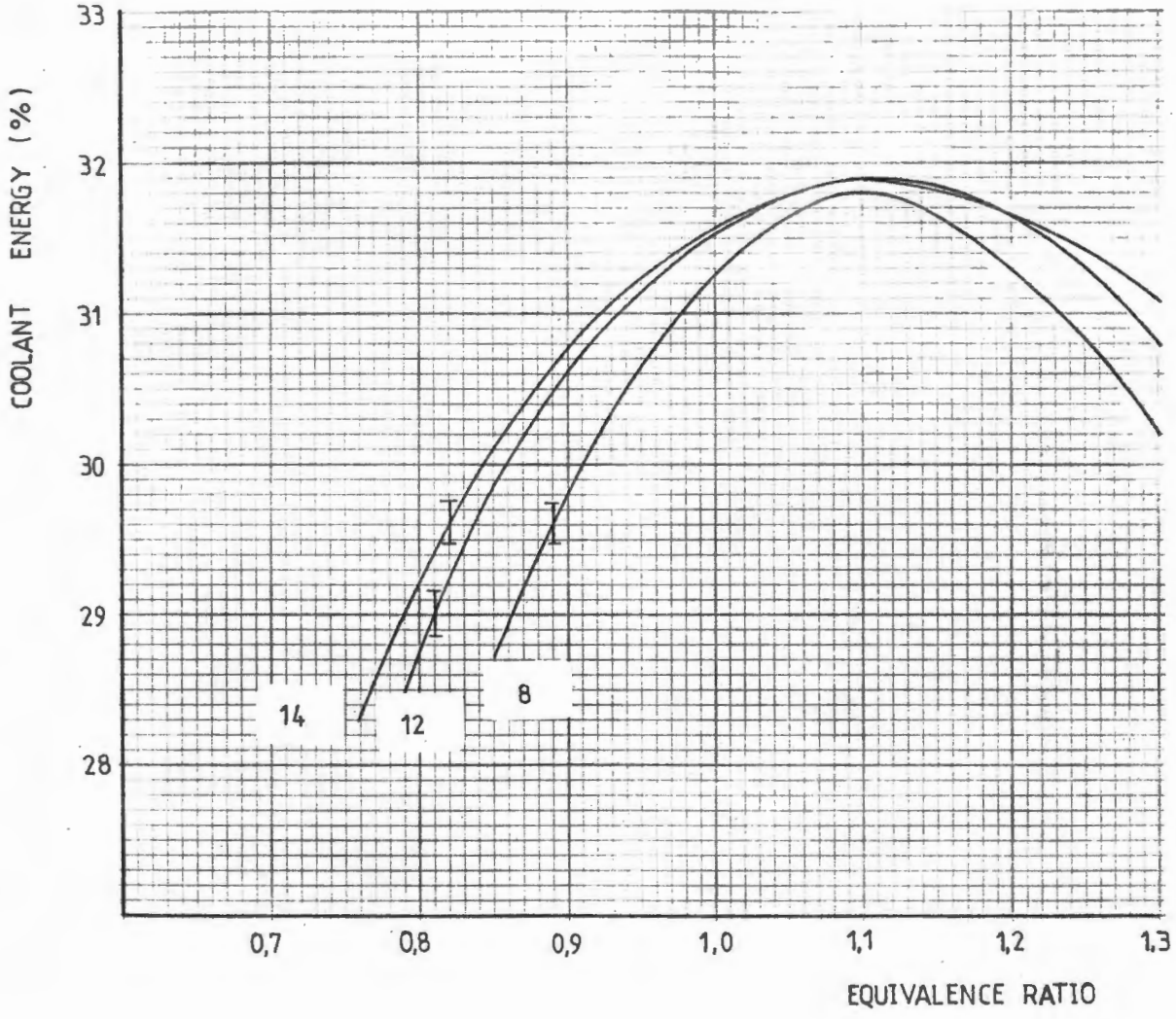

Figure 24. Effect of Compression Ratio on Coolant Energy

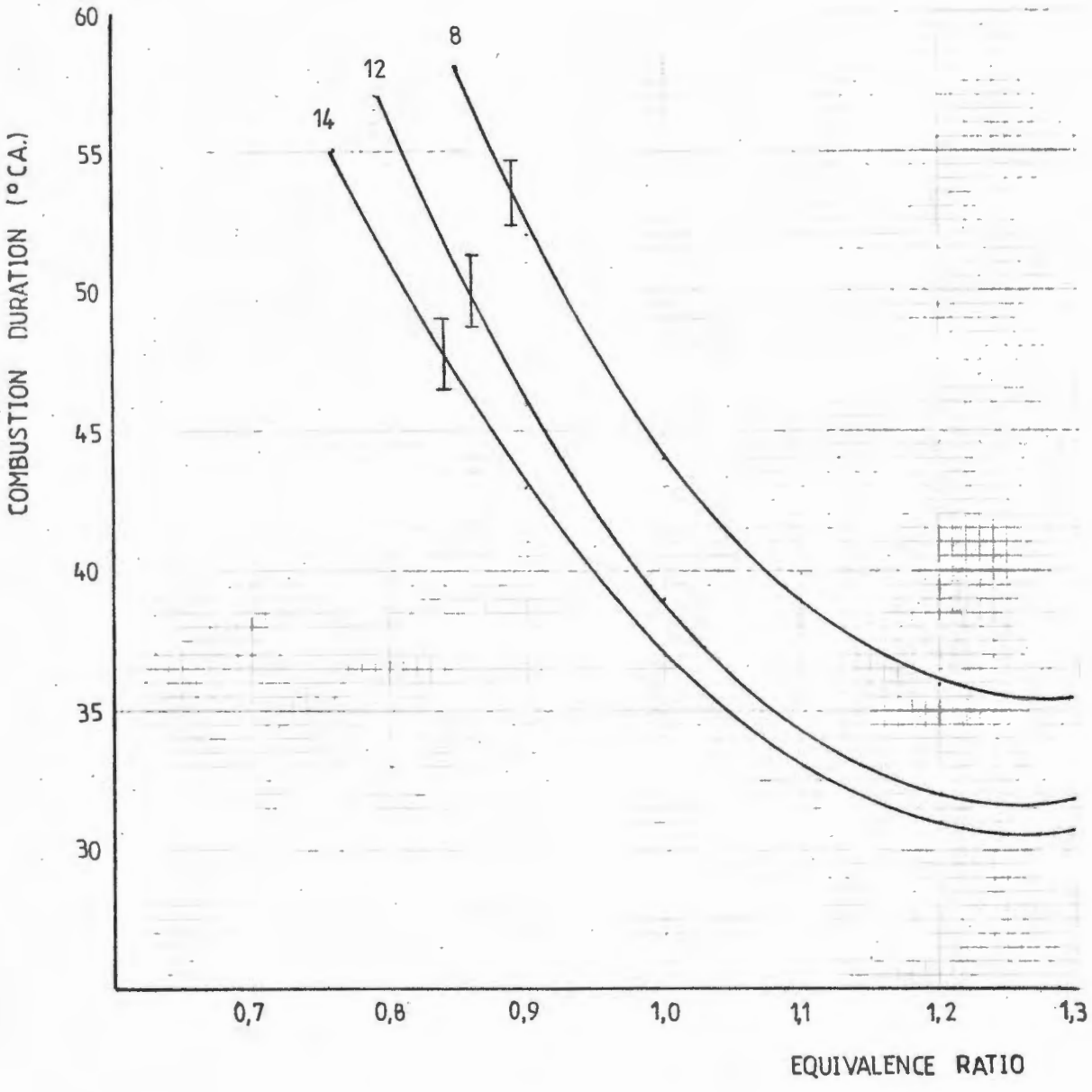

Figure 25. Effect of Compression Ratio on Combustion Duration

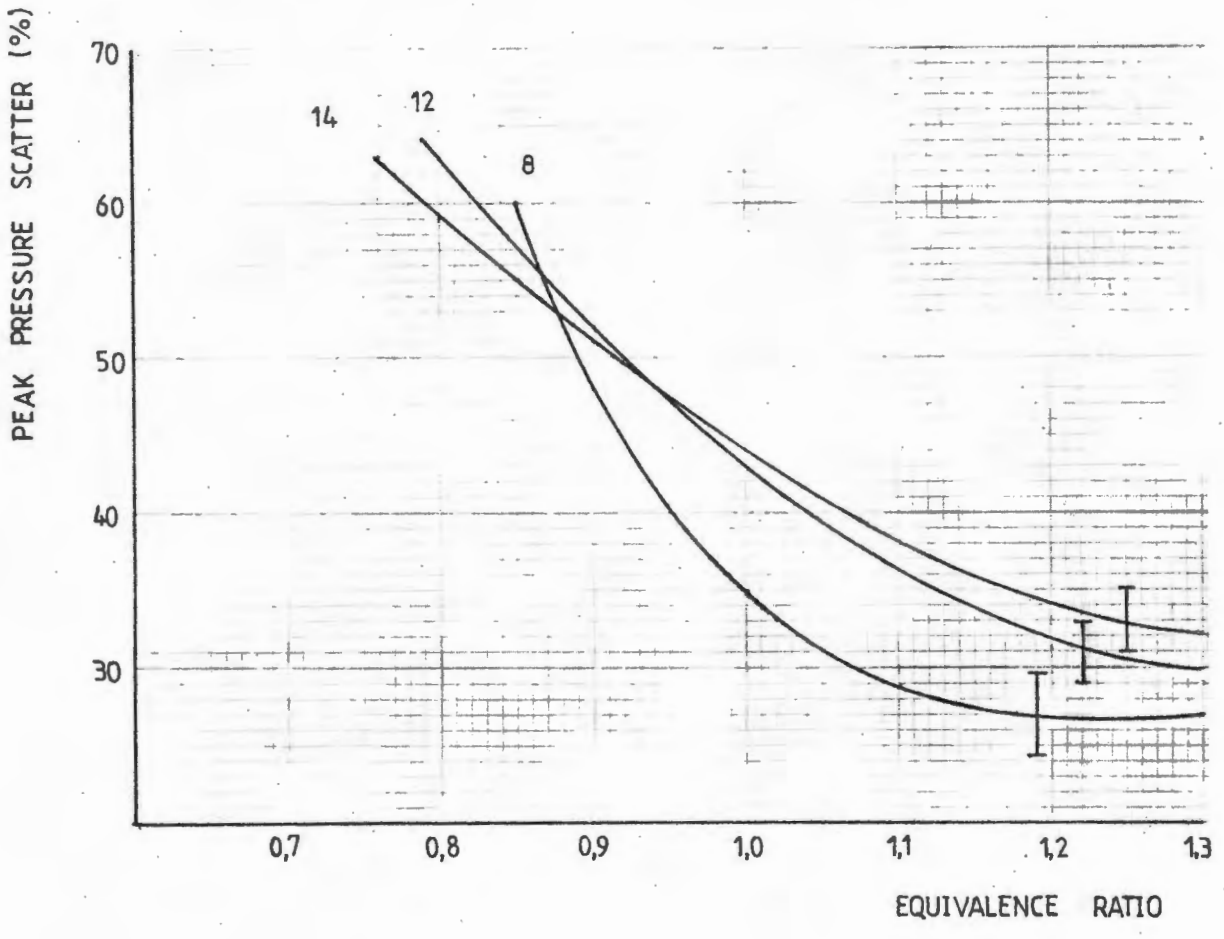

Figure 26. Effect of Compression Ratio on Peak Pressure Scatter

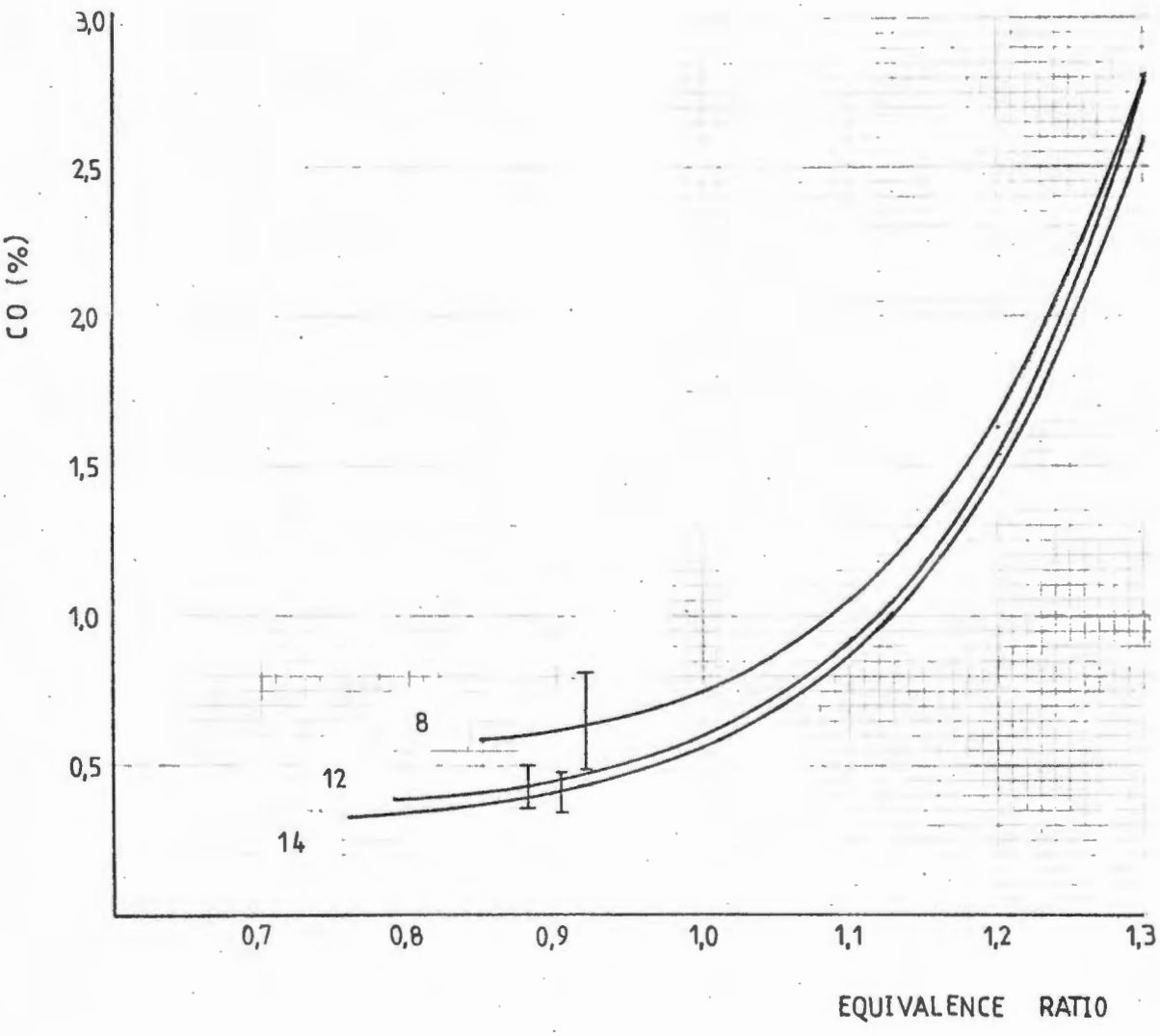

Figure 27. Effect of Compression Ratio on CO Emissions

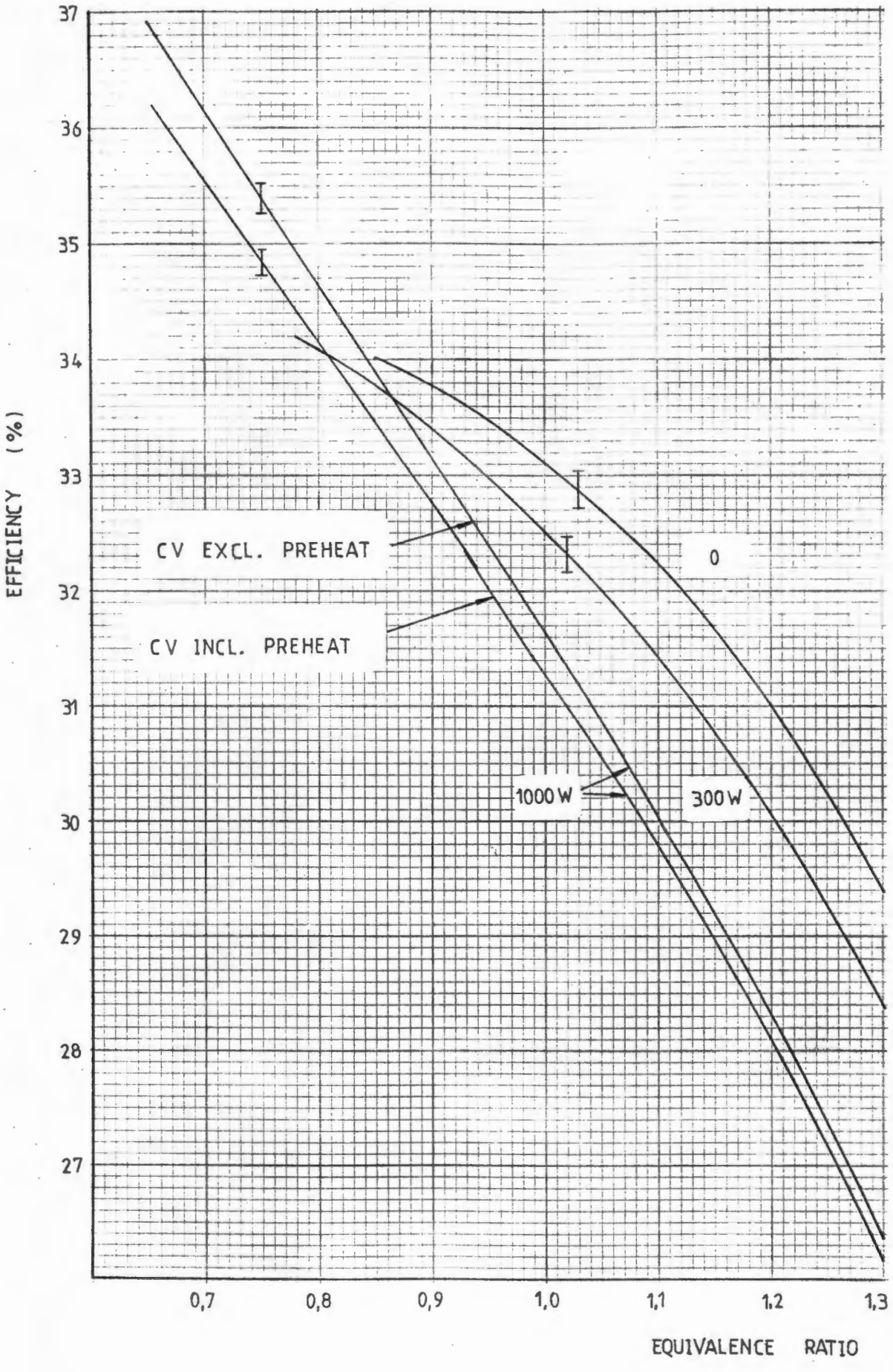

Figure 28. Effect of Air Preheat on Efficiency

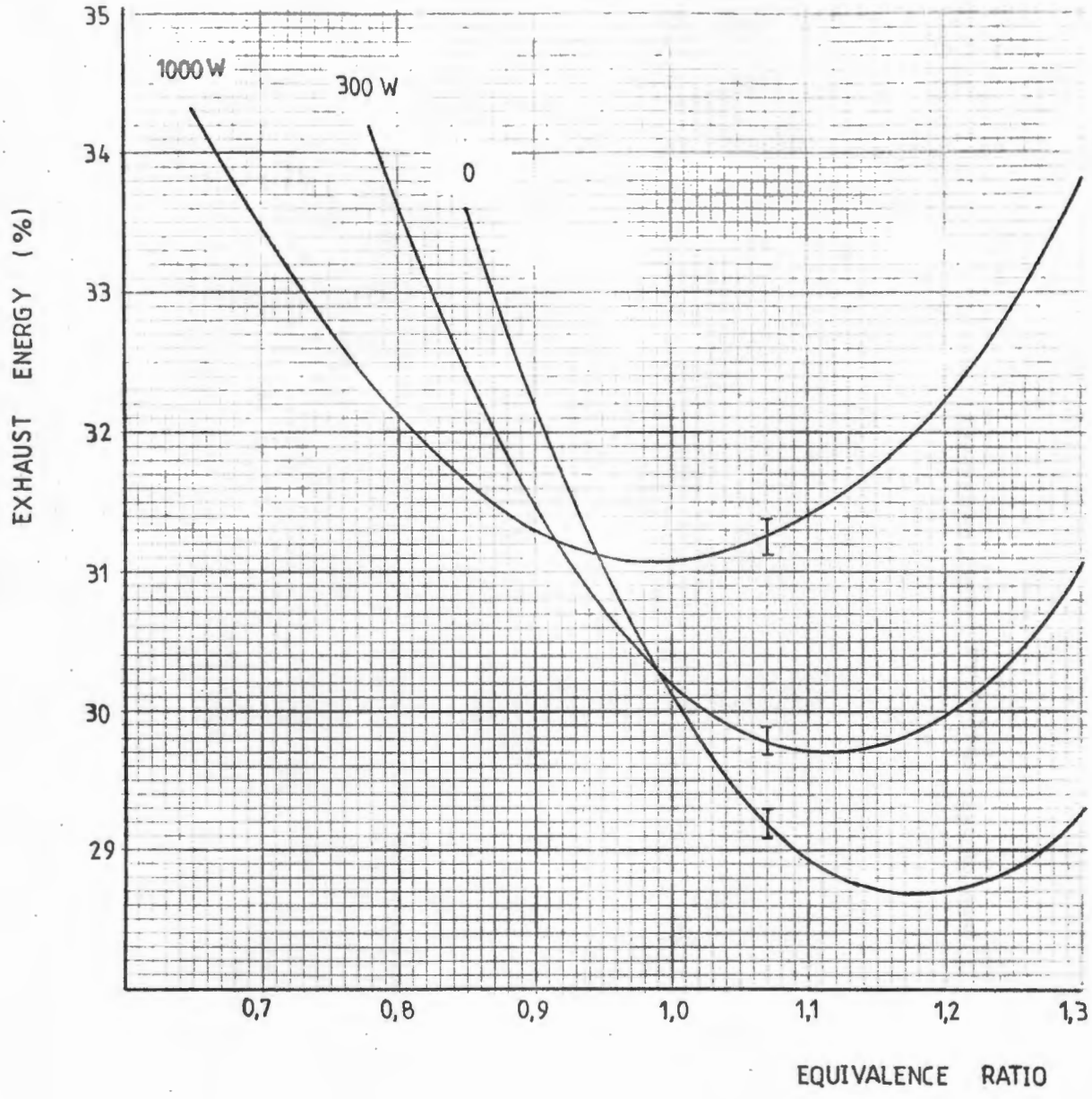

Figure 29. Effect of Air Preheat on Exhaust Energy

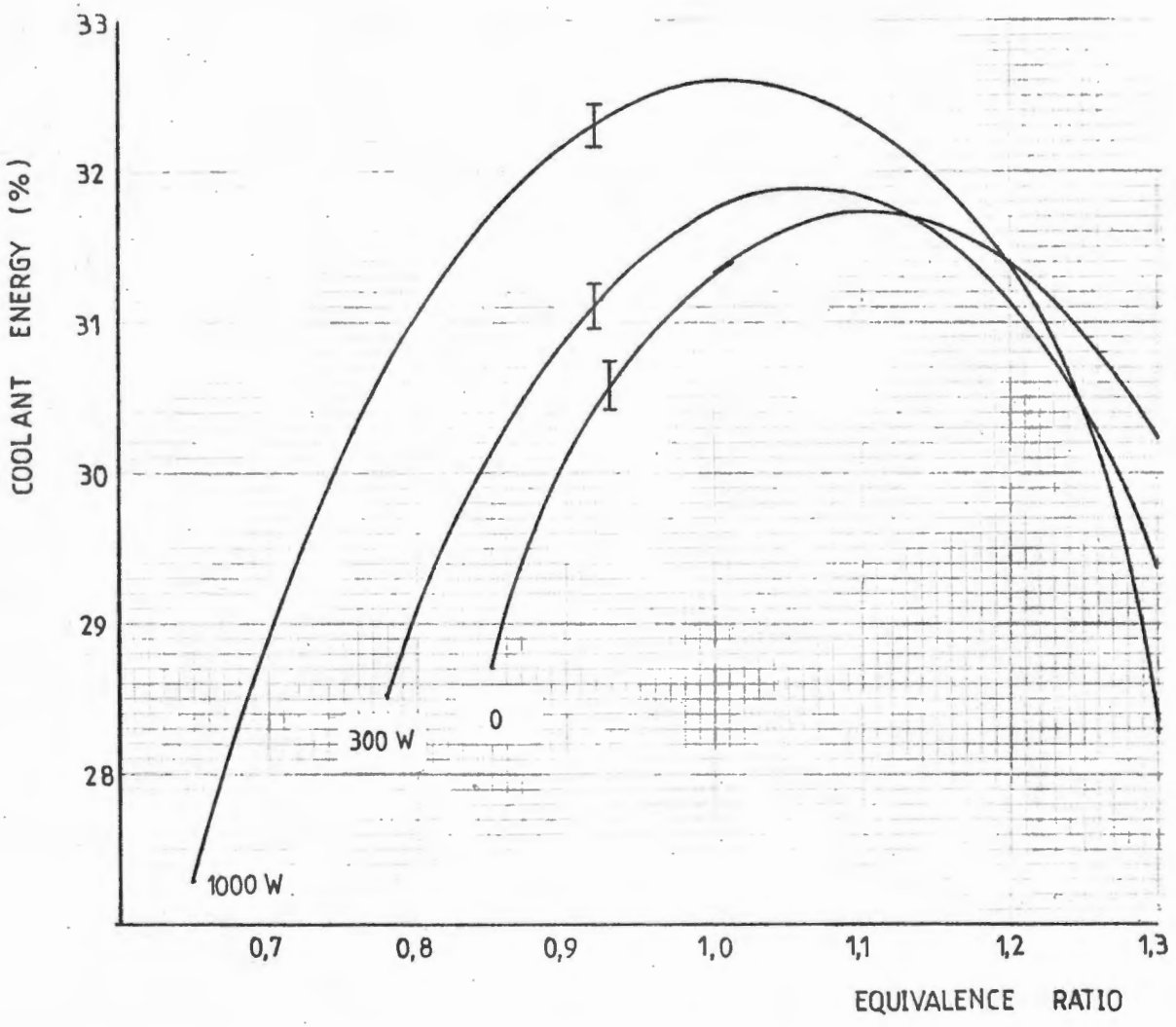

Figure 30. Effect of Air Preheat on Coolant Energy

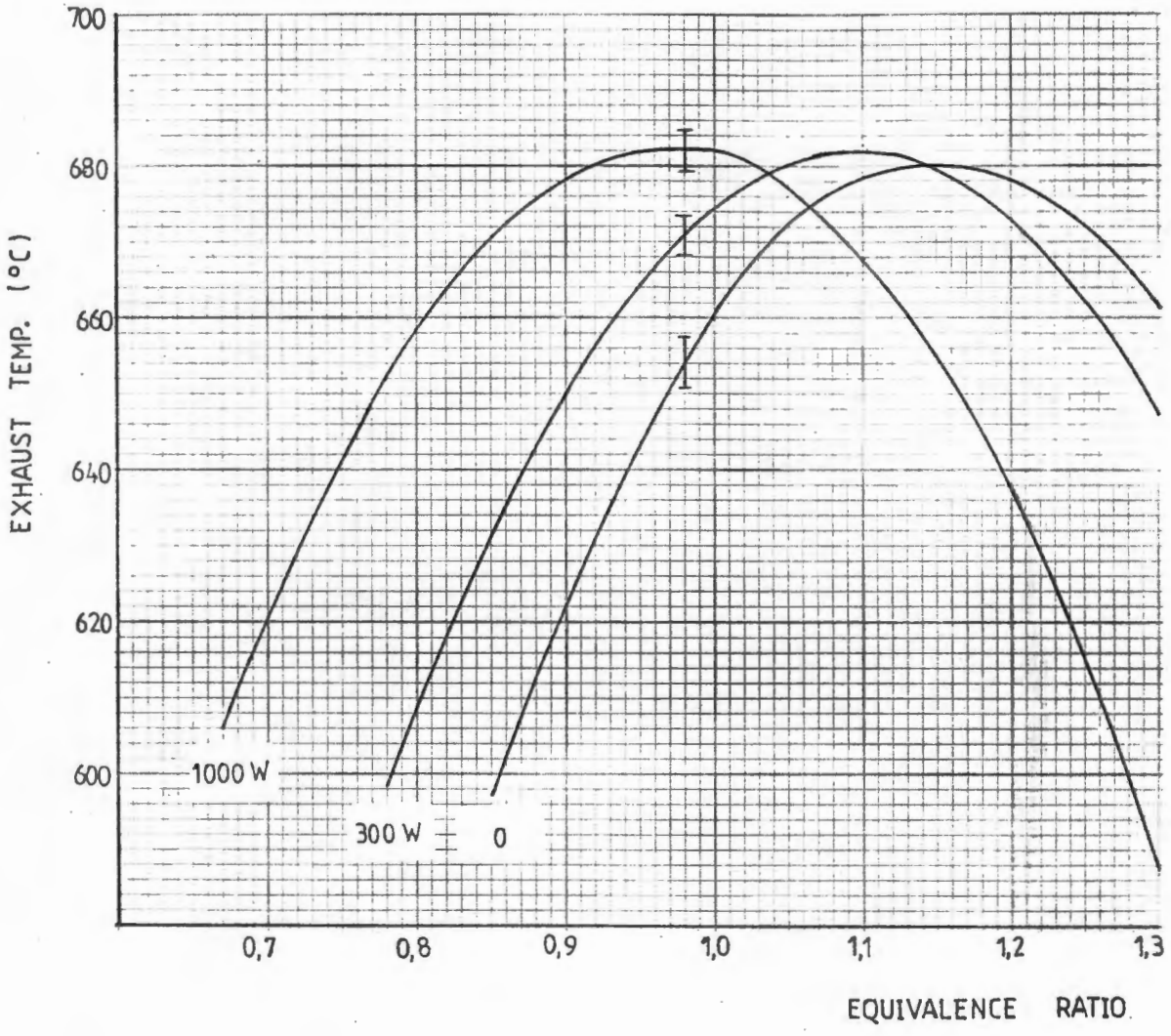

Figure 31. Effect of Air Preheat on Exhaust Gas Temperature

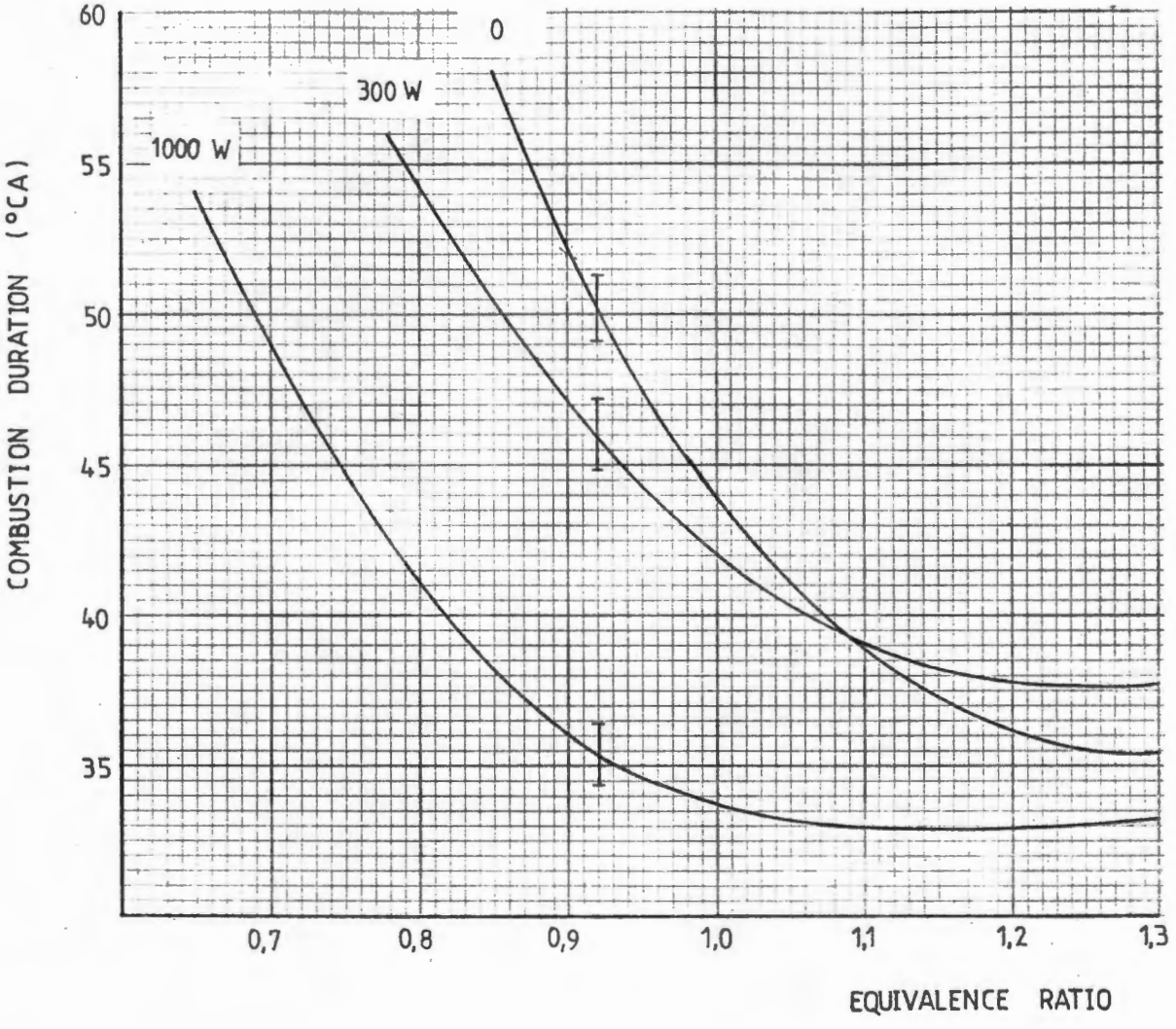

Figure 32. Effect of Air Preheat on Combustion Duration

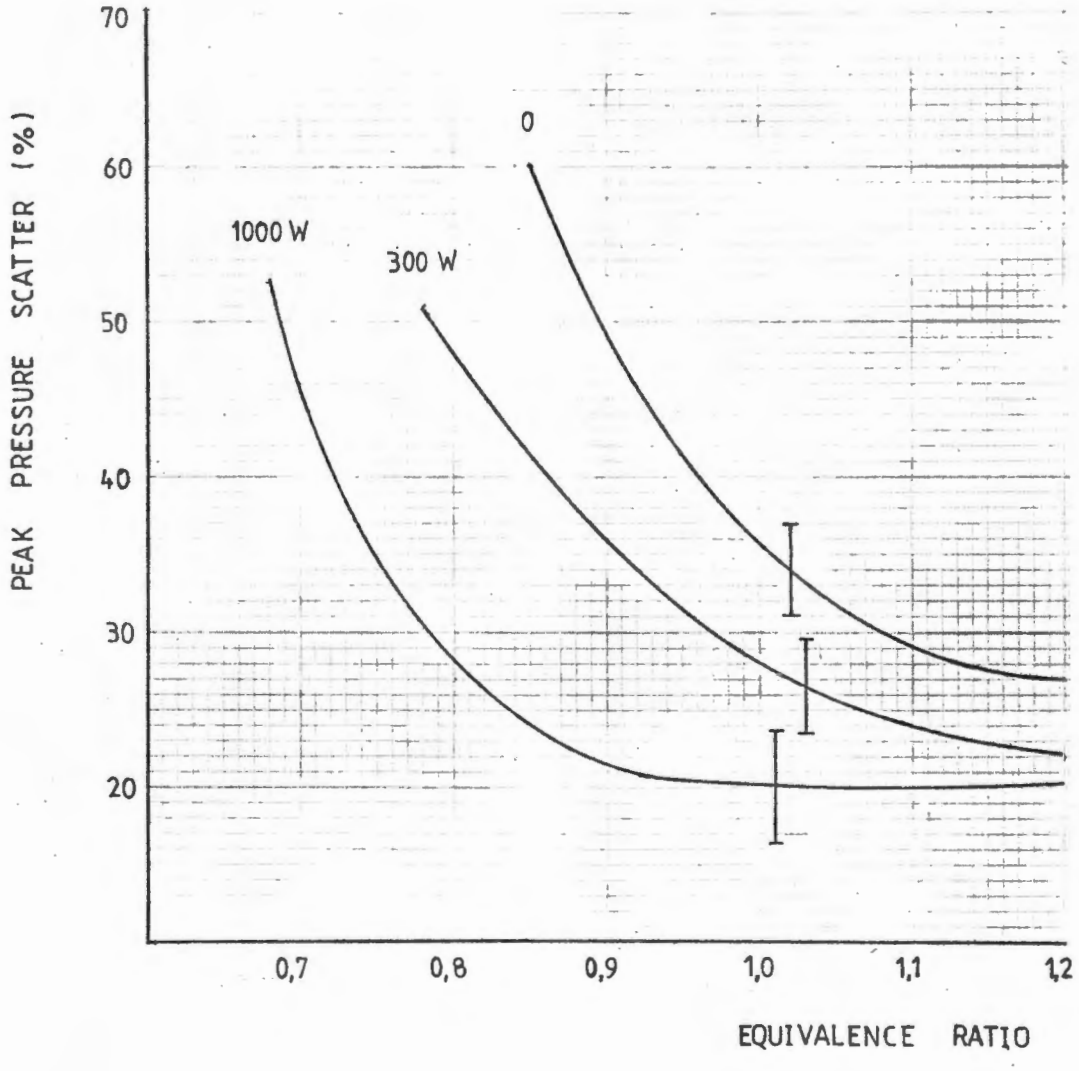

Figure 33. Effect of Air Preheat on Peak Pressure Scatter

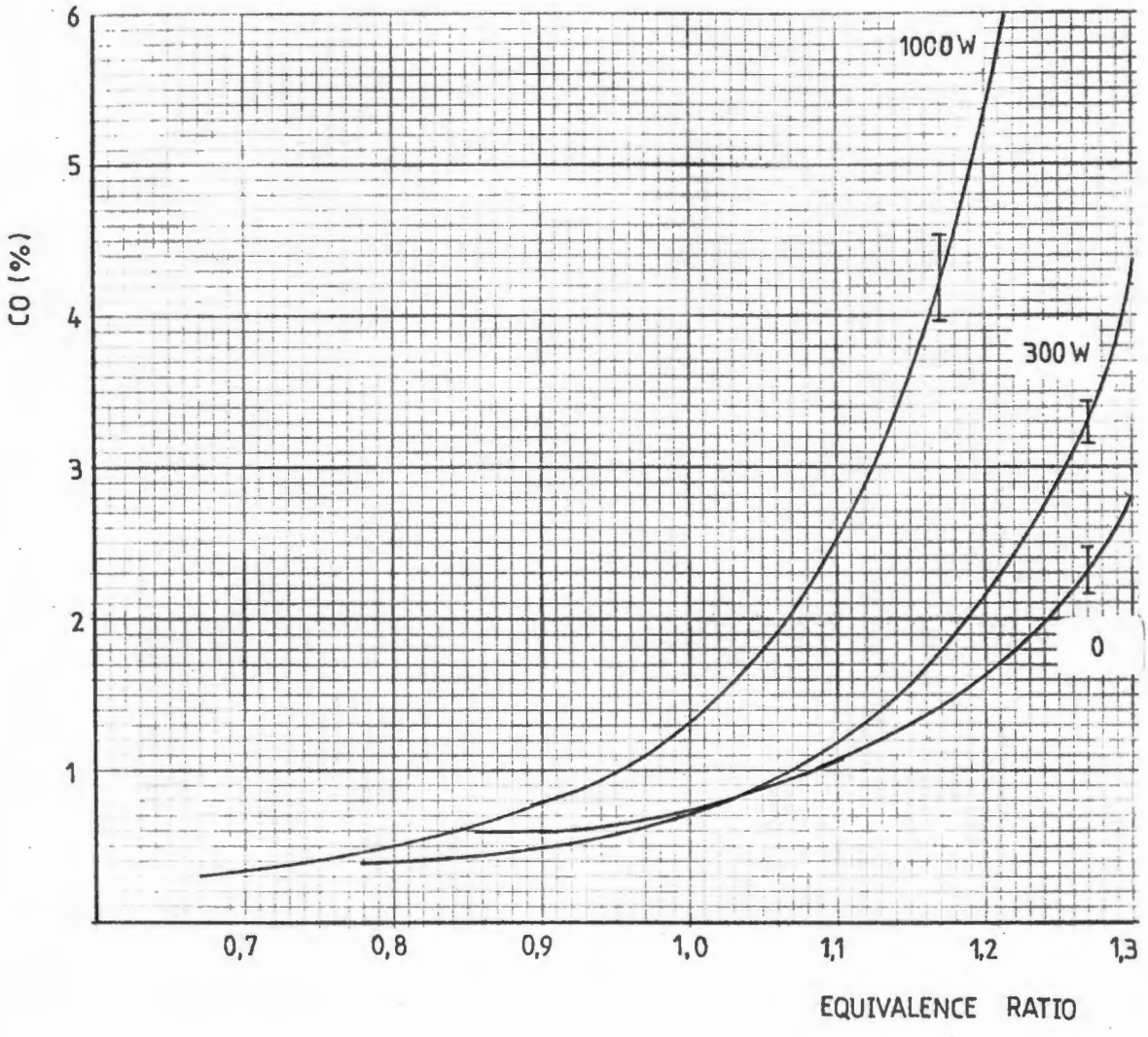

Figure 34. Effect of Air Preheat on CO Emissions

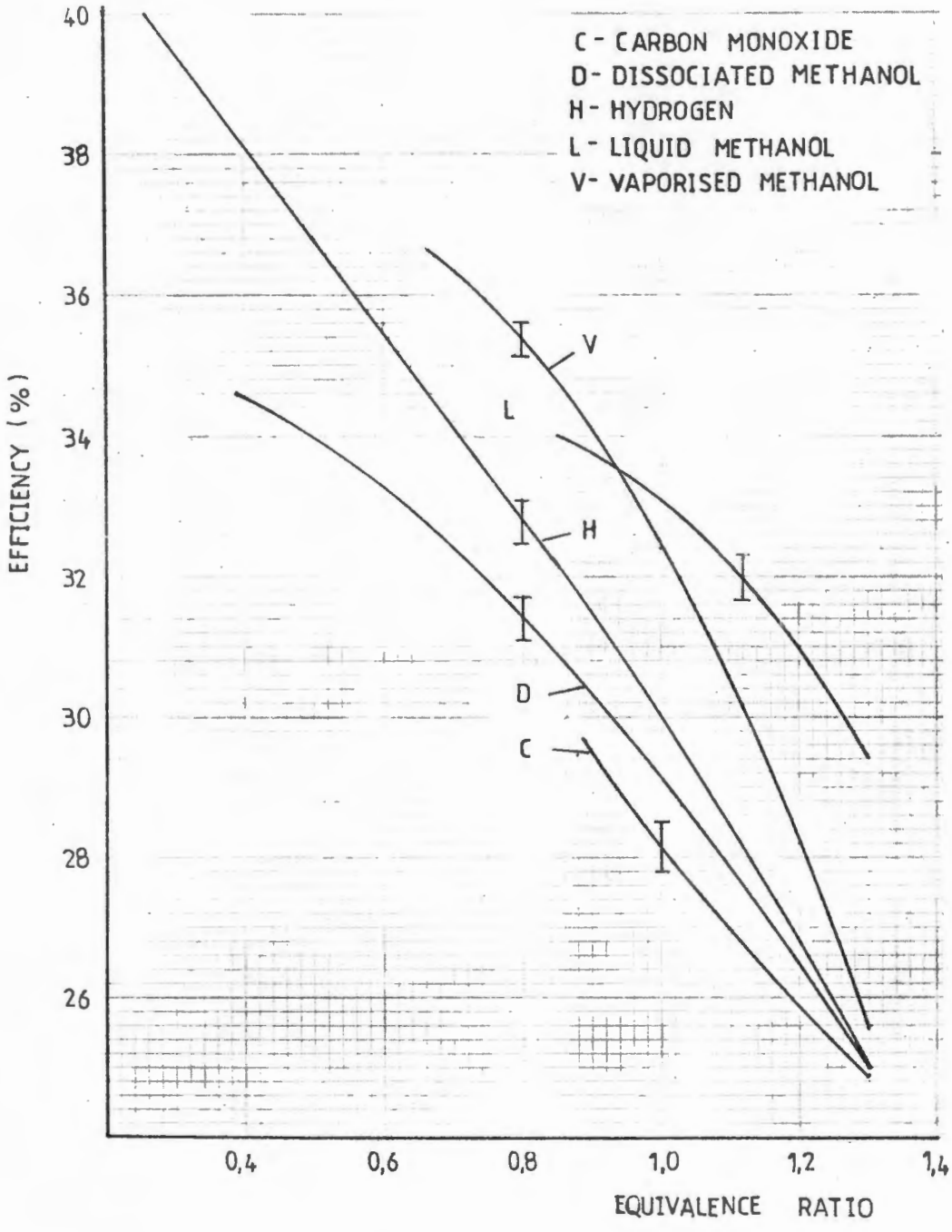

Figure 35. Effect of Fuel Type on Efficiency

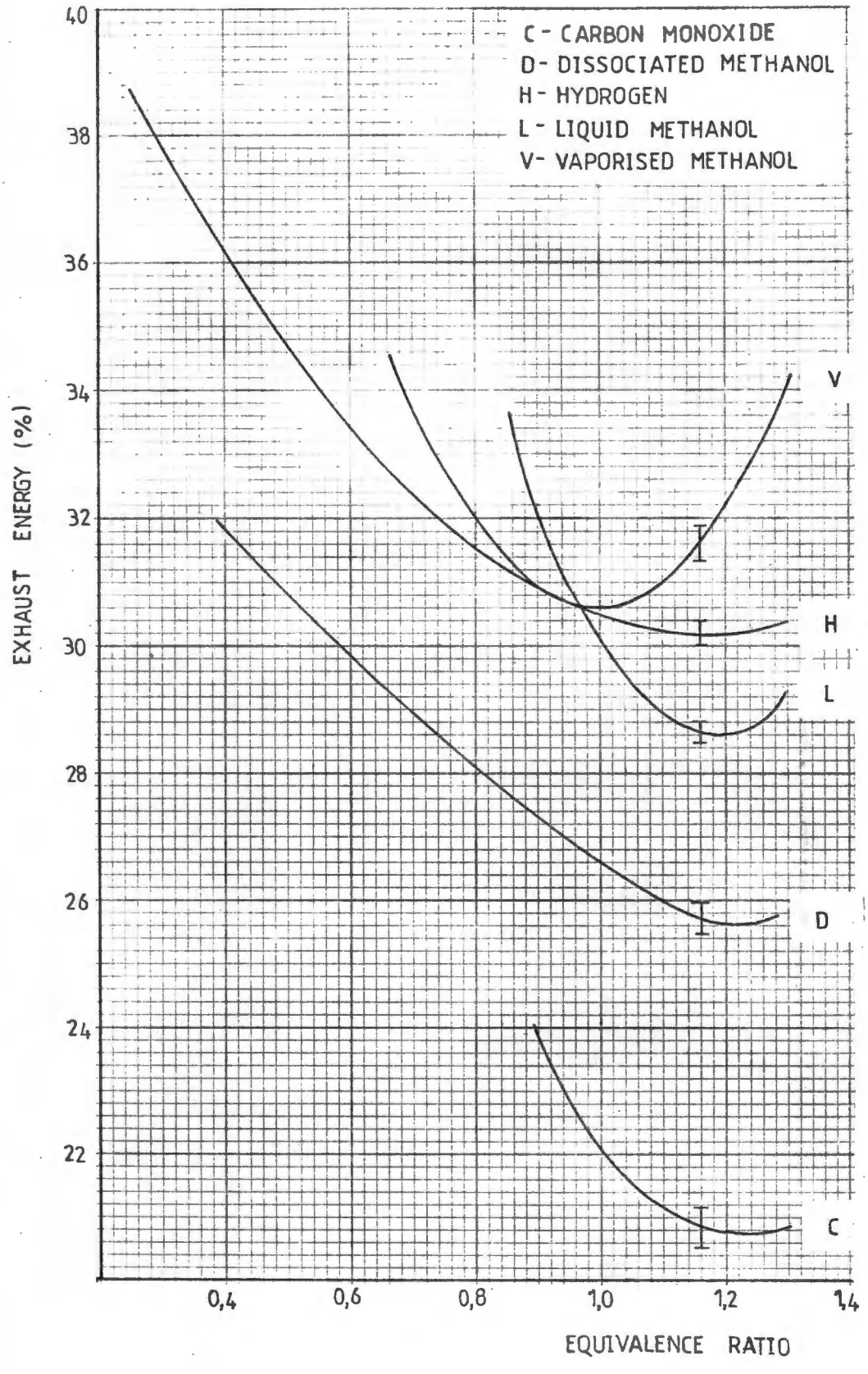

Figure 36. Effect of Fuel Type on Exhaust Energy

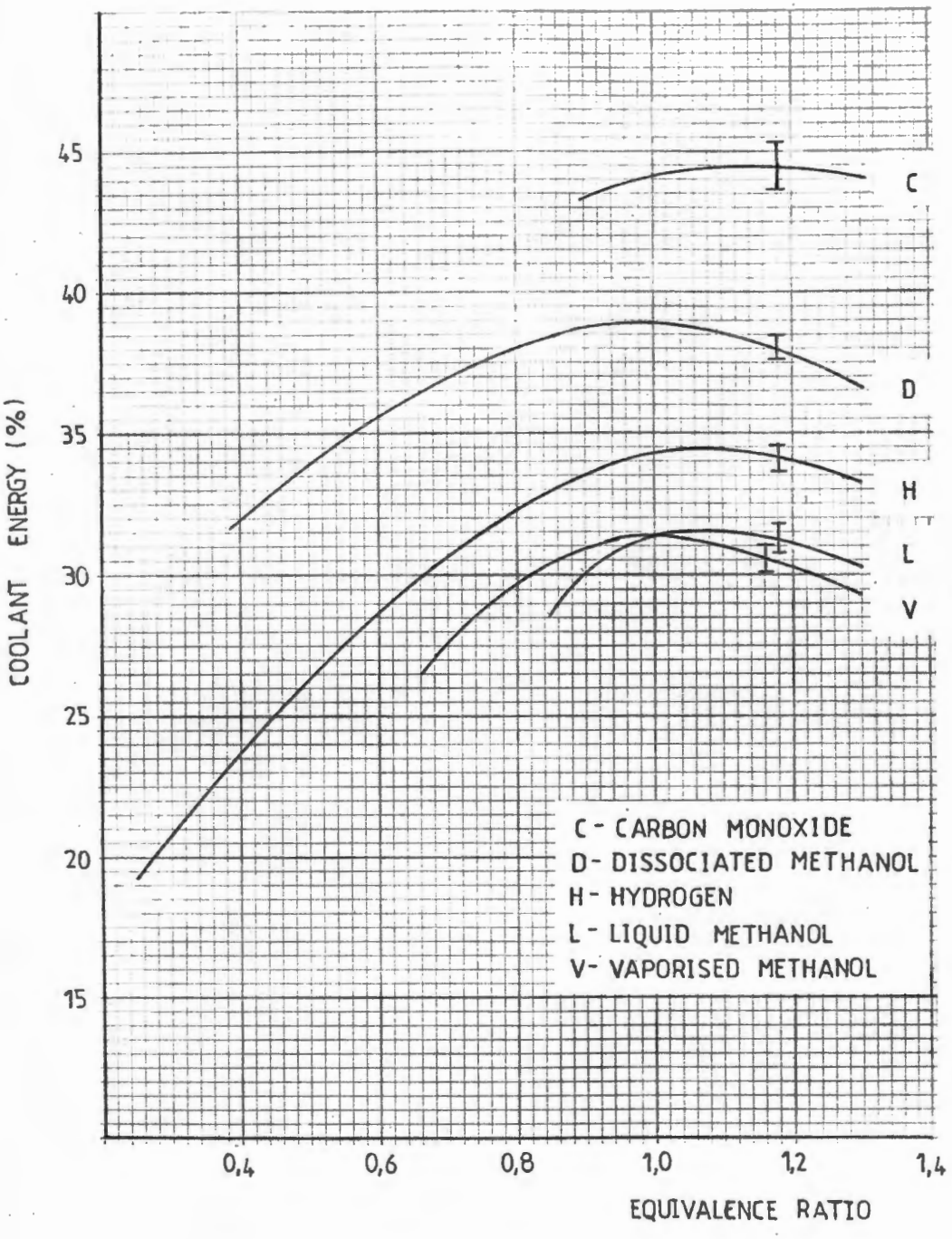

Figure 37. Effect of Fuel Type on Coolant Energy

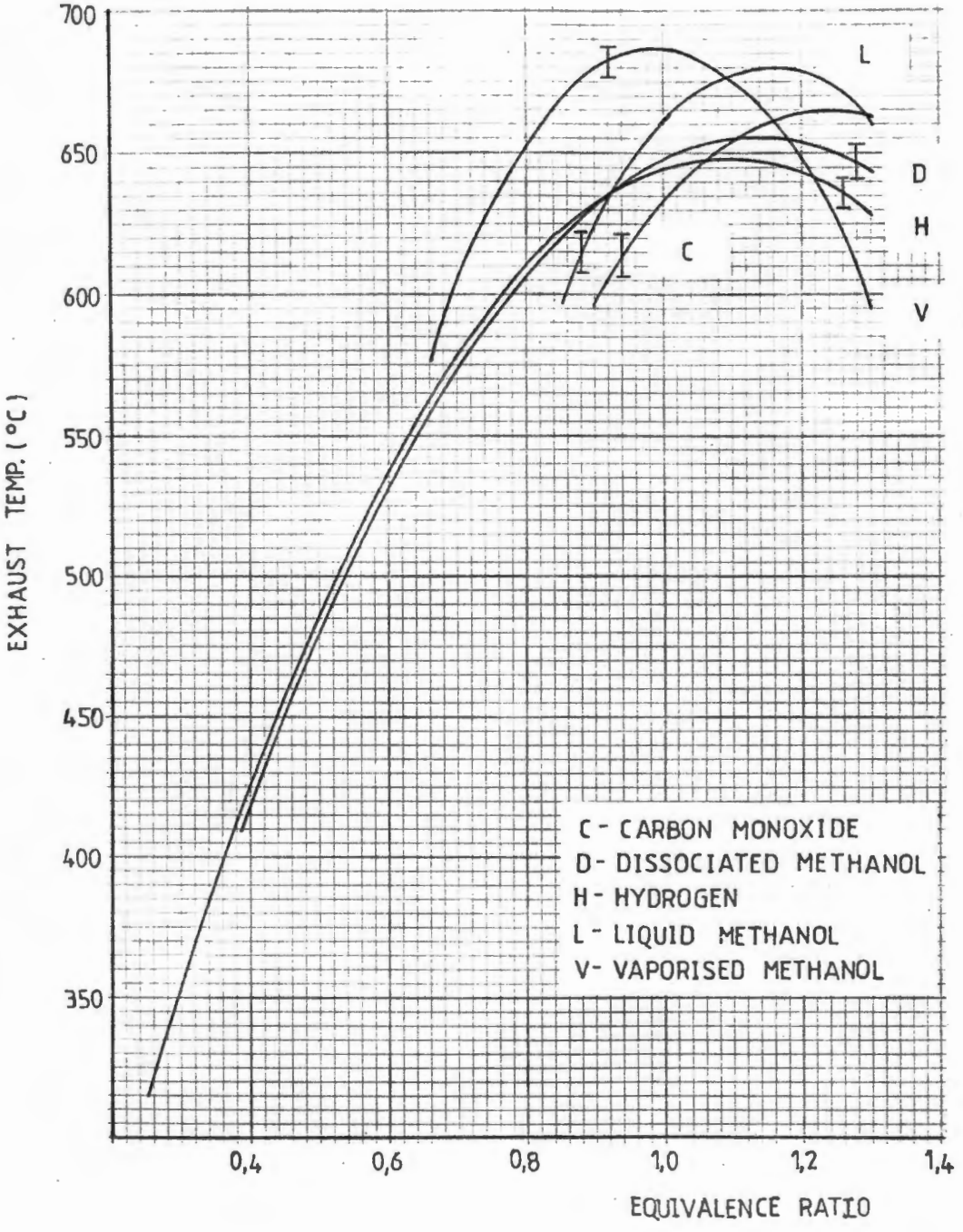

Figure 38. Effect of Fuel Type on Exhaust Temperature

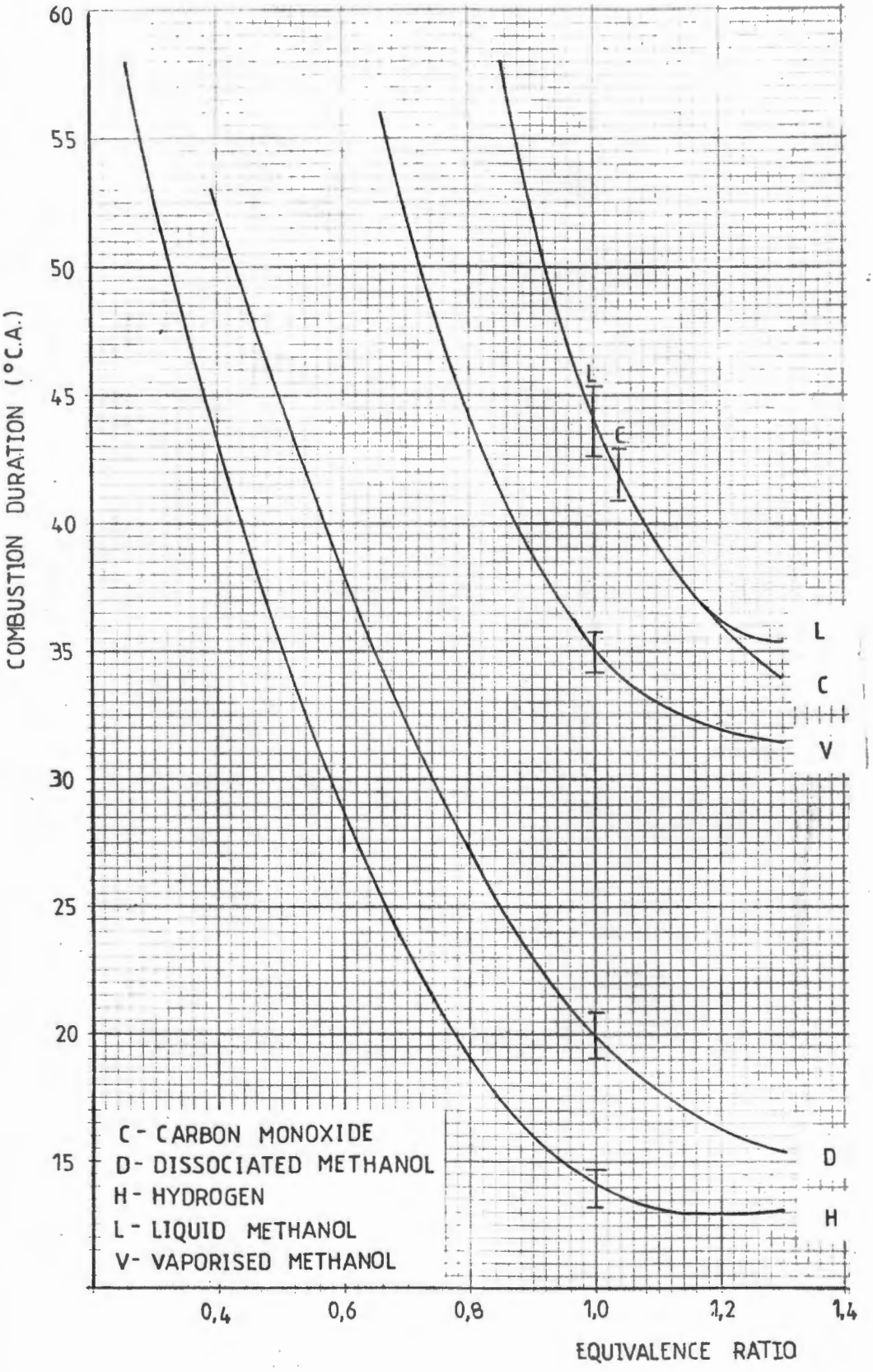

Figure 39. Effect of Fuel Type on Combustion Duration

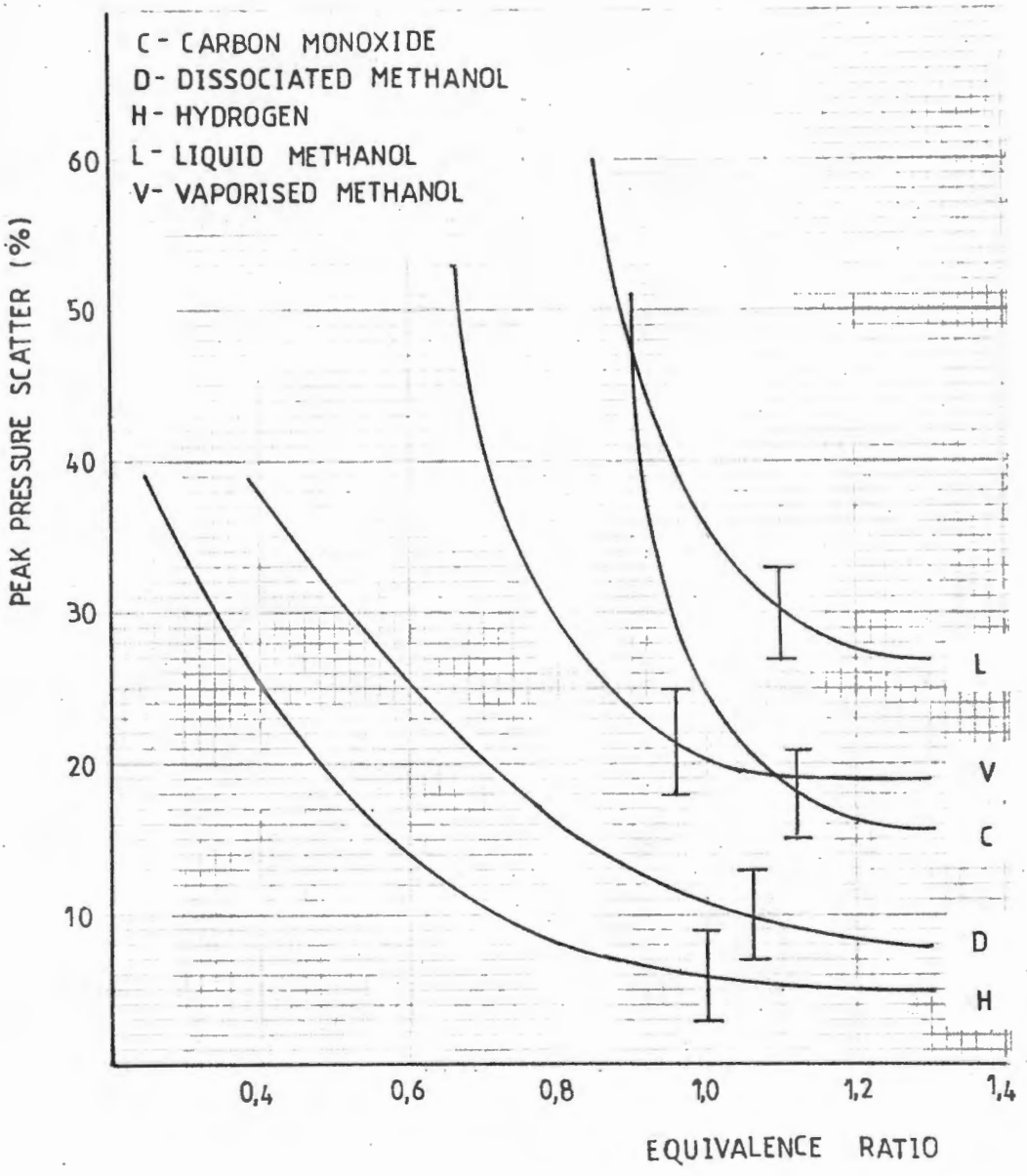

Figure 40. Effect of Fuel Type on Peak Pressure Scatter

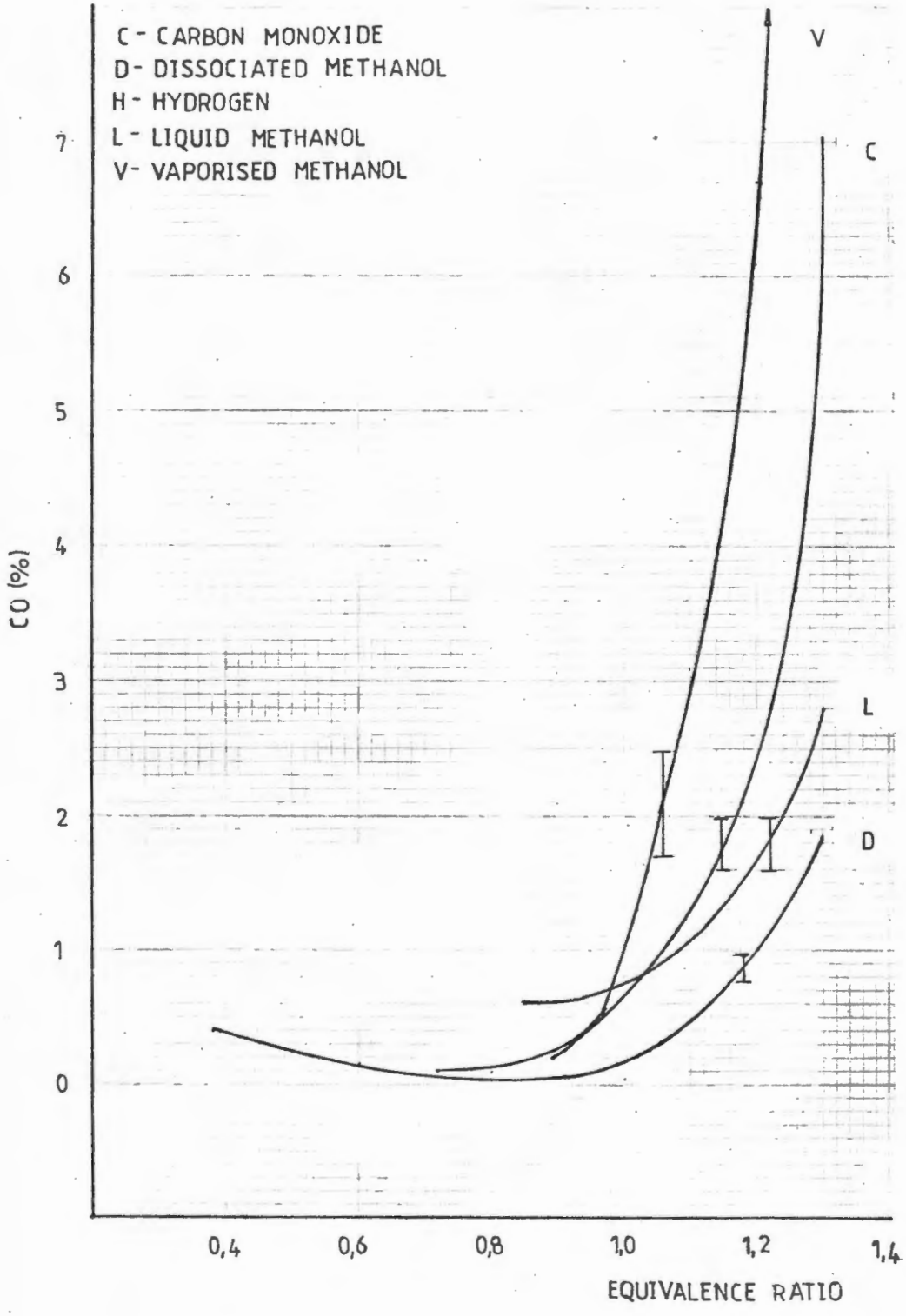

Figure 41. Effect of Fuel Type on CO Emissions

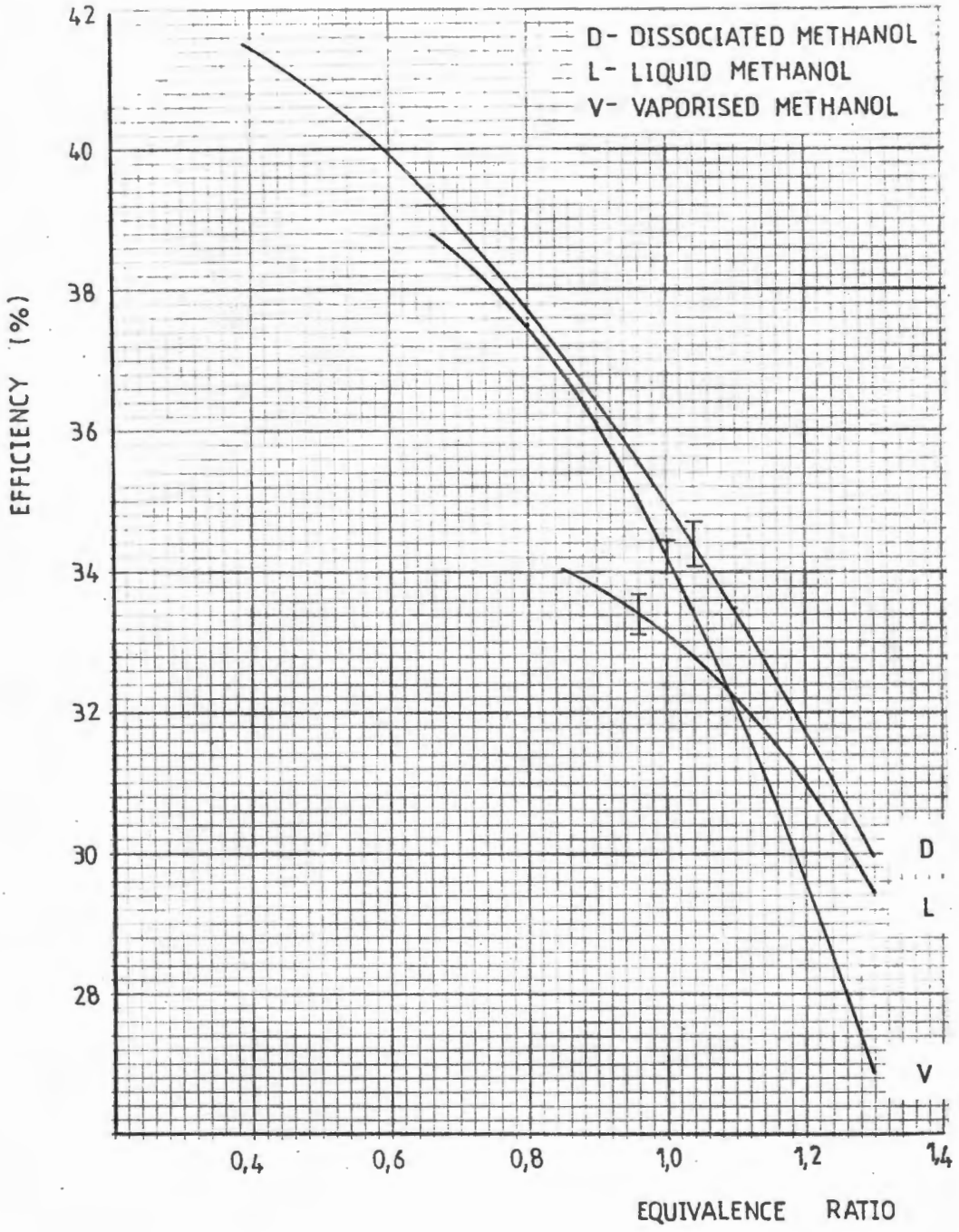

Figure 42. Efficiency based on the Calorific Value of Liquid Methanol

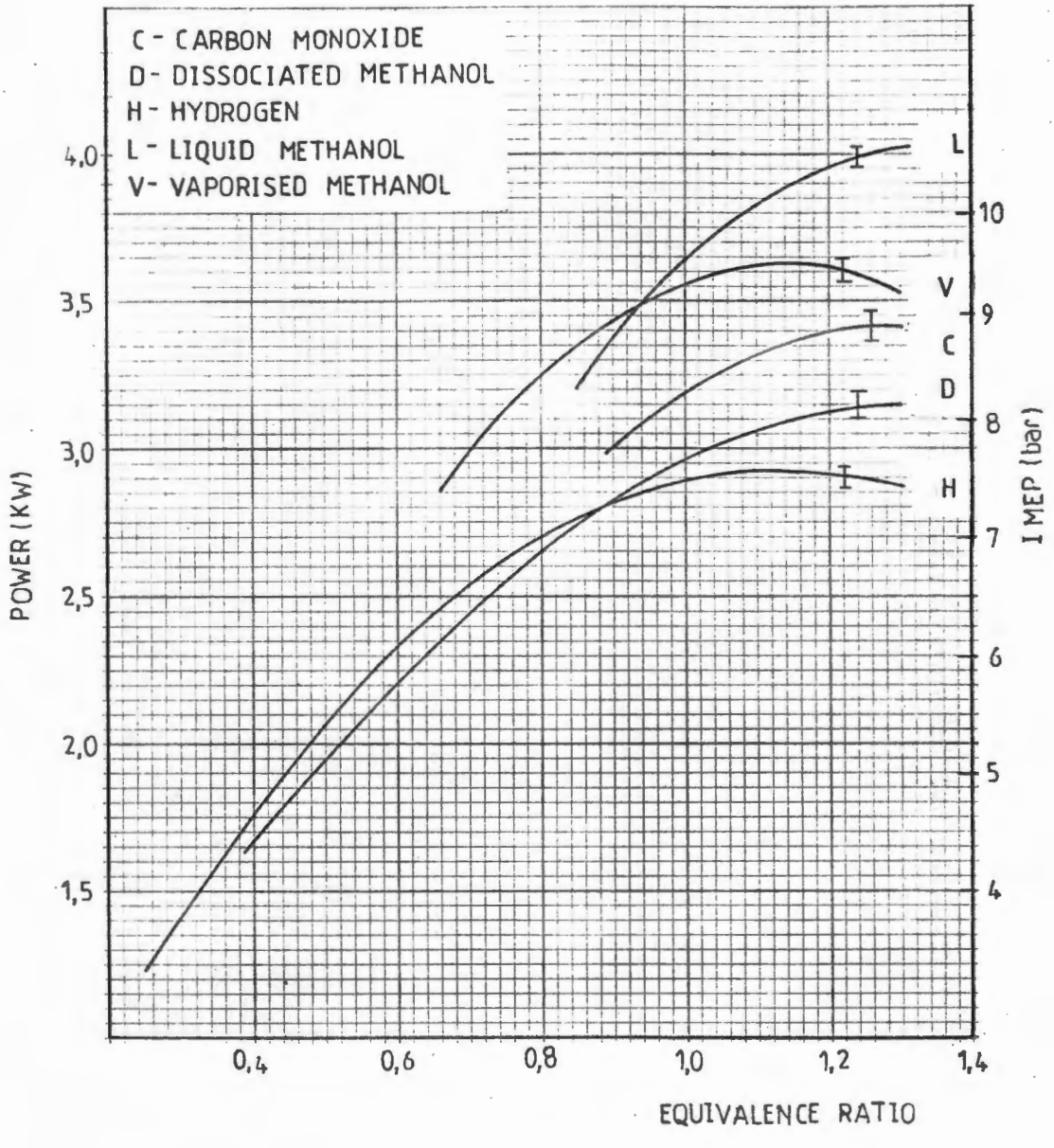

Figure 43. Effect of Fuel Type on Power

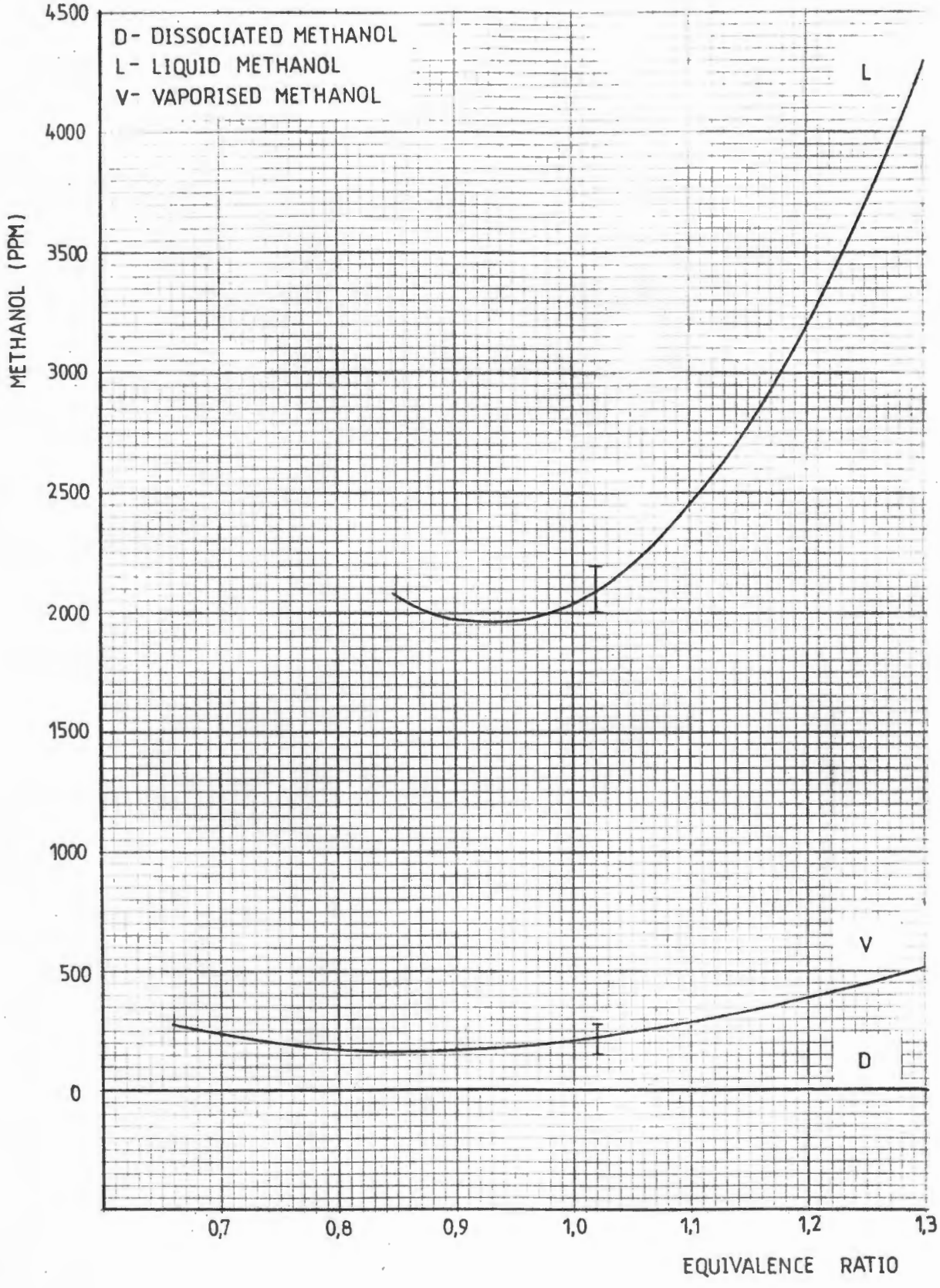

Figure 44. Effect of Fuel Type on Methanol Emissions

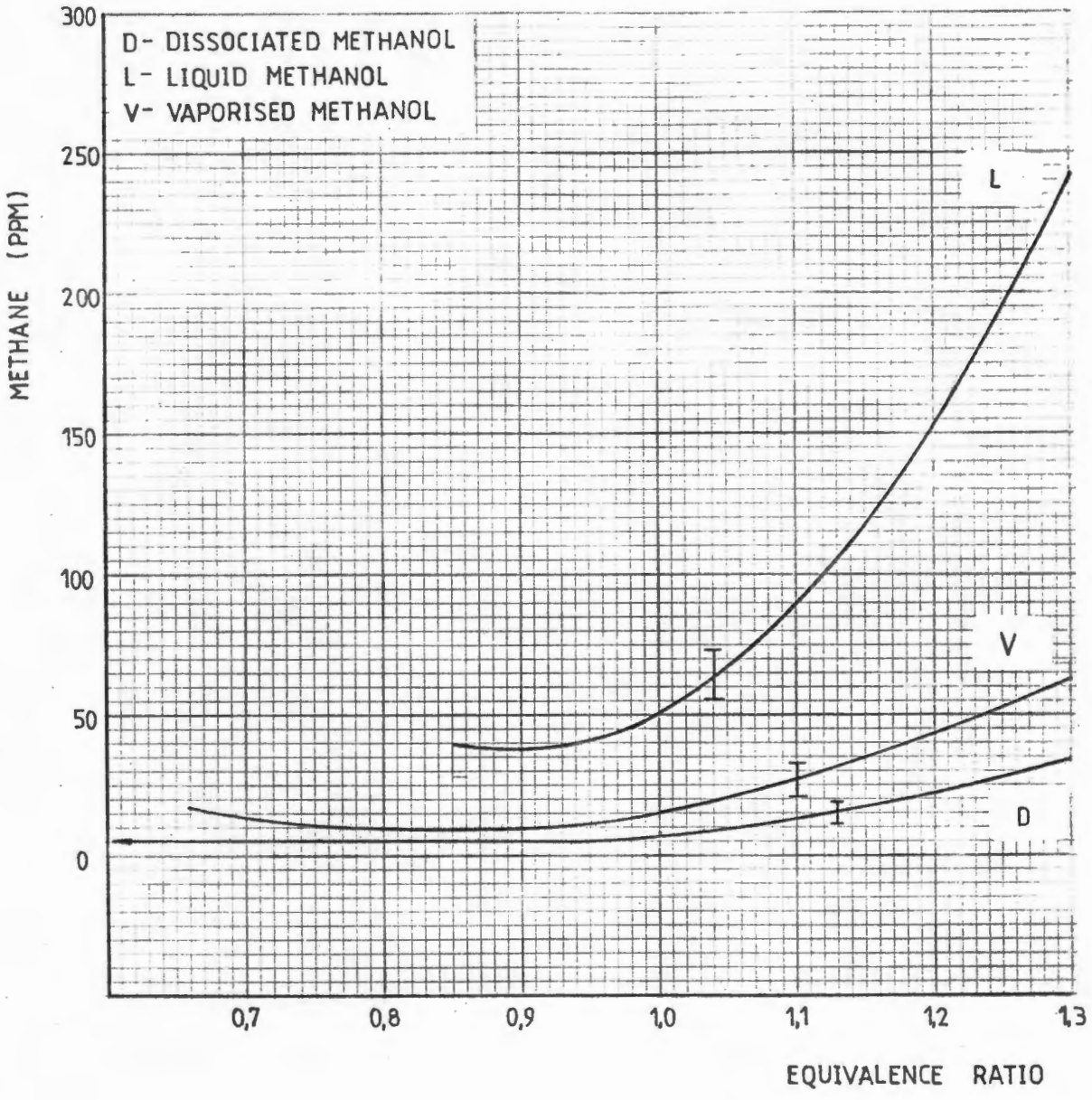

Figure 45. Effect of Fuel Type on Methane Emissions

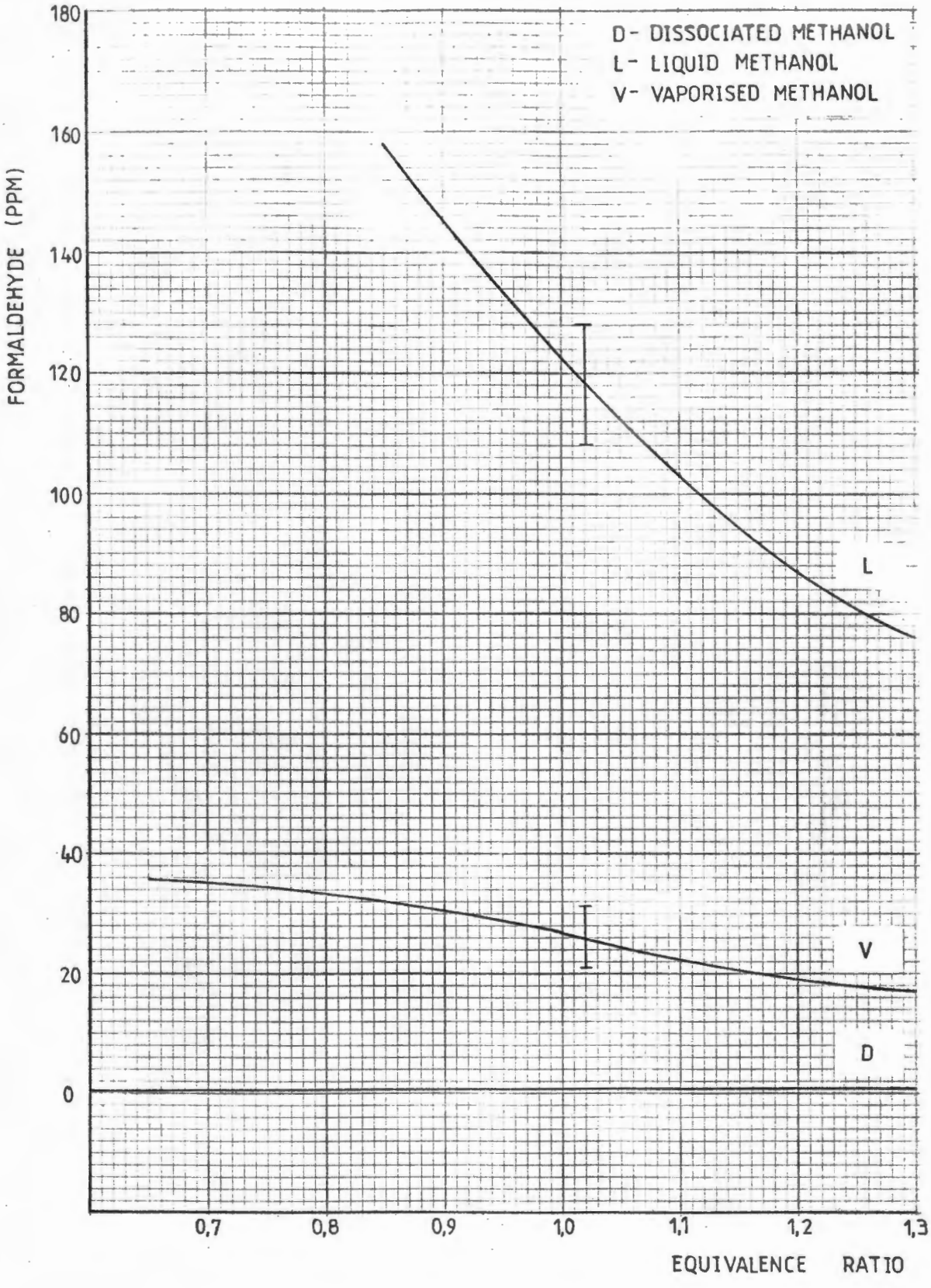

Figure 46. Effect of Fuel Type on Formaldehyde Emissions

8. DISCUSSION OF ENGINE PERFORMANCE

8.1 Effect of Compression Ratio on Engine Performance

The effect of compression ratio on engine performance is well documented in the literature. It is thus interesting to see that the results from the present investigation are largely in agreement with existing work and show that there was no gross error in the instrumentation.

Efficiency is clearly the parameter of fundamental interest and changes in other measured parameters will be used to support changes in efficiency.

A comparison may be made between the experimental results and the relationship derived from the literature. The experimental results for liquid methanol without air preheat gave efficiencies of 33,1, 36,5 and 37,1 at compression ratios of 8, 12 and 14 respectively and stoichiometric mixtures. Applying the relationship derived from the literature to the efficiency measured at a compression ratio of 8 gives efficiencies of 33,1, 36,2 and 37,4. Since the relationship was derived for use with compression ratios below 12 it appears less effective at high compression ratios where gain in efficiency diminishes.

Probably the most obvious advantage of higher compression ratios is the increased expansion ratio. This is clearly shown when increasing compression ratio from 8 to 12 by the 3,7 percentage point drop in exhaust energy. This was accompanied by a 3,1 percentage point increase in efficiency and 0,3 percentage point increase in coolant energy.

The effect of increased squish created by the higher compression ratio is seen in the reduced combustion duration and CO emissions. But the increase in cylinder turbulence also increased the peak pressure scatter.

8.2 Effect of Air Preheat on Engine Performance

Air preheat is of interest because of the relative ease with which air to an internal combustion engine may be heated using waste heat. This was seen as a means to increase the proportion of methanol vaporised before ignition and in so doing to improve the efficiency.

The amount of methanol which can be vaporised for a given air temperature may be calculated theoretically from a simple energy balance; vaporisation of the methanol will stop either when the air temperature has dropped sufficiently for it to be saturated with vapour or when all the methanol has evaporated. Table 3 relates the preheat to the mixture temperature and percentage methanol vaporised at stoichiometric conditions, ambient temperature of 20°C and when sufficient time is available for equilibrium to be reached.

Table 3. Theoretical Effect of Air Preheat on Vaporisation for a Stoichiometric Mixture and Initial Temperature of 20°C

Preheat (W)	Mixture Temp. (°C)	% Vaporised
0	-10	17
300	6	44
1000	56	100

During the experimental work the temperature of the fuel-air mixture was measured just upstream of the inlet valve. From these results the percentage methanol vaporised could be calculated. This has been done for stoichiometric conditions in Table 4.

Table 4. Measured Effect of Air Preheat on Vaporisation for a Stoichiometric Mixture and Initial Temperature of 20°C

Preheat (W)	Mixture Temp.(°C)	% Vaporised
0	9	6
300	48	9
1000	116	56

These results show that insufficient time was available for equilibrium to be reached. Where good mixture preparation is important the standard intake system is generally replaced with a high capacity baffled mixing chamber.

In the present investigation increasing air preheat was accompanied by a loss in efficiency over most of the operating range, even if the calorific value of the fuel excludes the preheat energy. Increased preheat does however increase the LML with a resultant gain in efficiency when operating near the LML. The reduction in efficiency is in agreement with the results of a computer model reported by Taylor [59]. No explanation of the phenomenon was given. In another investigation using propane as the fuel, air preheat was found to increase the LML and efficiency in the lean region without any reduction in efficiency over the normal fuel-air mixture range [30].

Trends in the energy rejected to the coolant and exhaust are of little value since the effect of air preheat changes over the range of fuel-air mixtures for no apparent reason. Consideration of the more fundamental parameters appears more informative in this case.

The reduction in combustion duration with increasing preheat is as a result of the higher flame speed when the mixture temperature is increased. This may be expected to increase the efficiency as the cycle moves closer to the top dead centre combustion of the Otto cycle. Increasing preheat also leads to a reduction in peak pressure scatter. This may be interpreted as a lower percentage of cycles with incomplete combustion

and should lead to an increase in efficiency.

However, the two most interesting parameters are the CO in the exhaust gas and the exhaust temperature. Air preheat will increase the peak cycle temperature which will increase the dissociation of CO_2 according to the following reaction:

$$CO_2 \rightleftharpoons CO + \tfrac{1}{2}O_2$$

The reaction from left to right is strongly endothermic. Now, even though the expansion ratio is constant, the exhaust gas temperatures for rich mixtures decrease with increased preheat. This can be explained in terms of the incomplete recombination of the O_2 and CO molecules, which is a slower reaction than the dissociation reaction because it occurs at lower temperatures during the expansion stroke and will be incomplete when exhausted from the cylinder.

The increased dissociation that accompanies increased preheat will thus absorb energy which is not recovered in the incomplete recombination reaction and will appear as an increase in CO in the exhaust gas. As mentioned previously, the effect is only prevalent for rich mixtures and appears to explain the loss in efficiency with increased preheat in this region.

These results are in contrast to those reported by Hilden and Parks [19] for vaporised methanol. They reported a lower efficiency for the vaporised methanol but with reductions of 60 - 80% in CO emissions. No reason for the lower efficiency was apparent.

Returning to the results for exhaust energy, the increase in exhaust energy with air preheat for rich mixtures appears surprising since the exhaust gas temperature decreases. However, this effect appears to be due to the relatively large percentage of CO, which has 21% higher specific heat capacity than CO_2, in the exhaust.

8.3 Effect of Fuel Type on Engine Performance

Table 5 summaries the results for the efficiencies of the different fuels.

Table 5. Effect of Fuel Type on Engine Efficiency (%)

Equivalence Ratio	Fuel				
	Liquid Methanol	Vaporised Methanol	Dissociated Methanol	Hydrogen	Carbon Monoxide
0,4	-	-	34,2	38,2	-
0,8	-	35,5	30,7	32,8	-
1,0	33,1	32,4	29,1	29,8	28,2
1,2	31,0	28,4	27,8	26,7	25,5

The results will be considered first for vaporised methanol, then for dissociated methanol.

8.3.1 Vaporised Methanol

Vaporised methanol initially appears to be a very promising fuel with shorter combustion duration and less peak pressure scatter than with liquid methanol fuel. In fact, vaporised methanol does offer improved efficiency over liquid methanol fueling for equivalence ratios less than 0,9. However, this improvement appears to be due simply to an extension in the LML, permitting operation at leaner mixtures than with liquid methanol.

For equivalence ratios greater than 0,9 there is evidence of the same problem that was encountered with air preheat. Efficiency is being reduced due to the endothermic dissociation of CO_2, without complete recombination. There is the same drop in exhaust temperature and increase in CO emissions as the mixture becomes richer than stoichiometric.

The trend in coolant and exhaust energy is similar to that for air preheat.

8.3.2 Dissociated Methanol

From the review of the literature, dissociated methanol fueling was expected to result in a lower efficiency than for liquid

methanol fueling, but the decrease measured experimentally was greater than expected. It was only at the LML that dissociated methanol was able to equal the efficiency of liquid methanol.

This problem may be considered in two stages. Firstly, there is the comparison between dissociated methanol and hydrogen and secondly between hydrogen and liquid methanol.

The lower efficiency for dissociated methanol in comparison with hydrogen is due to the presence of carbon monoxide which shows some unfavourable combustion characteristics:

(i) The abundance of carbon atoms in the fuel results in a lumincus flame with an increase in heat lost to the ccolant by radiation, which is not reccvered by reduced energy in the exhaust gas.

(ii) An increase in combustion duration to that of liquid methanol.

(iii) A significant increase in peak pressure scatter.

(iv) When combined with hydrogen to form dissociated methanol, there is a 21% reduction in the ratio of moles of product to moles of reactant for combustion of dissociated methanol as ccmpared to hydrogen and liquid methanol. This is probably the main reason for reduced efficiency.

However, this decrease in the product : reactant mclar ratio also resulted in lower peak cylinder pressures and thus lower peak temperatures. This in turn should reduce the dissociation of CO_2 to CO and must have had a beneficial effect on efficiency and CO emissions.

The lower efficiency for hydrogen in comparison with liquid methanol is not immediately apparent. Only for equivalence ratios less than 0,7 does hydrogen offer a higher efficiency than liquid methanol.

The combustion duration of hydrogen for equivalence ratios greater than 0,6 is extremely short and facilitates ccmplete

combustion near top dead centre. The peak pressure scatter is also lower than for any other fuel and indicates that adequate mixing of the hydrogen-air charge has occured.

However, it appears that this rapid combustion may indirectly be responsible for the reduction in efficiency. The concept of combustion knock has already been presented. Now, it appears that the pressure waves set up in the cylinder as a result of combustion knock are responsible for an increase in the heat transfer through the boundary layer. For equivalence ratios greater than 0,8 hydrogen shows coolant energy losses approximately 3 percentage points higher than for liquid methanol while having comparable exhaust energy losses. This is more than sufficient to account for the lower efficiency of hydrogen.

At this point it is necessary to recall that the primary objective in dissociating the methanol was the recovery of waste heat amounting to 20% of the net calorific value of methanol. Thus for dissociation of methanol onboard a vehicle, the efficiency will be based on the net calorific valve of liquid methanol and the resultant efficiency is shown in figure 42. Also shown in figure 42 is the efficiency for vaporised methanol where the heat of vaporisation has been recovered from waste heat. The potential of vaporised methanol to improve thermal efficiency is apparent for equivalence ratios of 0,7 - 1,0 where vaporised and dissociated methanol show effectively the same overall efficiency.

Figure 43 shows that both hydrogen and dissociated methanol show a significant loss in power in comparison with liquid methanol. Table 6 compares the measured change in indicated power (with respect to liquid methanol) to the theoretical change in power assuming similar combustion efficiency and an equivalence ratio of 1.

Table 6. Measured and Theoretical Change in Power with Fuel Type at Stoichiometric Conditicns with respect to Liquid Methanol

Conditions	Fuel				
	Liquid Methanol	Vaporised Methancl	Disso-diated Methanol	Hydrogen	Carbon Monoxide
Experimental	0	-1,9%	-18,7%	-20,7%	-12,1%
Theoretical	0	-12,3%	-15,3%	-19,9%	-6,3%

8.4 Evidence of Abnormal Combustion with Dissociated Methanol

The presence of various forms of knock with hydrogen fueling has already been dealt with. A distinction was made between combustion knock due to an abnormally high rate of flame propagation and detonation knock due tc autoignition and explosion of the end gas. Generally, most investigators reported that "knock" limited mixture strength to below stoichiometric even for compression ratios of 8.

In this investigation dissociated methanol and hydrogen behaved similarly with respect to knock phenomena. Thus further investigation of these phenomena was carried out with hydrogen fueling because of the greater ease of operation on a single gas.

The engine was operated on hydrogen at a compressicn ratio of 8 and MBT spark timing for mixture strengths up tc 30% rich. The only evidence of abnormal combustion was the presence of "rough running" for mixture strengths richer than stoichiometric, which appeared as very low amplitude, high frequency pressure pulsations on the oscilloscope. These could only be recorded on film by leaving the camera shutter cpen as the trace swept across the oscilloscope screen. Figure 47a is a typical pressure-crank angle diagram for a 10% rich mixture at which point the engine was running "rough".

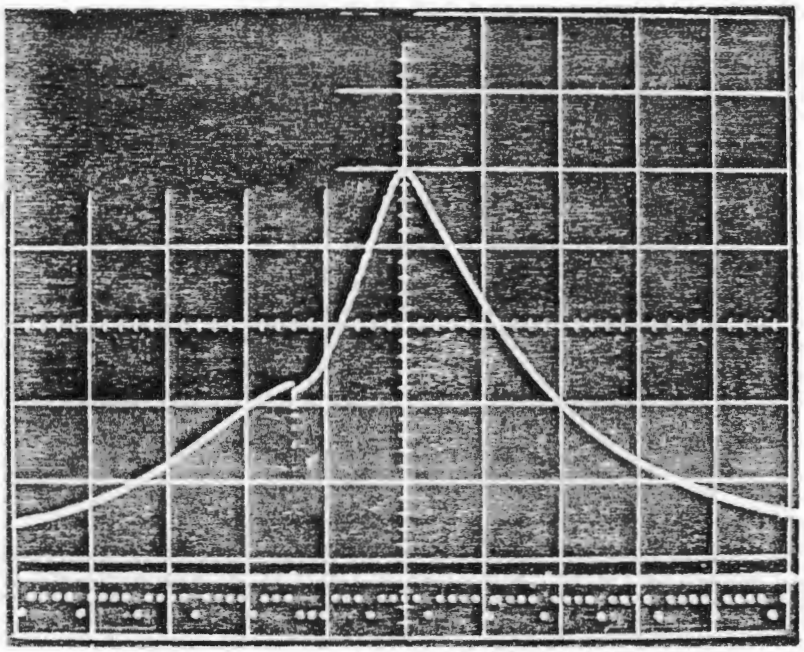

Figure 47a. Typical Indicator Diagram for a 10% Rich Hydrogen Mixture with Engine Roughness Present

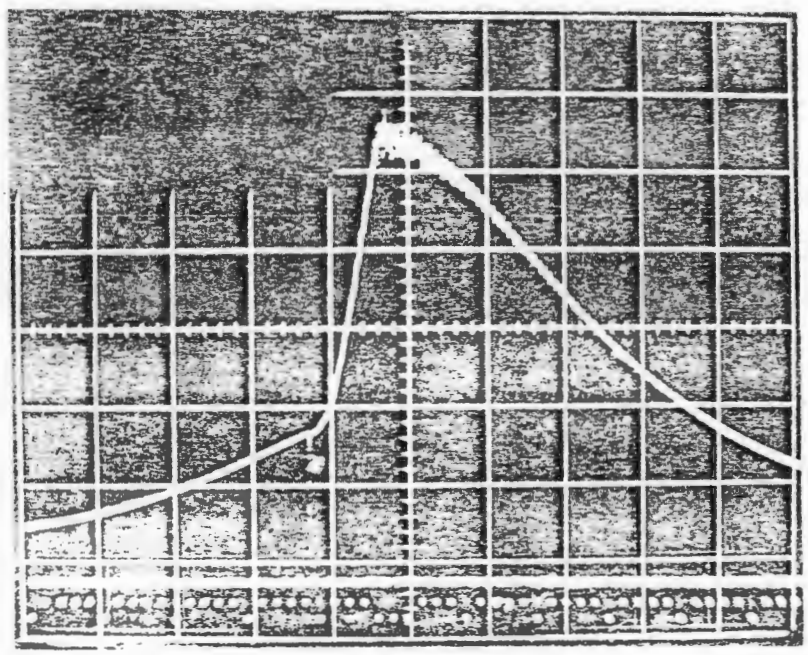

Figure 47b. Typical Indicator Diagram for a 10% Rich Hydrogen Mixture with Advanced Spark Timing and Knock apparently Present.

In ccntrast to this a definite knock, almost a thudding, was heard when either the spark timing was advanced or compression ratio raised to 12 at MBT spark timing, still with a 10% rich mixture. Figure 47b is a pressure-crank angle diagram obtained with an advanced spark timing. The pulsations were now of a much larger amplitude than anything which had been experienced during testing.

The detailed investigation of abnormal combustion phenomena was beyond the scope of the present work, but these tests have highlighted the fact that engines running on liquid or vaporised methanol would be able to benefit from high compression ratios unusable with dissociated methanol.

An extreme example will be used by way of illustration. The dissociated methanol engine will probably be limited to a compression ratio close to 8 to minimise abnormal combustion, while it has been found that a compression ratio of 14 may be used with the liquid methanol fueled engine. Then at an equivalence ratio of 0,8 the dissociated methanol engine will have an efficiency of 36,8% (based on the calorific value of liquid methanol) as against 38,8% for the liquid methanol engine.

Further evidence of abnormal combustion with hydrogen was encountered in extremely rare preignition and backfire. Figure 48a is a pressure-crank angle diagram showing an isolated preignition. Figure 48b shows the events in the cylinder which preceded a backfire. The cycle in which backfire occurred is shown by the lowest curve. There is absolutely no indication that the backfire was initiated by preignition.

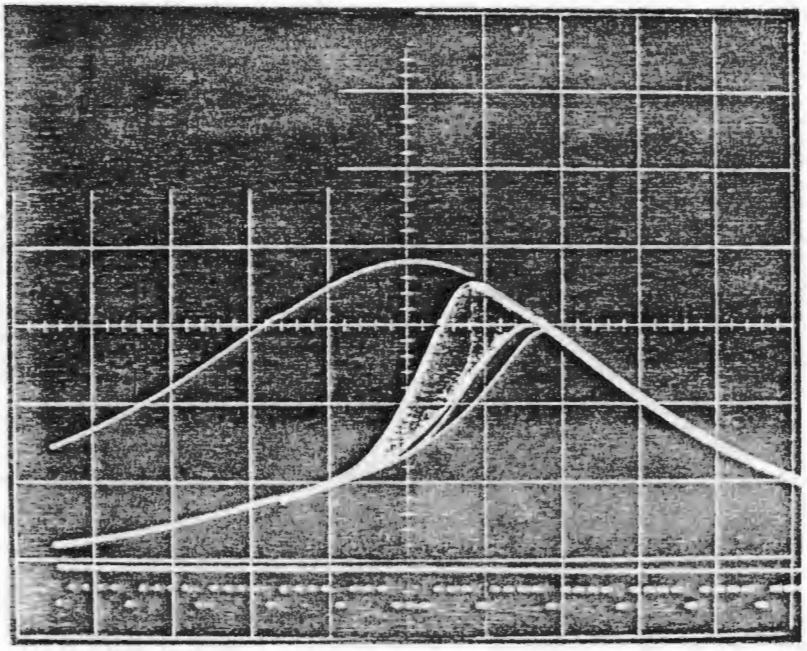

Figure 48a. Indicator Diagram showing Preignition with Hydrogen Fueling

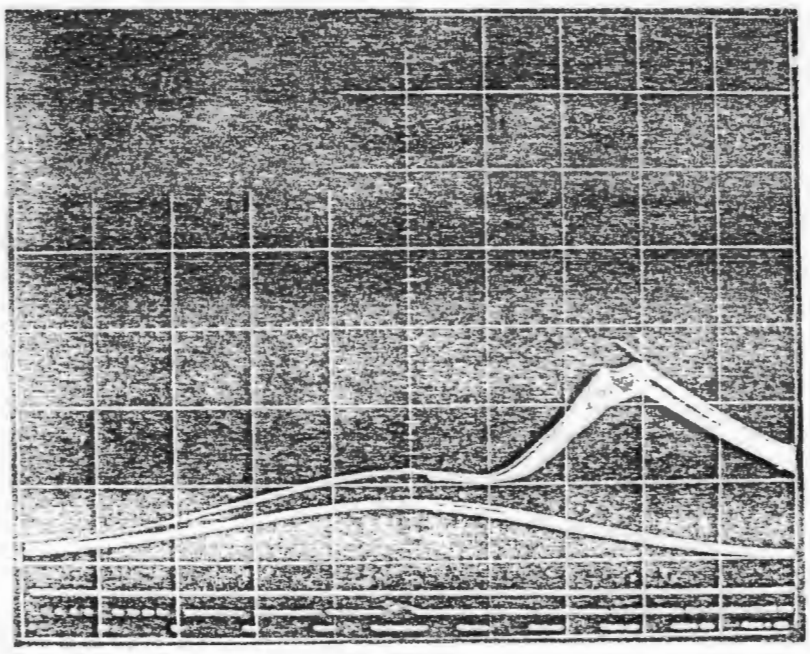

Figure 48b. Indicator Diagram showing events preceding a Backfire with Hydrogen Fueling

9. DISCUSSION OF EXHAUST EMISSIONS

9.1 Methanol Emissions

In the present investigation methanol emissions are effectively synonymous with UBF emissions since methane emissions (the other major constituent of UBF) are an order of magnitude lower than methanol.

Figure 44 shows that vaporisation of methanol is accompanied by an order of magnitude decrease in methanol emissions. This is as a result of the more homogeneous in-cylinder fuel-air mixture (no pockets of rich mixture) and absence of liquid fuel accumulation in the cylinder quench zone. The difference in methanol emissions between liquid and vaporised fuel for mixtures leaner than stoichiometric corresponds to 1,5% of the methanol in the original charge.

Comparison with the results of previous investigations, Figure 7, shows that the emissions with liquid methanol in the present investigation were somewhat higher, probably due to the deliberately poor mixture preparation. The results for the reduction in methanol emissions accompanying vaporisation are in agreement with those in Figure 9.

No methanol was detected (i.e. less than 10 ppm) for dissociated methanol fueling. Pefley claimed some erratic trace concentrations [14] but any synthesis of methanol according to the reaction:

$$2H_2 + CO \rightleftharpoons CH_3OH$$

will be inhibited by temperatures above 300°C since the reaction is exothermic.

9.2 Methane Emissions

Methane was the only hydrocarbon compound detected in the exhaust gas for dissociated methanol fueling. The source of this methane was probably the recombination of carbon monoxide and

hydrogen according to the reaction:

$$CO + 3H_2 \rightleftharpoons CH_4 + H_2O$$

This reaction has been shown to proceed readily at temperatures above 200°C in the presence of iron [14].

Previous investigations suggested that incomplete combustion may have been the cause of the poor efficiency of dissociated methanol. The presence of substantial concentrations of methane in the exhaust gas would have supported this theory. However, figure 45 shows conclusively that methane emissions are particularly low with dissociated methanol.

9.3 Formaldehyde Emissions

The formaldehyde emissions are presented in figure 46. The emissions for liquid methanol fueling agree with the general trend of previous investigations, figure 8, with the exception of the results of Hilden and Parks [19] and Pischinger and Kramer [37].

The trend for the reduction in formaldehyde emissions accompanying vaporisation is opposite to that reported by Hilden and Parks, figure 9, but that was from somewhat irregular curves.

Probably the most interesting aspect is the relation between methanol and formaldehyde emissions, since it has been proposed that formaldehyde is one of the oxidation products of unburnt methanol.

Considering first dissociated methanol, the absence of both unburnt methanol and formaldehyde offers some support to the theory.

Considering liquid and vaporised methanol next, it is found that an increase in methanol emissions is accompanied by an increase in formaldehyde for mixtures leaner than stoichiometric. For mixtures richer than stoichiometric an increase in methanol emissions has no effect on formaldehyde emissions.

It appears that these effects can be satisfactorily explained with respect to the pyrolytic decomposition of formaldehyde and the dehydrogenation of methanol [35].

Pyrolytic decomposition of formaldehyde occurs at temperatures above 400°C and may be represented by the following reactions:

$$HCHO + \tfrac{1}{2}O_2 \rightleftharpoons HCOOH \text{ (formic acid)}$$
$$HCHO + \tfrac{1}{2}O_2 \rightleftharpoons CO + H_2O$$
$$HCHO + O_2 \rightleftharpoons CO_2 + H_2O$$

The dehydrogenation of methanol is essentially complete at 500°C and is represented by the following reaction:

$$CH_3OH \rightleftharpoons HCHO + H_2$$

The relative rate of dehydrogenation of methanol and decomposition of formaldehyde will determine the final concentration of formaldehyde in the exhaust gas. The dehydrogenation reaction is active at all mixture strengths while the decomposition reaction is most effective at lean mixtures where there is an excess of oxygen.

However, it appears that at the temperatures experienced in the exhaust, the dehydrogenation reaction is faster than the decomposition reaction in the presence of oxygen and hence the high formaldehyde concentrations with lean mixtures.

In the absence of oxygen, i.e. a rich mixture, the dehydrogenation reaction is relatively slow while the decomposition reactions are limited by the availability of oxygen. This means that for rich mixtures, the unburnt methanol in the exhaust gas will probably remain unreacted.

10. SYSTEM DESIGN FOR ONBOARD DISSOCIATION OF METHANOL

The preceding discussion has assumed the availability of hydrogen and carbon monoxide from an onboard dissociation reaction. In fact, without the recovery of waste heat through onboard dissociation, dissociated methanol is considerably less attractive as a future automctive fuel than pure hydrogen. The following discussion considers the system design for onboard dissociation of methanol from the reaction itself to considerations of vehicle operation as reported in the literature.

10.1 Dissociation Reaction

The fundamental reaction may be represented as follows:

$$CH_3OH_{(l)} \rightleftharpoons 2H_{2(g)} + CO_{(g)}$$

The enthalpy of reaction is approximately 4000 kJ/kg at 298 K (equivalent to 20% of the net calorific value of methanol). The dissociation reaction proceeds from left to right. From equilibrium considerations the dissociation is complete at 200°C and atmospheric pressure or 300°C and 10 bar pressure [60].

There is usually insufficient time for equilibrium to be reached with the result that the yield will be less than that computed from equilibrium considerations. In addition, the reaction does not proceed in isolation but is accompanied by side reactions producing such products as dimethyl ether and methane. In order to reduce the effect of these difficulties, a catalyst is generally used in the reaction. The function of the catalyst is to increase the rate at which equilibrium is approached and to suppress the side reactions.

Catalysts generally contain one or more of the oxides of zinc, copper, chromium and platinum [14]. The catalysts are made up into small porous pellets and are packed into a catalytic bed into which the gaseous feedstock is introduced. Because of their porosity the catalytic pellets have low thermal conductivity. Their effective surface to volume ratio is high and their heat capacity low.

10.2 Energy Considerations

The breakdown of energy required to dissociate methanol is given in Table 7 below, using thermodynamic data from reference [61].

Table 7. Breakdown of the Energy Required for Dissociation

Process	Temperature	Energy Required (kJ/kg)	% Total
Preheating	20 - 65°C	112	2
Vaporisation	65°C	1119	20
Superheating	65 - 300°C	436	8
Dissociation	300°C	3992	70
		5659	100

It is proposed that the methanol dissociation be accomplished with engine exhaust energy. It is thus necessary to compare the thermal energy available in the exhaust gas with the energy requirements listed in table 7.

In an automotive application the available exhaust energy is a function of engine load, fuel-air ratio, speed and other less important variables. Results from the experimental investigation can be used to predict available energy at full load and low speed only.

From figure 36 it can be seen that for dissociated methanol fueling a minimum of 26% of the net calorific value of dissociated methanol is available as thermal energy in the exhaust gas at an initial temperature above 600°C.

The limiting energy requirement for the dissociation reaction is the availability of 17% of the net calorific value as thermal energy at a temperature above 300°C.

For a typical exhaust gas composition and initial temperature of 650°C, it was found that 60% of the thermal energy in the exhaust gas was available above 300°C. This is equivalent to about 16% of the net calorific value and would probably be just insufficient to dissociate all the methanol in this particular

instance. In addition, since this energy has to be transferred against a temperature of 300°C, large heat transfer surfaces will be needed to counteract the small temperature difference at the lower end. In fact, dissociation of 100% of the fuel appears quite impracticable.

10.3 Hardware Development

A system for the onboard dissociation of methanol is one which will accept liquid methanol at ambient temperature and produce dissociated methanol subject to the availability of space and thermal energy onboard a vehicle.

Such a system may be divided into three elements:

(i) Vaporiser. Engine coolant is used to vaporise the liquid methanol at a temperature of about 65°C.

(ii) Superheater and dissociation reactor. Energy is supplied from the exhaust gas at a temperature of 350 - 600°C. The methanol vapour is introduced first into the superheater where a temperature of 300°C is attained. The superheated vapour is exposed to the catalyst at a temperature of 300°C - 400°C to promote dissociation to hydrogen and carbon monoxide.

(iii) Aftercooler. The product gas is cooled by engine coolant to increase its density prior to admission to the combustion chamber.

The only one of these elements to present any difficulty is the dissociation reactor itself. The fundamental problem is how to transfer the energy for dissociation into the reactor.

The low thermal conductivity of the catalyst limits the energy available from direct catalyst bed heating. On the other hand, if the energy is to be supplied by superheated vapour alone, then 1300°C of superheat is required, but thermal stability of the catalyst may be impaired by temperatures as low as 350°C [14], although this will depend on the particular catalyst.

This problem may be solved by improving the thermal conductivity of the catalyst and employing a series heating and dissociation system.

The catalyst includes a catalyst carrier in substantial excess which is used to provide a desirable distribution of pores and bulk density. By careful selection of a catalyst carrier with a relatively high thermal conductivity, such as alumina, it shcuild be possible to increase the transfer of energy by direct catalyst bed heating.

A series heating and dissociation system would consist of alternate superheat and dissociation stages. A sandwich type design would facilitate superheating the remaining vapour immediately following a dissociation stage in a single heat exchanger through which the exhaust gas flowed.

Results from actual investigations have shown that for a methanol flow rate of 10 kg/h (sufficient for a 2 l engine) approximately 4 l of catalyst would be required with a total reactor volume of about 7 l and system mass of 50 kg [4,14]. A conversion efficiency from liquid to dissociated methanol of 80% has been claimed for such a system [4]. The design of a typical system is shown in figure 48 [62].

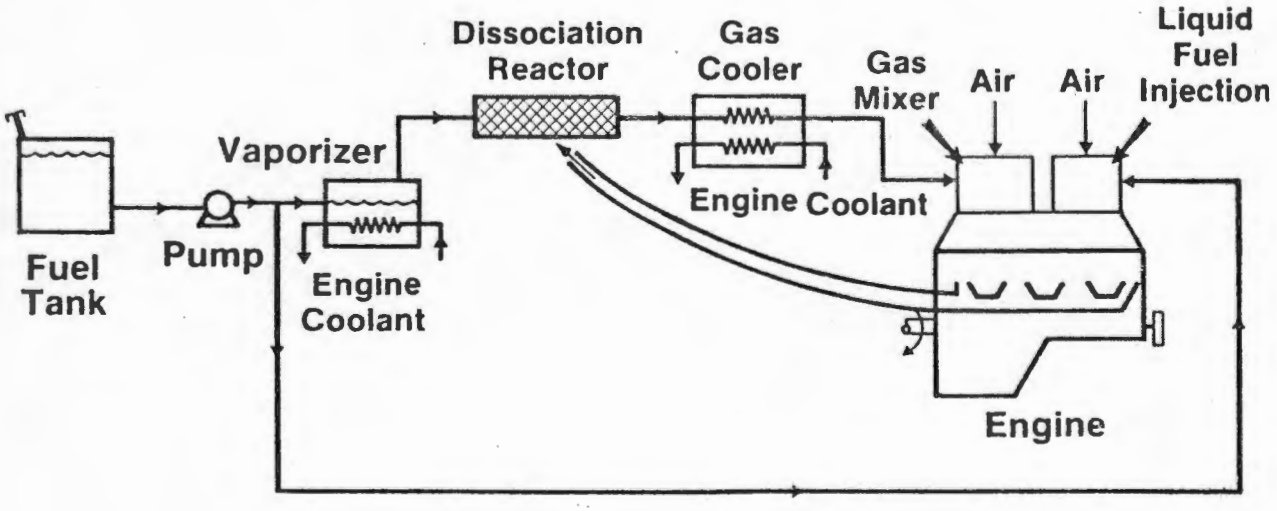

Figure 49. Design of a Dissociated Methanol Automotive Fuel System

10.4 Vehicle Operation

Only one report of a vehicle utilising onboard dissociation of methanol was found in the literature [4]. The report was remarkable in that no problems were reported, although no mention was made of how cold start-up was achieved or whether heavy acceleration was possible. However, it was mentioned that at high speed the exhaust temperature rises and reactor's performance improved. At low speed, under light load, a richer mixture was required than under normal operating conditions to prevent a drop in exhaust gas temperature since low power output was achieved by using very lean mixtures. Low exhaust gas temperatures were found to promote dehydration to dimethyl ether in preference to dissociation to hydrogen and carbon monoxide.

Endurance tests have revealed that some loss in the effectiveness of the catalyst may be expected within a hundred hours of operation [63]. The effects of cyclic on-off operation of the type expected in an automotive dissociation application have not been assessed, but the dissociation products act as a reducing agent on the catalyst and may help to maintain activity under cyclic loading conditions [14]. The condensation of methanol in the catalyst bed will be a problem since reheating and vaporisation of saturated pellets will adversely affect the performance of the catalyst.

The problems of cold start-up and heavy acceleration both have their origin in the dependency of the fuel supply on the availability of engine waste heat.

Three possible solutions are worthy of consideration:

(i) The use of reservoir and compressor to store some of the gaseous product above the system pressure. This would facilitate both cold start and high pressure fuel injection from the reservoir.

(ii) The supplementary injection of liquid methanol directly into the intake ports of the engine [62]. The liquid methanol would be used only for start-up

and when the output of the dissociation reactor is insufficient to meet the demand, such as under heavy acceleration.

(iii) A dual fuel system incorporating a partial dissociation reactor [14]. In this system a separate vaporiser and superheater unit is added to the superheater-dissociation reactor unit. A proportioning valve is used between these two units to enable the superheated methanol vapour to be routed either directly to the fuel admission system, i.e. bypassing the dissociation reactor, or via the dissociation reactor to the fuel admission system. The superheated vapour would only bypass the dissociation reactor in the proportion needed to meet the shortfall in the engine's demand for dissociated methanol. It was estimated that while it would take at least five minutes for the dissociation reactor to reach operating temperature from a cold start, superheated methanol vapour would be available within one minute.

The inherent disadvantages in both the second and third solutions is the need to supply the correct fuel-air ratio for varying mixtures of two completely different fuels.

In conclusion, it appears that dissociation of all the engine's fuel requirement will be impracticable in view of the insufficient high temperature energy available.

11. CONCLUSIONS

It has been shown that the dissociation of methanol onboard a vehicle using engine waste heat has the potential to improve thermal efficiency by up tc 10% in comparison with liquid methanol and to effectively eliminate the undesirable exhaust emissions associated with liquid methanol. This ccmbination of attributes is presently unmatched by any known fuel.

A fuel of this excellence is not, however, obtained without some penalty being incurred elsewhere. The penalty incurred with dissociated methanol is the need to achieve the dissociation onbcard a vehicle using engine waste heat. The dissociation reaction itself requires a temperature of 300°C in the presence of a catalyst. It appears that even with an ideal catalyst there is insufficient energy in the exhaust gas to dissociate all the methanol. In addition, the catalysts presently available will not be able to maintain their activity for an appreciable period and will be severely degraded by the thermal cycling encountered in an automotive application.

In addition to these difficulties there still remains the need to provide a dual fuel system, the contribution from dissociated methanol only becoming significant when the vehicle is used for a relatively long distance.

The investigation revealed that the potential of vaporised methancl to improve efficiency and reduce emissions was almcst comparable to dissociated methanol. There is no technical difficulty involved in vaporising methancl on board a vehicle and a prctotype vaporised methanol fueled vehicle is already in commercial use.

In ccnclusion, it appears that the benefits of dissociated methanol in regard to efficiency and emissions over and above thcse of vaporised methancl do not justify the considerably more complex hardware required.

12. REFERENCES

1. Newkirk, M.S. and Abel, J.L., "The Boston Reformed Fuel Car", SAE Paper 720670, 1972.

2. Ecklund, E.E. and Kester, E.L., "Hydrogen Storage on Highway Vehicles' Update '76", Proc. First World Hydrogen Energy Conference, Miami, Florida, 1976.

3. Ullman, A.Z. and Van Vorst, W.D., "Methods of On Board Generation of Hydrogen for Vehicular Use", Proc. First World Hydrogen Energy Conference, Miami, Florida, 1976.

4. Inagaki, T., Hirota, T. and Ueno, Z., "Combustion and Emission of Gaseous Fuel from Reformed Methanol in Automotive Engine", Proc. Third Int. Symp. on Alcohol Fuels Technology, Asilomar, California, 1979.

5. Rose, J.W. and Cooper, J.R., eds., "Technical Data on Fuel", 7th Ed., British National Committee World Energy Conference, London, 1977, pp. 249 - 296.

6. Bernhardt, W.W. and Lee, W., "Engine Performance and Exhaust Emission Characteristics of a Methanol-Fueled Automobile", Proc. Symp. on Future Automotive Fuels: Prospects, Performance and Perspective, Warren, Michigan, 1975.

7. Taylor, C.F., "The Internal Combustion Engine in Theory and Practice", Vol. 1, John Wiley & Sons, New York, 1960, p. 82.

8. Swain, M.R. and Adt, R.R., "The Hydrogen-Air Fueled Automobile", Seventh IECEC, San Diego, California, 1972.

9. Finegold, J.B. and Van Vorst, W.D., "Engine Performance with Gasoline and Hydrogen: A Comparative Study", in Hydrogen Energy, T.N. Veziroglu, Ed., Plenum Press, New York, 1975, pp. 685 - 696.

10. Woolley, R.L. and Germane, G.J., "Dynamic Tests of Hydrogen Powered IC Engines", Proc. First World Hydrogen Energy Conference, Miami, Florida, 1976.

11. Reed, T.B. and Lerner, R.M., "Methanol: A Versatile Fuel for Immediate Use", Science, 182, 1973, pp. 1300 - 1301.

12. Hilden, D.L. and Stebar, R.F., "Hydrogen Produced from Decomposition of Methanol During Engine Compression?", Science, 192, 1976, pp. 396 - 397.

13. Frame, G.A. and Varde, K.S., "A Study of Combustion and Engine Performance Using Electronic Hydrogen Fuel Injection", Proc. Fourth World Hydrogen Energy Conference, California, 1982.

14. Pefley, R.K., Saad, M.A., Sweeney, M.A., Kilgroe, J.D. and Fitch, R.E., "Study of Decomposed Methanol as a Low Emission Fuel : Final Report", Prepared by Office of Air Programs, Environmental Protection Agency, Contract No. EHS 70 - 118, 1971.

15. Finegold, J.G. and McKinnon, J.T., "Dissociated Methanol Test Results", Presented at the Automotive Technology Development Contractor Coordination Meeting, Dearborn, Michigan, 1982.

16. Brinkman, N.D., "Effect of Compression Ratio on Exhaust Emissions and Performance of a Methanol-Fueled Single-Cylinder Engine", SAE Paper 770791, 1977.

17. Kerley, R.V. and Thurston, K.W., "The Indicated Performance of Otto- Cycle Engines", SAE Transactions, 1962.

18. Koenig, A., Lee, W. and Bernhardt, W., "Technical and Economic Aspects of Methanol as an Automotive Fuel ", SAE Paper 760545, 1976.

19. Hilden, D.L. and Parks, F.B., "A Single-Cylinder Engine Study of Methanol Fuel - Emphasis on Organic Emissions", SAE Paper 760378, 1976.

20. Johnson, R.T., "A Comparison of Gasoline, Methanol, and a Methanol/Water Blend as Spark Ignition Fuels", Proc. Int. Symp. of Alcohol Fuel Technology, Wolfsburg, 1977.

21. Ebersole, G.D. and Manning, F.S., "Engine Performance and Exhaust Emissions : Methanol versus Isooctane", SAE Paper 720692, 1972.

22. King, R.O., Wallace, W.A. and Mahapatra, B., "The Oxidation, Ignition and Detonation of Fuel Vapours and Gases V. The Hydrogen Engine and Detonation of the End Gas by the Igniting Effect of Carbon Nuclei Formed by Pyrolysis of Lubricating Oil Vapour", Canadian Journal of Research, 26, 264, 1948.

23. Stebar, R.F. and Parks, F.B., "Emission Control with Lean Operation using Hydrogen Supplemented Fuel", SAE Paper 740187, 1974.

24. Ricardo, H.R., "Further Note on Fuel Research", Empire Motor Fuels Committee Reprint, Proc. Inst. Automotive Engineers, 18, 327, 1923.

25. Homan, H.S., De Boer, P.C.T. and McLean, W.J., "The Effect of Fuel Injection on NO_x Emissions and Undesirable Combustion for Hydrogen-Fueled Piston Engines", Int. Journal of Hydrogen Energy, 8, 131, 1983.

26. Mischke, A., Koerner, D. and Bergram, "The Mercedes-Benz Alcohol-Gas-Engine M407 hG", Fifth Int. Symp. on Alcohol Fuels Technology, Auckland, New Zealand, 1982.

27. Benson, R.S. and Whitehouse, N.D., "Internal Combustion Engines", Vol. 1, Pergamon, New York, 1979, p.123.

28. Patterson, D.J. and Henein, N.A., "Emissions from Combustion Engines and their Control", Ann Arbor Science, Michigan, 1980, pp. 133 - 135.

29. Patterson, pp. 117 - 128.

30. Quader, A.A., "Lean Combustion and the Misfire Limit in Spark Ignition Engines", SAE Paper 741055, 1974.

31. Espinola, S.A. and Pefley, R.K., "Alternate Fuel Influences on Emissions Test Procedures", Symp. on Chemistry of Oxygenates in Fuel, Kansas City, 1982.

32. Ito, K. and Yano, T., "Formaldehyde Emissions from a Spark Ignition Engine Using Methanol", Third Int. Symp. on Alcohol Fuels Technology, Asilomar, California, 1979.

33. Harrenstein, M.S., Rhee, K.T. and Adt, R.R., "Determination of Individual Aldehyde Concentrations in the Exhaust of a Spark Ignited Engine Fueled by Alcohol/Gasoline Blends", SAE Paper 790952, 1979.

34. Kappatos, D.C. and Coe, J., "An Investigation into the Reliability of Aldehyde Level Measurements for Emissions in Alcohol Fueled Cars", Fifth Int. Symp. on Alcohol Fuels Technology, Auckland, New Zealand, 1982.

35. Walker, J.F., "Formaldehyde", Reinhold, New York, 1944.

36. Ecklund, E.E. and Pefley, R.K., "Characterisation and Research Investigation of Alcohol Fuels in Automobile Engines", Final Report, DOE Contract No. DE-AC03-78CS, 1981.

37. Pischinger, F.F. and Kramer, K. "The Influence of Engine Parameters on the Aldehyde Emissions of a Methanol Operated Four Stroke Otto Cycle Engine", Third Int. Symp. on Alcohol Fuels Technology, Asilomar, California, 1979.

38. Benson, pp. 100 - 111.

39. Taylor, Vol. 2, pp. 29 - 31.

40. Chester, K.A., Adt, R.R., Rhee, K.T., Pappas, J.M. and Swain, M.R., "The Effect of Blending Methanol with Gasoline on the Lean Misfire Limit of a Multicylinder Carbureted Engine", Proc. Int. Symp. on Alcohol Fuel Technology Methanol and Ethanol, Wolfsburg, 1977.

41. Lee, R.C. and Wimmer, D.B., "Exhaust Emission Abatement by Fuel Variations to Produce Lean Combustion", SAE Paper 680769, 1968.

42. ASTM Manual of Engineering Test Methods for Rating Fuels, ASTM, 1952.

43. Anzilotti, W.F., Rogers, J.D., Scott, G.W. and Tomsic, V.J., "Combustion of Hydrogen as Related to Knock", Industrial and Engineering Chemistry, 46, 1954, pp. 1314 - 1318.

44. King, R.O. and Hayes, S.V., "The Oxidation, Decomposition, Ignition and Detonation of Fuel Vapours and Gases", Canadian Journal of Technology, 34, 1957.

45. Murray, R.G. and Schoeppel, R.J., "Emissions and Performance Characteristics of an Air-Breathing, Hydrogen Fueled Internal Combustion Engine", SAE Paper 719009, 1971.

46. King, R.O., Hayes, S.V., Allan, A.B., Anderson, R.W.P. and Walker, E.J., "The Hydrogen Engine : Combustion Knock and Related Flame Velocity, Transactions of Engineering Institution of Canada, 2, 143, 1958.

47. Taylor, Vol. 2, pp. 295 - 297.

48. Lynch, F.E., "Backfire Control Techniques for Hydrogen Fueled Internal Combustion Engines", in Hydrogen Energy, pp. 717 - 726.

49. Davies, L.P. and Bindon, J.P., "Manifold Explosions and other Combustion Phenomena in the Low Speed Hydrogen Fueled Spark Ignition Engine", The South African Mechanical Engineer, 26, January 1976.

50. British Standards Institution, "Methods for the Measurement of Fluid Flow in Pipes - Part 1 : Orifice Plates, Nozzles and Venturi Tubes", BS 1042, Part 1, 1964.

51. Tabaczynski, R.J., "Time Resolved Measurements of Hydrocarbon Mass Flow Rate in the Exhaust of a Spark-Ignition Engine", SAE Paper 720112, 1972.

52. Benson, R.S., "Measurement of Transient Exhaust Temperatures in IC Engines", The Engineer, 217, 1964.

53. Benson, pp. 106 - 111.

54. Patterson, pp. 309 - 312.

55. Sawicki, E., Hauser, T.R., Stanley, T.W. and Elbert, W., "The 3-Methyl-2-Benzothiazolone Hydrazone Test", Analytical Chemistry, 33, 1961.

56. Nebel, G.J., "Determination of Total Aliphatic Aldehydes in Auto Exhaust by a Modified 3-Methyl-2-Benzothiazolone Hydrazone Method", Analytical Chemistry, 53, 1981.

57. Harrington, J.A., "Application of a New Combustion Analysis Method in the Study of Alternate Fuel Combustion and Emission Characteristics", Proc. Symp. on Future Automotive Fuels : Prospects, Performance, and Perspective, Warren, Michigan, 1975.

58. Mclean, W.J., de Boer, P.C.T., Homan, H.S. and Fagelson, J.J., "Hydrogen as a Reciprocating Engine Fuel ", Proc. Symp. on Future Automotive Fuels : Prospects, Performance and Perspective, Warren, Michigan, 1975.

59. Taylor, Vol. 2, p. 4.

60. Paul, J.K., ed., "Methanol Technology and Application in Motor Fuels", New Jersey, 1978, pp. 39 - 53.

61. Hagen, D.L., "Methanol as a Fuel : A Review with Bibliography", SAE Paper 770792, 1977.

62. Finegold, J.G., Karpuk, M.E. and McKinnon, J.J., "Demonstration of Dissociated Methanol as an Automotive Fuel : System Design", Proc. Fourth Int. Symp. on Alcohol Fuels Technology, Sao Paulo, Brasil, 1980.

63. Kester, F.L., Konopka, A.J. and Camara, E.H., "On-Board Steam-Reforming of Methanol to Fuel the Automotive Hydrogen Engine", Tenth IECEC, Paper 759175, 1975.

64. Rogers, G.F.C. and Mayhew, Y.R., "Engineering Thermodynamics Work and Heat Transfer", 2nd Ed., Longmans, London, 1978, pp. 320 - 336.

65. British Standards Institution, "Specification for Methanol ", BS 506, 1966.

66. Prothero, A., "Computing with Thermochemical Data", Combustion and Flame, 13, 1969.

67. McNair, H.M. and Bonelli, E.J., "Basic Gas Chromatography", 5th Ed., Consolidated Printers, Berkley, California, 1969, p. 21.

68. McNair, p.67.

69. Spark, A.D., Private Communication, April 1983.

70. Richmond, S.B., "Statistical Analysis", 2nd Ed., Ronald Press, New York, 1964, pp. 350 - 378.

71. Daniel, C. and Wood, F.S., "Fitting Equations to Data", Wiley-Interscience, New York, 1971, p. 23.

72. Richmond, p. 432 - 442.

APPENDIX A

DEFINITION OF THERMAL EFFICIENCY

Considerable uncertainty surrounded the methods employed to determine the thermal efficiencies reported in the literature. As a result it was seen to be necessary to state explicitly how this was done and the values used. The approach used here follows that of reference [64].

The thermal efficiency of a power plant is conventionally expressed as:

$$\eta = \frac{W}{Qnet}$$

where η = thermal efficiency
W = net work per unit fuel supplied
$Qnet$ = net calorific value (or lower heating value) of fuel

Consideration will first be given to the calorific value term. Calorific values are defined in terms of the number of heat units liberated when unit mass of fuel is burnt completely in a calorimeter under specified conditions. For solid and liquid fuels the calorific value is determined in a constant volume calorimeter, while a constant pressure calorimeter is used for gasecus fuels. The difference between calorific values at constant volume and constant pressure is calculated from a knowledge of the difference between the number of product and reactant moles in the gaseous phase and in the present investigation was always less than 0,2%, an amount which was neglected.

The term "net" used in conjunction with calorific value means that the water in the products is in the vapour phase, as occurs in real engines. "Gross" calorific value means water in the products is in the liquid phase and consequently is numerically greater than the net value. For methanol the gross value is 6% higher than the net value.

Net calorific values used in this report refer to the fuel actually entering the cylinder. Thus, if the methanol has been vaporised, then the net calorific value for vapour was used in the efficiency calculation.

In the present investigation, net calorific values were calculated from heats of formation given in references [61, 64] and are as follows:

Liquid methanol:	19915	kJ/kg
Vaporised methanol:	21099	kJ/kg
Dissociated methanol ($2H_2 + CO$):	23958	kJ/kg
Hydrogen:	120915	kJ/kg
Carbon Monoxide:	10106	kJ/kg

The next term to be considered is the net work. This may be either the work delivered to the flywheel (brake work) or the actual work done by the working fluid on the piston (indicated work). Using these definitions results in the brake thermal efficiency and indicated thermal efficiency, respectively. Indicated thermal efficiency was selected for the present investigation for two reasons:

(i) Results from similar work on single cylinder engines are invariably quoted in this form.

(ii) Friction losses in a single cylinder test engine are not representative of those in a multicylinder automotive engine.

The next step was to establish the most suitable method cf measuring the indicated power. The two methods most commonly used are:

(i) Area of indicator cards

(ii) Addition of motoring power to brake power

The use of indicator cards is complicated by the cycle-to-cycle variation in pressures encountered. Because of this, some means of averaging successive cycles must be used. In addition, the area of the card must be measured reproducibly, a feat which cannot be accomplished manually.

The second method involves the measurement of brake power and the power required to motor the engine at the same conditions. This method assumes that the total friction losses during motoring are equal to the similar losses obtained during firing. However, two obvious differences are lower cylinder pressures and temperatures under motoring conditions.

Indicated efficiencies measured by these two methods should not differ by more than about 2% [17].

For the purposes of the present investigation, reproducibility of the results was more important than accuracy since changes were to be measured relative to liquid methanol.

APPENDIX B

OUTLINE OF ENERGY BALANCE CALCULATION

The system under consideration is shown schematically in figure 50.

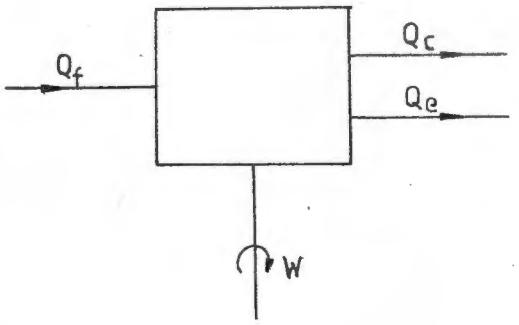

Q_f = energy in fuel
W = indicated work
Q_c = energy in coolant
Q_e = energy in exhaust gas

Figure 50. Energy Balance Schematic

The energy in the fuel was determined as the product of the fuel flow rate and net calorific value.

The indicated work was determined as the sum of the brake work and friction losses measured by a balance attached to the swinging field dynamometer. Indicated power was corrected to an ambient temperature of 25°C.

The energy in the coolant was determined as the product of coolant flow rate and energy transferred to the ccolant while flowing through the cylinder head. The flow rate was measured by a rotameter for which calibration constants were supplied by the manufacturer. These constants enabled the rotameter to be calibrated for the coolant (distilled water) at the operating temperature (70°C).

The energy in the exhaust gas required a knowledge of the exhaust gas composition, for which the following combustion equation was set up (for methanol):

$$A(CH_3OH) + B(0{,}210_2 + 0{,}79N_2) + C(H_2O) \longrightarrow D(CO_2) + E(CO) + F(O_2) + G(H_2O) + 0{,}79B(N_2)$$

A was calculated from the fuel flow rate (corrected for ambient temperature) and B from the air flow rate. C accounted for the moisture in the air measured by a wet and dry bulb thermometer and was used to determine the value of B in conjunction with the flow meter measurements.

The exhaust gas composition was then determined by mass balances for carbon, hydrogen and oxygen and actual measurements of carbon monoxide concentrations. This resulted in four equations in four unknowns but could not be solved implicitly because the carbon monoxide was expressed as a concentration. The solution was found by the Newton-Raphson iterative method.

The temperature and composition of the exhaust gas was used to calculate the thermal energy in the exhaust gas as the difference between the enthalpy just downstream of the exhaust valve and the enthalpy at ambient temperature. Enthalpies were calculated using sixth order polynomials [66].

The sum of the indicated work, coolant energy and exhaust energy was in general not equal to the energy in the fuel, since the fuel was not completely oxidised. Instead, the energy available was calculated from the difference between the enthalpy of the fuel and the enthalpy of the exhaust gas, both at ambient temperature. The difference between this value and the sum of the three energy terms was the unaccounted energy. The unaccounted energy was monitored continuously and found to be approximately 5% of the energy available at rich mixtures and 1% at lean mixtures. For the energy terms to be of comparative value for the different fuels it was essential that this unaccounted energy did not change with fuel type. Fortunately it was found to be a function of equivalence ratio only and no trend with fuel type coulo be found.

APPENDIX C

DETAILS OF FUELS USED

Methanol

Chemical grade methanol manufactured to BS506 specifications [65] was used throughout the test programme. The standard lays down that the methanol shall be clear and free from matter in suspension and shall consist essentially of methanol, CH_3OH. The relative density at 20°C should be 0,792 - 0,795.

The methanol was stored in 200 l drums and pumped to the engine's fuel tank daily. Measurements of the relative density were made regularly but it was found tc be constant at approximately 0,792. Even after several days exposure to the atmosphere the relative density changed negligibly.

Hydrogen

High purity grade hydrogen was used, with a minimum purity of 99,9%. The only significant impurity was nitrcgen.

Carbon Monoxide

Commercial grade carbon monoxide was used, with a minimum purity of 98,0%. The impurities were nitrogen (0,8 - 1%) and oxygen and argon (0,4%).

APPENDIX D

ENGINE PERFORMANCE RESULTS

The results of the 191 engine tests carried out are tabulated on the following pages. The following symbols are used:

ϕ	-	equivalence ratio
η	-	indicated efficiency
Qe	-	exhaust energy
Qc	-	coolant energy
Pi	-	indicated power
Te	-	exhaust gas temperature
θ_c	-	combustion duration
CO	-	carbon monoxide concentration in exhaust gas
PPs	-	peak pressure scatter

Fuel: Liquid methanol
Compression Ratio: 8
Air Preheat: 0

ϕ	η(%)	Qe(%)	Qc(%)	Pi(kW)	Te(^{o}C)	θ_c(^{o}CA)	CO(%)	PPs(%)
0,850	33,8	33,8	28,7	3,21	596	58	0,50	56
0,851	34,0	33,4	28,4	3,19	597	57	0,53	56
0,854	33,8	33,4	28,7	3,22	601	57	0,54	55
0,859	34,2	33,4	28,6	3,25	599	57	0,55	54
0,860	33,7	33,2	28,9	3,22	606	56	0,59	54
0,881	34,0	32,8	29,3	3,30	617	54	0,60	48
0,894	33,8	32,2	29,5	3,31	622	53	0,58	45
0,895	33,7	32,4	29,8	3,36	622	52	0,55	47
0,901	33,8	31,9	29,5	3,37	620	53	0,59	44
0,909	33,8	31,7	29,7	3,37	629	53	0,62	43
0,912	34,0	31,9	30,0	3,39	629	52	0,54	43
0,916	33,6	31,8	30,0	3,40	634	52	0,61	42
0,923	33,4	31,5	30,2	3,41	630	53	0,51	40
0,935	33,4	31,5	30,2	3,44	635	50	0,59	41
0,948	33,4	31,2	30,3	3,45	641	48	0,61	38
0,961	33,6	30,8	30,8	3,51	644	48	0,59	36
0,990	33,0	30,3	31,1	3,59	659	45	0,69	33
1,01	33,1	29,9	31,1	3,65	661	44	0,68	31
1,06	32,5	29,1	31,8	3,74	671	39	1,01	28
1,11	32,3	28,8	31,5	3,87	681	38	1,24	26
1,18	31,0	28,7	31,3	3,98	681	37	1,65	24
1,22	30,6	28,6	31,1	3,97	678	35	1,92	34
1,24	30,2	29,0	30,8	4,01	676	36	2,21	24
1,27	30,1	29,2	30,6	4,05	667	37	2,41	24
1,32	29,4	29,4	29,8	4,03	657	36	2,90	24

Fuel: Liquid methanol

Compression Ratio: 12

Air Preheat: 0

ϕ	η(%)	Qe(%)	Qc(%)	Pi(kW)	Te(^{o}C)	θ_c(^{o}CA)	CO(%)	PPs(%)
0,793	38,3	30,3	28,8	3,32	539	55	0,39	61
0,796	38,0	29,9	28,3	3,37	537	55	0,42	63
0,803	38,2	29,7	28,7	3,37	541	55	0,44	63
0,813	37,8	29,6	29,1	3,43	542	53	0,41	57
0,830	37,7	29,3	29,0	3,43	552	54	0,42	55
0,851	37,7	29,1	29,6	3,56	565	52	0,42	55
0,880	37,6	28,3	30,4	3,62	575	48	0,45	56
0,891	37,4	27,8	30,1	3,71	576	45	0,46	51
0,908	37,2	27,9	30,8	3,72	584	45	0,45	52
0,924	37,0	27,4	30,4	3,75	584	43	0,51	45
0,955	36,9	26,6	31,1	3,83	590	43	0,54	43
0,983	36,9	26,9	31,2	3,99	603	40	0,60	43
0,998	36,5	26,4	31,6	3,98	601	40	0,65	44
1,02	36,4	26,2	31,9	4,09	611	37	0,68	43
1,03	36,1	26,2	31,6	4,04	608	36	0,70	43
1,09	35,3	25,8	31,7	4,21	615	36	0,95	40
1,14	34,6	25,4	32,0	4,23	621	33	1,12	39
1,19	33,9	25,7	31,9	4,36	621	31	1,51	37
1,20	33,5	25,7	31,6	4,32	617	32	1,56	35
1,23	33,4	25,8	31,6	4,42	618	32	1,93	31
1,29	31,8	26,2	30,6	4,46	607	34	2,63	28
1,33	30,9	26,9	30,2	4,43	596	35	3,22	29

Fuel: Liquid methancl

Ccmpression Ratio: 14

Air Preheat: 0

ø	η (%)	Qe(%)	Qc(%)	Pi(kW)	Te(^{o}C)	θ_c(^{o}CA)	CO(%)	PPs(%)
0,760	39,3	29,4	27,5	3,34	522	56	0,38	62
0,760	39,3	29,7	27,9	3,35	517	56	0,40	61
0,769	39,1	29,6	28,0	3,33	524	55	0,34	61
0,780	38,8	29,0	28,1	3,42	525	54	0,38	56
0,799	38,8	29,0	28,6	3,40	531	53	0,37	56
0,816	38,4	28,7	29,1	3,55	545	49	0,39	55
0,843	38,6	28,1	29,2	3,63	553	46	0,37	53
0,870	38,1	27,7	30,2	3,70	555	45	0,45	50
0,889	38,1	27,0	30,0	3,69	565	45	0,42	54
0,908	38,0	26,9	30,3	3,76	564	41	0,49	49
0,925	37,9	26,7	30,8	3,86	572	40	0,54	50
0,964	37,6	26,1	31,1	3,92	578	38	0,59	49
0,992	37,2	26,1	31,4	4,00	589	38	0,66	44
1,00	36,9	25,9	31,3	4,04	586	38	0,63	42
1,05	36,2	25,3	31,9	4,14	599	35	0,69	40
1,09	36,2	25,1	32,1	4,20	597	35	0,92	41
1,15	35,0	25,0	31,7	4,33	599	31	1,25	35
1,20	34,7	24,8	31,6	4,39	607	32	1,48	31
1,27	33,1	25,0	31,1	4,48	600	32	2,19	26
1,31	32,5	24,9	30,8	4,51	598	31	2,65	29

Fuel: Liquid methanol
Compression Ratio: 8
Air Preheat: 300 W

ø	η (%)	Qe(%)	Qc(%)	Pi(kW)	Te(^{o}C)	θ_c(^{o}CA)	CO(%)	PPs(%)
0,776	34,2	34,4	28,3	3,03	593	58	0,36	53
0,779	34,0	34,3	28,5	3,11	596	56	0,38	51
0,788	34,0	34,1	28,5	3,16	604	57	0,39	50
0,811	34,1	33,2	29,3	3,24	608	55	0,42	47
0,826	34,0	32,8	29,4	3,30	625	53	0,39	43
0,840	33,7	32,7	29,8	3,29	622	50	0,40	40
0,891	33,5	31,8	30,7	3,51	642	48	0,45	36
0,905	33,2	31,2	31,0	3,55	652	48	0,51	36
0,931	33,1	30,8	31,3	3,61	658	45	0,48	32
0,964	32,7	30,4	31,6	3,76	667	44	0,55	29
0,983	32,7	30,4	31,5	3,78	668	43	0,69	27
0,998	32,4	30,3	31,5	3,79	678	44	0,68	29
1,03	32,3	30,0	32,1	3,87	683	40	0,80	27
1,09	31,5	29,8	31,7	3,97	679	39	1,22	23
1,14	30,7	29,6	31,8	4,00	681	39	1,58	22
1,17	30,6	29,9	31,2	4,02	678	37	1,71	21
1,23	29,6	30,3	30,5	3,98	671	37	2,31	21
1,27	29,1	30,5	30,1	3,98	658	39	3,54	21
1,31	28,0	31,1	29,0	3,90	645	39	4,95	18
1,36	27,4	31,9	27,9	3,85	625	41	7,17	18

Fuel: Liquid methanol
Compression Ratio: 8
Air Preheat: 1 000 W

ø	η(%)	Qe(%)	Qc(%)	Pi(kW)	Te(°C)	θ_c(°CA)	CO(%)	PPs(%)
0,646	36,3	34,6	27,3	2,55	594	57	0,34	69
0,650	36,2	34,6	27,1	2,57	596	55	0,33	67
0,658	35,7	34,2	27,7	2,60	598	52	0,31	67
0,691	35,8	33,3	28,0	2,71	618	50	0,36	54
0,713	35,2	33,4	28,7	2,76	625	47	0,38	48
0,740	35,1	33,1	29,2	2,85	640	44	0,41	38
0,778	34,7	32,6	30,4	2,88	654	42	0,47	30
0,820	33,7	32,1	30,7	3,02	664	41	0,48	26
0,839	33,7	31,7	30,9	3,03	669	37	0,51	24
0,871	33,1	31,5	31,4	3,07	674	38	0,64	23
0,899	32,4	31,4	31,8	3,19	679	35	0,72	20
0,941	31,8	30,9	32,0	3,26	683	36	0,91	20
0,953	32,0	31,2	31,8	3,22	681	35	0,96	20
0,980	31,7	30,8	31,9	3,27	681	33	1,23	18
0,993	31,1	31,0	32,4	3,32	683	32	1,31	19
1,00	31,4	31,2	32,3	3,31	680	33	1,39	21
1,04	30,7	31,3	31,9	3,33	685	32	1,72	19
1,07	30,2	31,2	31,8	3,35	671	31	2,04	20
1,10	29,7	31,1	31,6	3,39	668	33	2,66	19
1,17	28,6	31,7	30,8	3,30	646	32	4,34	20
1,21	27,6	32,5	30,8	3,36	633	33	5,80	21
1,24	27,1	33,1	29,8	3,30	619	33	7,37	20
1,29	26,0	33,3	28,9	3,22	596	33	11,0	20

Fuel: Vaporised methanol

Compression Ratio: 8

Air Preheat: 0

ø	η (%)	Qe(%)	Qc(%)	Pi(kW)	Te(^{o}C)	θ_c(^{o}CA)	CO(%)	PPs(%)
0,661	37,0	34,7	26,3	2,79	582	54	0,05	53
0,663	37,0	34,6	26,5	2,84	582	54	0,05	52
0,691	36,2	33,7	27,3	2,97	594	53	0,07	45
0,755	35,7	32,8	28,8	3,16	628	49	0,07	34
0,760	35,7	32,7	28,6	3,13	634	48	0,05	33
0,811	35,3	31,5	29,5	3,27	651	44	0,08	28
0,870	34,4	30,7	30,4	3,40	668	40	0,11	24
0,898	34,3	30,9	30,6	3,39	676	39	0,08	23
0,901	34,2	31,1	30,8	3,44	675	38	0,12	23
0,930	33,3	30,9	30,8	3,44	685	36	0,11	22
0,957	33,0	30,5	31,4	3,54	686	37	0,24	23
0,988	32,9	30,7	31,4	3,53	694	36	0,90	20
1,01	32,0	30,6	31,5	3,53	693	34	0,97	20
1,03	32,0	30,3	31,2	3,61	683	32	1,04	21
1,08	31,0	30,7	31,5	3,57	677	31	1,59	20
1,13	30,0	31,1	31,2	3,66	676	32	3,10	20
1,15	29,3	31,8	30,8	3,62	665	33	3,74	20
1,19	28,1	31,8	30,5	3,65	647	32	5,64	21
1,26	26,6	33,4	29,6	3,63	624	34	8,85	22
1,28	25,8	33,6	29,4	3,53	607	34	9,63	23
1,35	23,8	35,4	28,3	3,52	568	36	13,80	25

Fuel: Dissociated methanol

Compression Ratio: 8

Air Preheat: 0

ϕ	η (%)	Qe(%)	Qc(%)	Pi(kW)	Te(^{o}C)	θ_c(^{o}CA)	CO(%)	PPs(%)
0,391	34,4	31,6	31,2	1,67	416	52	0,49	38
0,394	34,8	31,6	31,6	1,62	404	52	0,53	38
0,459	33,9	31,4	33,4	1,84	446	48	0,42	32
0,508	33,9	30,4	33,7	1,96	486	42	0,22	29
0,570	33,4	29,9	34,9	2,17	515	38	0,18	25
0,592	32,8	29,7	35,3	2,24	516	38	0,14	24
0,651	32,6	29,1	36,4	2,34	544	32	0,05	21
0,680	32,8	28,7	37,3	2,42	563	35	0,05	20
0,703	32,2	29,0	37,2	2,45	565	30	0,05	19
0,771	31,4	28,2	38,2	2,57	596	31	0,05	17
0,824	31,4	27,7	37,9	2,72	620	28	0,05	15
0,886	30,4	27,3	38,3	2,77	623	25	0,05	13
0,913	29,7	27,1	39,0	2,84	626	21	0,05	13
0,971	29,8	26,9	39,1	2,92	650	19	0,08	12
0,997	29,1	26,4	39,1	2,98	653	21	0,10	11
1,02	28,6	26,2	39,2	2,97	651	20	0,14	11
1,06	28,8	26,6	38,9	3,04	650	18	0,15	10
1,07	28,6	26,1	39,0	3,04	654	20	0,18	10
1,13	27,1	25,8	38,3	3,06	652	19	0,35	9
1,16	26,9	25,5	37,6	3,12	646	19	0,76	8
1,21	26,6	25,1	38,0	3,09	660	17	1,13	8
1,29	25,5	25,2	37,0	3,18	636	16	1,84	7
1,34	23,9	25,1	35,7	3,17	632	16	2,25	7

Fuel: Hydrogen
Compression Ratio: 8
Air Preheat: 0

ø	η(%)	Qe(%)	Qc(%)	Pi(kW)	Te(°C)	θ_c (°CA)	CO(%)	PPs(%)
0,247	40,1	38,8	18,3	1,21	317	57	0	39
0,249	39,8	38,5	18,2	1,23	310	59		41
0,273	40,0	38,0	19,3	1,28	339	57		36
0,298	39,7	37,8	20,0	1,38	350	52		35
0,330	38,8	37,4	21,1	1,50	381	48		37
0,371	38,6	36,6	22,4	1,69	401	45		32
0,407	38,3	36,2	23,4	1,74	423	43		26
0,453	37,3	35,0	24,9	1,94	455	42		27
0,497	36,9	34,8	26,4	2,07	482	37		19
0,571	36,3	33,6	28,2	2,23	518	30		18
0,594	35,6	33,6	28,6	2,24	527	31		15
0,661	35,0	32,6	30,1	2,42	554	26		11
0,734	33,5	31,9	31,2	2,54	584	20		9
0,773	33,3	31,4	31,7	2,66	604	22		10
0,840	32,1	31,5	32,9	2,74	615	18		8
0,910	31,4	30,8	33,3	2,82	634	16		7
0,982	30,4	30,8	34,1	2,81	641	16		7
1,03	29,3	30,2	34,7	2,87	642	15		6
1,10	28,2	30,4	34,1	2,96	646	13		5
1,17	27,4	29,9	34,2	2,90	646	13		5
1,22	26,7	30,3	34,0	2,86	636	14		5
1,28	25,3	30,0	33,6	2,90	637	14		5

Fuel: Carbon monoxide

Compression Ratio: 8

Air Preheat: 0

Ø	η (%)	Qe(%)	Qc(%)	Pi(kW)	Te(^{o}C)	θ_c(^{o}CA)	CO(%)	PPs(%)
0,887	28,9	23,7	42,9	3,01	594	53	0,15	53
0,888	28,9	24,0	43,4	3,02	591	54	0,18	54
0,894	28,8	24,1	43,3	2,98	596	54	0,19	50
0,910	28,4	23,3	43,3	3,06	599	52	0,26	47
0,923	28,4	23,6	43,5	3,01	604	50	0,29	39
0,957	27,9	23,1	43,9	3,17	622	46	0,45	36
0,980	28,1	22,6	43,7	3,20	628	43	0,55	30
0,998	27,7	22,4	44,3	3,22	629	44	0,63	25
1,01	27,8	21,8	43,9	3,17	635	43	0,69	27
1,04	27,7	21,7	44,0	3,23	638	41	0,81	21
1,09	27,5	21,2	44,5	3,34	651	38	1,37	17
1,11	27,5	21,0	44,4	3,33	652	37	1,61	16
1,17	27,3	21,1	44,5	3,39	664	36	2,57	16
1,22	27,0	20,9	44,2	3,43	663	35	3,70	17
1,27	26,9	20,8	44,5	3,43	668	35	5,27	17
1,28	27,1	20,9	44,2	3,42	664	37	5,77	18

APPENDIX E

CALIBRATION FOR EMISSIONS ANALYSIS

Methane and Methanol

The concentrations of methane and methanol were measured with a gas chromatograph equipped with a FID. The response of the FID is proportional to the mass of carbon in the sample for a particular species [67]. This made calibration particularly easy since relatively few samples were needed to establish the response of the FID to a particular species. The range over which calibration was required was established by analysing actual exhaust samples over the whole engine operating range. Calibration was then performed over this range.

Calibration of the response to methane was performed with methane of 600 ppm concentration in nitrogen. The sample bottles mentioned previously were used to dilute the methane to the required concentration. The bottles were partially evacuated and then filled from a sample bag containing 600 ppm methane at atmospheric pressure. 0,3 ml samples of this mixture were then injected into the gas chromatograph. The resultant calibration was 38,5 area units per ppm methane (volume basis) in a 0,3 ml sample.

Calibration of the response to methanol was performed with analytical grade methanol. An initial volume of 1 ml was withdrawn with a pipette and diluted with distilled water. 1 μl samples of this mixture were then injected into the gas chromatograph. The resultant calibration was 20,1 area units per ppm methanol in a 0,3 ml gas sample.

From these results the ratio of the response to the carbon atom in methanol to that in methane was 0,52. A value of 0,47 has been reported in the literature for a similar FID [68].

Formaldehyde

The response of the MBTH method to formaldehyde was calibrated by using samples spiked with known amounts of formaldehyde. The formaldehyde was used in the form of analytical grade formalin, which was assayed by a commercial laboratory to contain 20,7 g formaldehyde per 100 ml. This is significantly below the 37 g per 100 ml claimed by the manufacturer. Since there was no evidence of precipitation in the bottle, the calibration was performed immediately following the assay on the advice of the analyst [69].

The method employed to obtain the correct concentration of the calibration sample was one of successive dilution in distilled water. 1 ml of formalin was withdrawn with a pipette and after dilution in water, 1 ml of the solution was added to 20 ml of MBTH reagent. 1 ml of this solution was withdrawn and processed as for the exhaust samples. The formalin solution was then further diluted and the procedure repeated.

The absorbance was found to be proportional to the mass of formaldehyde in the sample. Figure 51 relates the mass of formaldehyde in the impinger to the measured absorbance. The standard error of the estimate is shown for 22 samples. The concentration of formaldehyde in the exhaust gas could then be calculated from this relationship once the volume of exhaust gas drawn through the impinger was known.

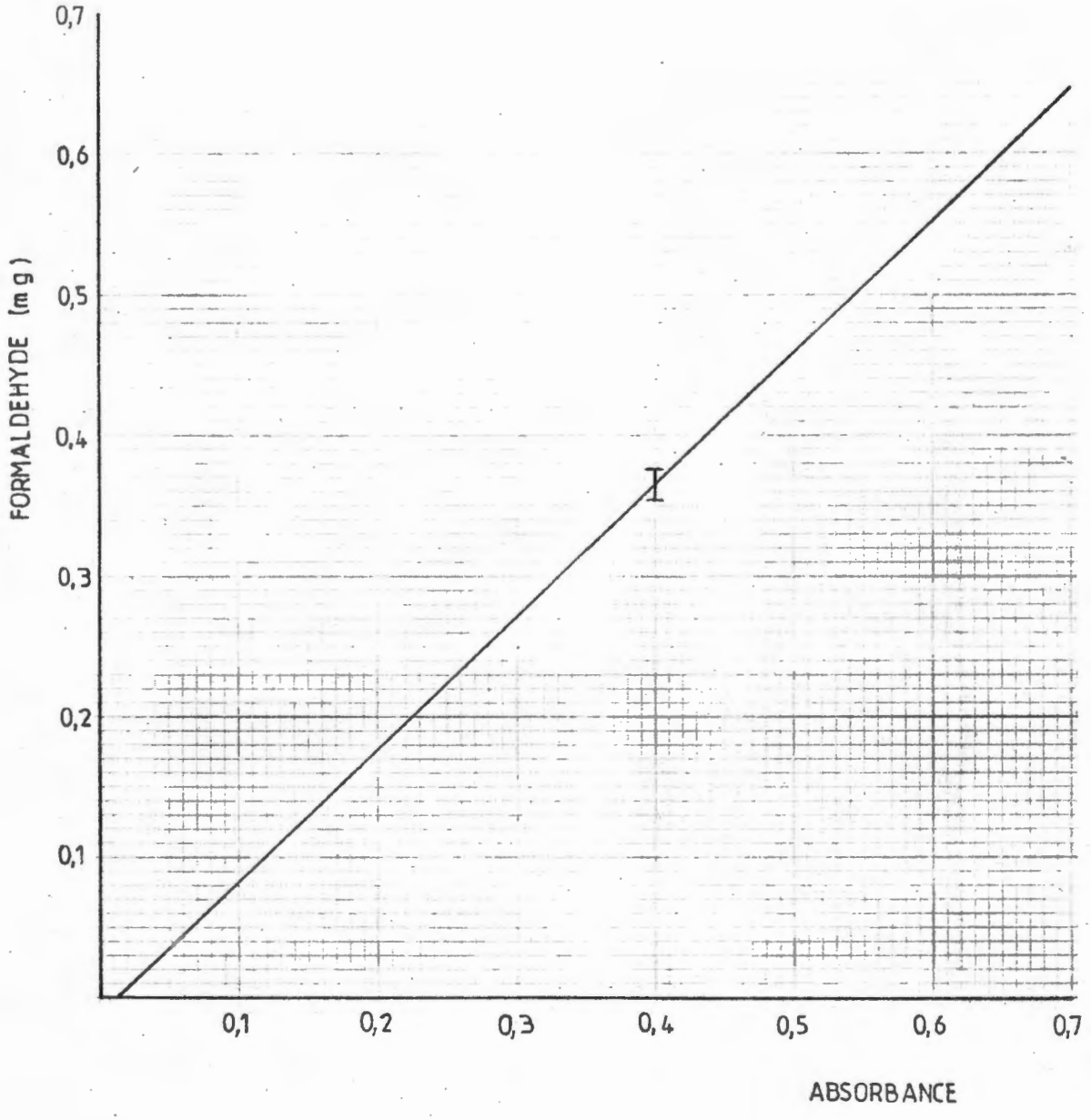

Figure 51. MBTH Calibration Curve

APPENDIX F

EMISSIONS RESULTS

Liquid Methanol

Ø	CH_3OH (ppm)	CH_4 (ppm)	HCHO (ppm)
0,856	2060	24	155
0,868	2053	36	144
0,890	2011	31	153
0,909	1958	37	160
0,916	2013	47	148
0,938	1940	40	162
0,956	1965	46	153
0,985	1973	43	150
0,994	2085	61	122
1,01	1960	66	108
1,03	2217	59	112
1,03	2280	64	106
1,07	2407	73	98
1,10	2441	102	118
1,13	2560	98	92
1,17	3021	111	82
1,20	3361	134	86
1,23	3321	178	80
1,26	3840	221	88
1,32	4550	264	76

Vaporised Methanol

ø	CH_3OH (ppm)	CH_4 (ppm)	HCHO (ppm)
0,671	240	14	38
0,690	220	13	41
0,714	260	13	44
0,728	261	13	35
0,757	165	10	43
0,804	110	10	38
0,830	215	11	30
0,872	207	10	38
0,893	67	13	31
0,911	156	13	38
0,912	168	11	33
0,969	240	14	25
0,985	204	15	31
1,01	265	14	21
1,05	171	18	18
1,07	253	18	23
1,11	301	27	18
1,19	358	46	24
1,23	312	38	16
1,28	498	59	22

Dissociated Methanol

ø	CH_3OH (ppm)	CH_4 (ppm)	HCHO (ppm)
0,401	< 10	6	< 1
0,410		5	
0,487		5	
0,528		6	
0,611		6	
0,659		4	
0,723		8	
0,794		4	
0,809		8	
0,836		7	
0,946		9	
1,05		11	
1,12		14	
1,21		23	
1,24		26	
1,28		34	

APPENDIX G

DETAILS OF DATA REDUCTION

The need for a regression of the dependent variable against the independent variable has already been discussed. The details of how this was carried out will now be presented.

Least squares regression may be used to fit a curve to the data such that the sum of the squares of the deviations about that curve is less than the sum of the squares of the deviations about any other line of the same mathematical type [70].

This, however, means that the type of curve must be decided on before starting. The curves considered for the present investigation were polynomials, exponentials and Hoerl's special functions [71]. Hoerl's special functions ($f(x)=ax^b e^{cx}$) were used where polynomial and exponential curves both failed.

An example of the method used will be given for the efficiency curve. From the numerous results in the literature an idea of the shape of the curve was obtained. The exponential curve was not suitable since its shape was concave where the efficiency curve was convex. Next, polynomials of various degrees were tried. The criteria of acceptance or rejection were as follows:

(i) Shape of the curve (number of points of inflexion)

(ii) Coefficient of determination

(iii) Standard Error of the estimate

By way of explanation, the coefficient of determination may be interpreted as the percentage of the total variation in the dependent variable that is associated with variation in the independent variable [72]. The standard error of the estimate may be interpreted in such a way that if the deviations about the regression line are normally distributed, then it may be said that 68% of the deviations will lie within a distance of

one standard error of the estimate from the line [72].

In the case of the efficiency curves second order polynomials had coefficients of determination greater than 97%. As the order of the polynomial increased, the coefficient of determination showed very little increase although the standard errors of the estimate were noticeably reduced. This is understandable since, for instance, a third order polynomial has two points of inflexion and can follow the data more closely. However, the resultant third order curve often showed a point of inflexion when approaching the lean limit, which was a property of the curve and not the data.

Thus second order polynomial functions were used for the efficiency curves. One standard error of the estimate was represented by an I at a convenient point on the curve. That this method offered a reasonable indication of the uncertainty in the results was established by the following test. The engine was prepared for an efficiency test with fuel-air mixture set close to stoichiometric. The efficiency was measured, then the spark timing and load were changed. The spark timing and load were then reset, not necessarily to their previous values but to the values determined by the same method as used previously. Again efficiency was measured. This process was repeated 12 times and the standard deviation calculated from the results. The standard deviation so obtained was approximately $\frac{1}{2}$ of the standard error of the estimate. Since data used to determine the standard error of the estimate were obtained over a number of days, the difference between the standard error of the estimate and standard deviation was believed to be due to day-to-day variations in operating conditions.

It is possible to compute prediction intervals for the true means of the distributions of efficiency for fixed values of the equivalence ratio. If the regression curve is a straight line, the prediction intervals are represented by curved lines which are closest to the regression line at the mean equivalence ratio. This is because statistically the estimate of the efficiency is less precise as the distance from the mean equivalence ratio increases.

The experimental data have been plotted together with the fitted curves and standard error of the estimate in Appendix H. It is clear from these that prediction intervals do not reflect the actual distribution of the experimental data as effectively as the standard error of the estimate does.

APPENDIX H

EXPERIMENTAL DATA AND CURVES FITTED FOR ENGINE EFFICIENCY

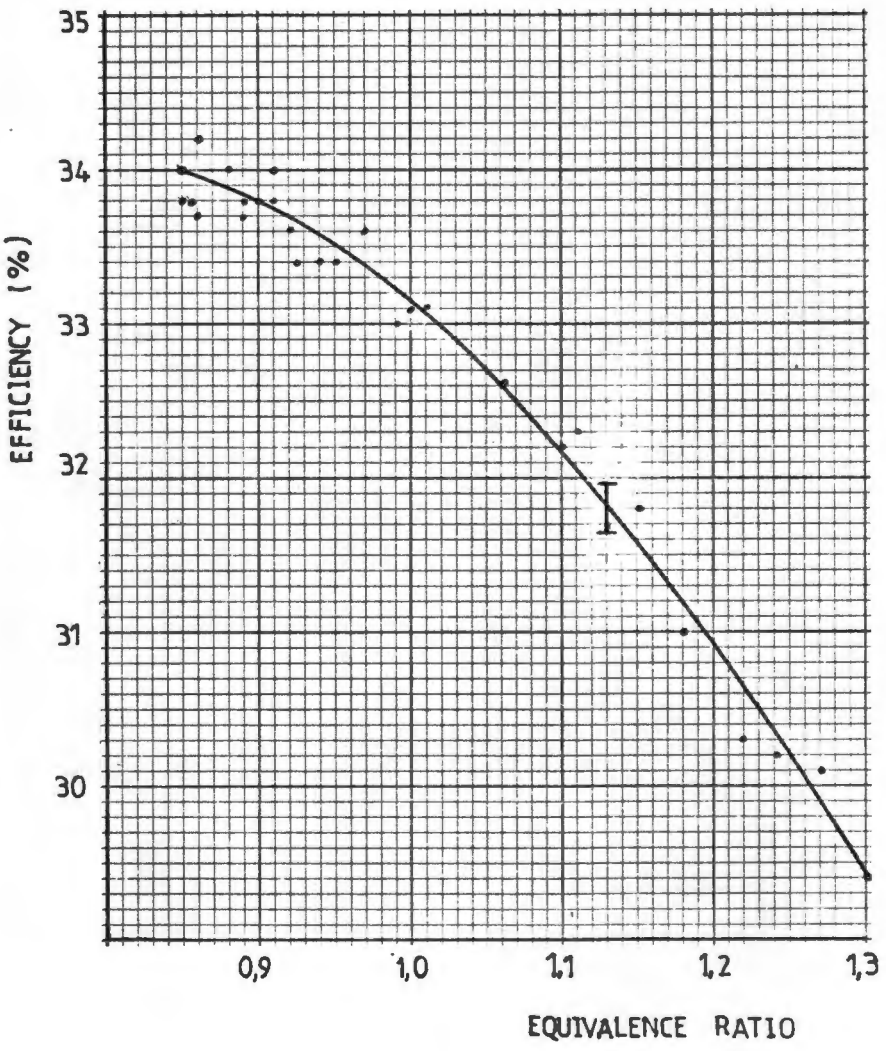

Figure 52. Experimental Data and Fitted Curve for Liquid Methanol Fueling

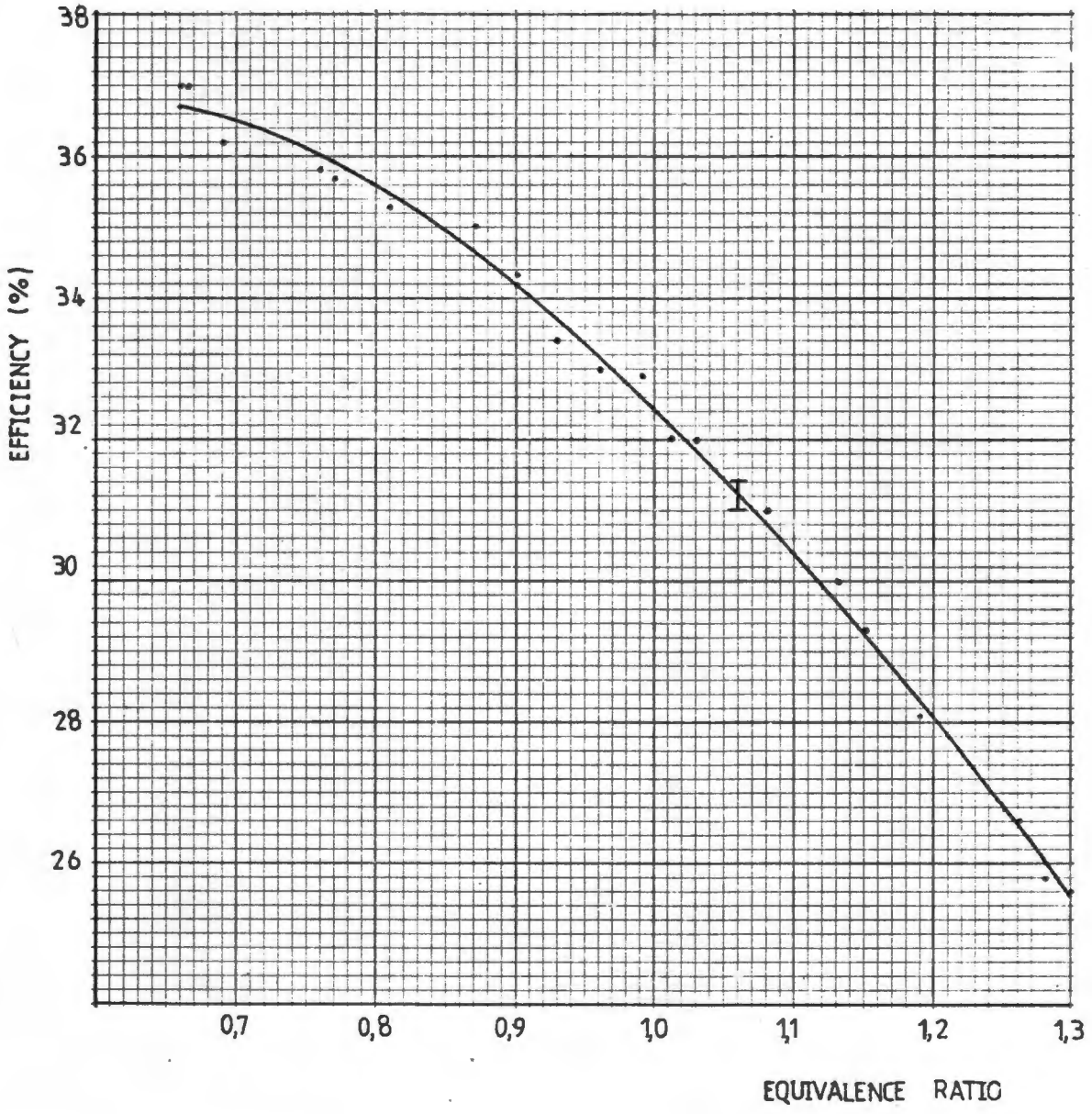

Figure 53. Experimental Data and Fitted Curve for Vaporised Methanol Fueling

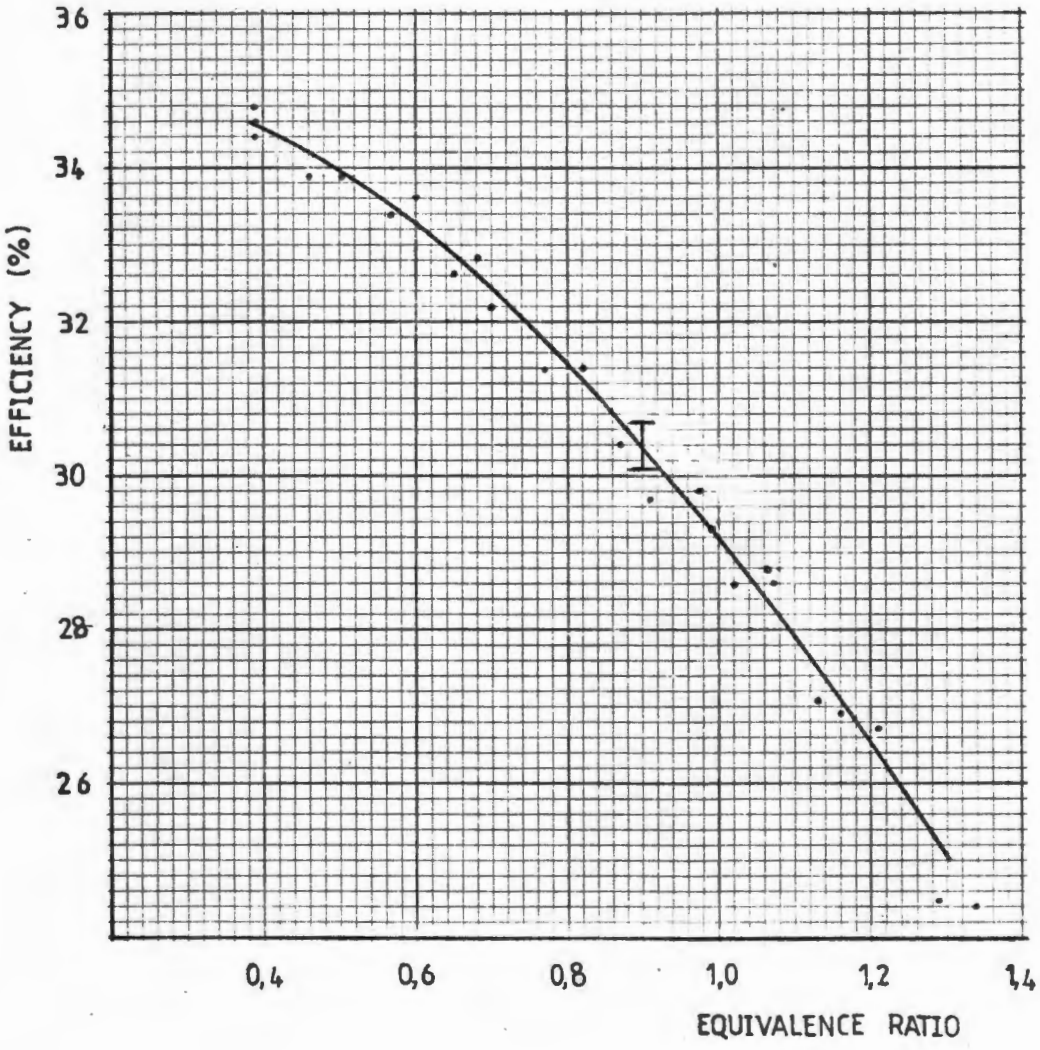

Figure 54. Experimental Data and Fitted Curve for Dissociated Methanol Fueling